Monopile gripper:

Optimized design of a seabed monopile gripper

Deepakraj Thangaraju

TU Delft

Van Oord
Marine ingenuity

Monopile gripper:

Optimized design of a seabed monopile gripper

by

Deepakraj Thangaraju

to obtain the degree of Master of Science
at the Delft University of Technology,

Student number:	4806778	
Thesis committee:	Prof. dr. ir. A. Metrikine,	TU Delft, Chairman
	Ir. J. S. Hoving,	TU Delft, Supervisor
	Ir. R. J. N. J. Luiken,	Van Oord, Supervisor

This thesis is confidential and cannot be made public until January 29^{th}*, 2023.*

An electronic version of this thesis is available at `http://repository.tudelft.nl/`.

TU Delft

Van Oord
Marine ingenuity

Abstract

To increase the benefit of wind energy, the next generation wind turbines are becoming larger and are moving into deeper waters. This significantly increases the size and weight of the corresponding monopile support structures. In current practice, the majority of monopiles are installed using jack-ups or floating vessels using so-called monopile gripper frames. Both vessels have their advantages and disadvantages. Jack-ups are limited by weather conditions and lifting capacity depending on the jack-up legs. For floating vessels, it is difficult to achieve stability and verticality of the monopile during installation, because the gripper frame moves with the vessel. This reduces the operating weather condition for installation of monopiles using a floating vessel.

To operate in larger weather windows and to be able to lift larger loads, Van Oord is investigating the use of a monopile gripper on the seabed, so that the gripper frame is no longer subject to the motions of the vessel. To install a monopile support structure using a seabed gripper, the monopile gripper frame is installed first. The monopile is then slewed into the gripper frame, which is able to hold the monopile in position and vertical while hammering it. After the installation of the monopile, the seabed gripper structure is removed and transported to the location where the next monopile is to be installed. This thesis covers the optimized design of such a re-usable seabed monopile gripper. First, the different options for the gripper structure and its foundation currently available in practice are identified from a literature study. Suitable concepts for the gripper structure are generated based on the requirements, of which the two optimal concepts are selected based on a Multi Criteria Analysis (MCA). A four-legged Jacket and a Tripod are chosen as the best concepts for the gripper structure using either Helical piles or Suction buckets for its foundation.

A preliminary design of both the gripper structure and the foundation is done to identify the initial member sizing and reactions of the piles at the seabed. A FEM model of the gripper structure including a soil model is created in ANSYS and analysed for both members and joints in ULS conditions. Due to the required opening on one side of the gripper structure (to slew in the monopile), the stresses at the joints of the gripper frame are higher than anticipated and strengthened accordingly. Based on the soil-structure interaction, the four-legged jacket structure is selected as the best concept, because its piles are further apart than for the tripod structure, thereby leading to minimal interaction between the piles of the gripper structure and the installed monopile. Still, both helical piles or suction bucket can be used as the foundation for jacket. A fatigue analysis shows that the gripper frame is subjected to cyclic loads that lead to high bending stresses at the joints leading to possible failure. Based on this, certain modifications have been made to the gripper structure to properly distribute the stresses.

A case study has been performed comparing the monopile installation by a floating vessel with and without seabed gripper. This case study shows that the time taken and cost associated with monopile installation using the jacket gripper structure is most economical using suction buckets. However, modification of the installation using helical piles may lead to time- and cost-reduction compared to using suction buckets. However, installation without using a seabed gripper is more economical compared to with using a seabed gripper.

From this thesis, it is thus concluded that a four-legged jacket structure with either helical piles or suction buckets is an optimal seabed gripper structure. However, it is not an economical solution to use seabed gripper for monopile installation for Van Oord.

Preface

Pursuing my masters in TU Delft and also doing my graduation in Van Oord, was one of the best decisions in my life. This thesis was a wonderful experience and a learning opportunity to develop my knowledge in offshore industry. This conceptual topic lead me to learn varieties of things

I would like to express my gratitude to Prof. dr. Andrei Metrikine, Ir. Jeroen Hoving and Ir. Ralph Luiken for being a part of my graduation committee and guiding me throughout my project. I feel grateful and my sincere thanks to Ir. Ralph Luiken, who gave me this opportunity to be part of the structural team and most importantly for guiding me throughout my project from whom I learnt a lot. I also would like to thank Ir. Jeroen Hoving, for guiding me as the university supervisor and spending time on me and giving feedback on my work. I would like to thank my whole structural team whom I worked with and especially Menno Jorna and Jori Kappen for guiding me and helping with my project and ANSYS.

Finally, I would like to thank my family for letting me pursue my dreams and continuously supporting me without any doubts. I deeply appreciate my friends both in India and Delft, especially Alexandra Kalpakoglou and Patrick Symes, with whom we did group studies and brain storming throughout our Masters which helped a lot.

It was a wonderful experience being in a foreign country and learning its people and culture. Without you all I would not be at this point, Thank you so much!!!

Deepakraj Thangaraju
Delft, January 2021

Contents

Abbreviations

MP	Monopile
VO	Van Oord
VOOW	Van Oord Offshore Wind bv
OW	Offshore Wind
WTG	Wind Turbine Generator
EPCI	Engineering, Procurement, Construction and Installation
MPT	Monopile Template
BFS	Bottom Founded Structures
FS	Floating Structures
HS	Hybrid Structures
NMS	Noise Mitigation System
MCA	Multi Criteria Analysis
GBS	Gravity Based Structure
CPT	Cone Penetration Test
GDP	Gentle Driving of Pile
AR	Advancement Ratio
SW	Self-Weight
MSL	Mean Sea Level
COG	Center Of Gravity
FEA	Finite Element Analysis
APDL	ANSYS Parametric Design Language
ULS	Ultimate Limit State
FLS	Fatigue Limit State
SCF	Stress Concentration Factor
DFF	Design Fatigue Factor
TP	Transition Piece

1

Introduction of the thesis

1.1. Van Oord

Van Oord is a leading international contractor specialising in dredging, marine engineering and offshore projects (oil, gas and wind). In 2007, Van Oord Offshore Wind bv (VOOW) was established as a separate business unit for Offshore Wind (OW) to perform all the activities related to offshore wind farm construction. VOOW are responsible for the Engineering, Procurement, Construction and Installation (EPCI) of many offshore wind farms in Europe. They are adapting the latest technology and operates the world's most advanced fleet, which constitute of specialised vessels and dedicated equipment and tools[1]. Van Oord also focuses on the environmental impacts during projects and innovates new technologies to reduce those impacts.

Engineering, procurement and construction (EPCI) of the entire offshore wind farm includes the design and installation of foundations, scour protection, infield cables, offshore high voltage substations, export cables, dredging/back-filling works, WTG installation and onshore works.

This thesis focuses on the foundation part of the EPCI process, where it deals with the installation of the monopile foundation using a seabed gripper.

1.2. Offshore wind turbines

Sustainability is a key factor in most of the government's energy policies. Wind energy is one of the major components towards clean green energy. Onshore wind farms are not appreciated due to site availability and public acceptance. Offshore conditions are favourable for wind farms as they have better wind characteristics and have more space. In countries like the Netherlands, Denmark, Germany, France, UK, etc. there are many offshore wind farms that are being built in the seas like North Sea, Baltic Sea, etc.

The monopile structure is by far the most common foundation concept for the offshore wind turbines, owing to the simple yet robust design by comparison with other foundation concepts; it is well suited to mass-fabrication and the installation method, based on conventional impact driving, is robust in most soil conditions [9]. Monopile diameter's of up to 10 m are claimed to be feasible in water depths up to 60 m [9]. However, larger turbines and deeper water will challenge the technical feasibility of the monopile, particularly as wave action will increasingly interfere with the dynamics of the turbine structure [9]. In this thesis, the monopile is taken

as the foundation for offshore wind turbines and focuses on stabilizing the MP during the installation into the seabed.

1.3. Traditional Installation of a monopile using a gripper frame

In current practice, monopiles are usually installed using a jack-up vessels or floating vessels.

Jack-up vessels have legs, which are lowered to the seabed when at the construction location. These legs have spud cans at their bottom, which penetrates into the soil. These penetrations are based on the soil properties and the spud can designs. The penetration of the spud cans must provide sufficient capacity for the vessel, so that the hull can be lifted above water and can do the operation with negligible disturbances. However, the waves hitting the legs can still limit the installation process. Preloading is then done to ensure the proper transfer of loads from the legs to the soil. After the monopile has been installed, the vessel is jacked-down and moved to the next location for another monopile installation.

Offshore wind industry tends to prefer jack-up vessels in higher sea states compared to floating vessel, as they provide stability and are easier to obtain verticality of the monopile due to the relatively negligible disturbances from the waves.

An example of the operation of the jack-up vessel is shown below and its schematic representation is shown in Figure 1.1 [1].

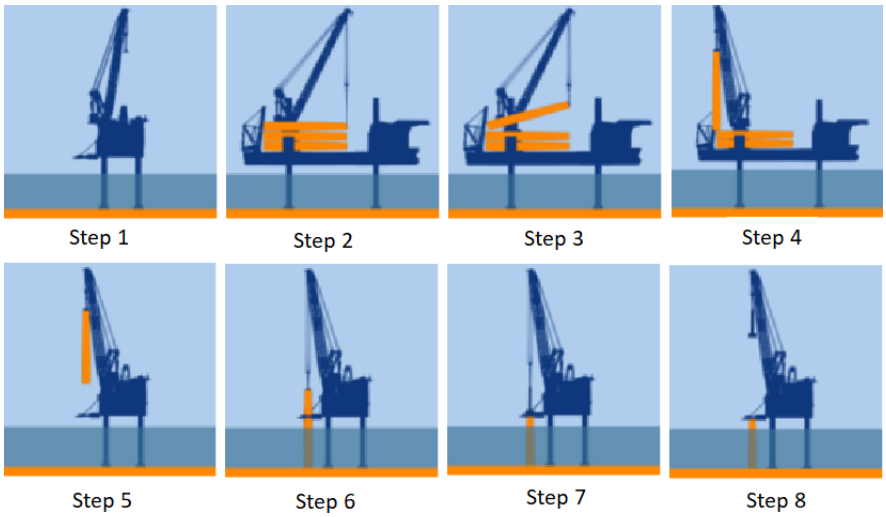

Figure 1.1: An example of the operation of a jack-up vessel[1]

The steps involved in the installation of a monopile using a jack-up vessel are[1]:

1. Jacking-up the vessel and installing the gripper frame.
    - First, the legs are lowered and preloaded.
    - While preloading, the legs penetrates the soil to certain depth until it provides sufficient capacity.
    - Meanwhile the gripper frame is slid to the side of the vessel and positioned.
    - After that, a Noise Mitigation System (NMS) (i.e. bubble curtains) is placed around the vessel.
2. Hook the monopile onto the lifting gear.

3. Up-end the monopile.
4. Monopile up-ended.
5. Slew monopile into position over gripper.
6. Lower the monopile into the gripper.
    - Initially, the gripper frame is fully opened to have an easier lowering of the monopile.
    - After lowering, the gripper frame is closed.
    - The arms in the gripper frame make the monopile vertical.
7. Placing the hammer on top of the monopile and driving to desired depth.
    - For some cases, when the hammer needs to pass the gripper frame, the frame is opened and the monopile is hammered to desired depth without use of the gripper. At this point, the monopile has sufficient penetration to stand vertically.
    - After hammering, the hammer and the noise mitigation system is removed and the gripper frame is slid back on-board.
8. Survey and demobilisation.

The operation of the floating vessel is the same as shown in Figure 1.1 except Step 1. In floating vessels, dynamic positioning system is used to ensure the vessel is in position throughout the installation of the monopile.

1.4. Monopile gripper frame

A traditional monopile gripper frame is a support structure on board the vessel which holds the monopile in position during installation. The monopile is held in place by the gripper frame using hydraulic gripper arms. Based on the design of the gripper frame, the hydraulic arms are placed at various locations, such that the force given by the arms makes the monopile vertical. An example of the location of the gripper frame and the installed gripper frame in Aeolus is shown in Figure 1.2 and 1.3 respectively.

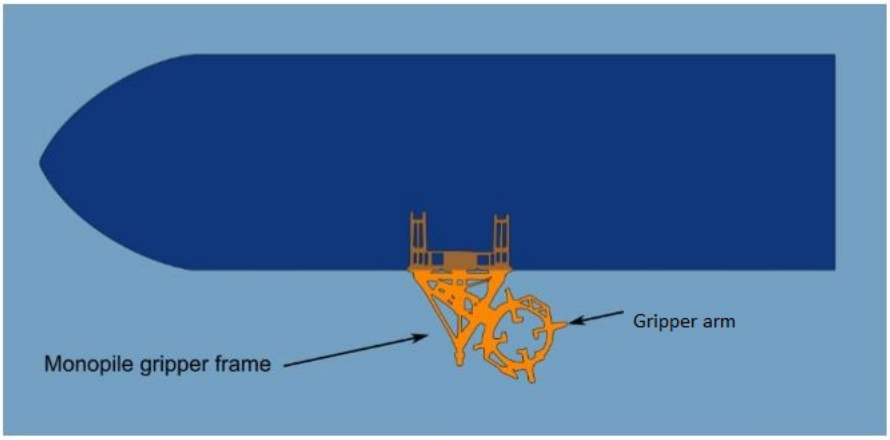

Figure 1.2: Location of the monopile gripper on the vessel Aeolus [1].

When the monopile is subject to environmental loading during installation, the monopile tends to incline. The initial inclination of the monopile while slewing into the gripper frame is

Figure 1.3: Gripper frame installed in the vessel Aeolus [1].

made vertical by an opposing force given by the gripper arm. After the monopile is vertical, the gripper arms simply hold the monopile in position, and the later environmental loading is transferred as a force applied to the gripper arm. This way the monopile stays in its vertical position, within the allowable tolerances, throughout the installation process.

The monopile is only restricted in its horizontal motion, not in its vertical motion. For this reason, rollers are attached at the point of contact between the gripper arm and the monopile. This allows rotations (with respect to vertical axis) and vertical translations yet restrict horizontal translations. If the gripper restricts vertical motion, it hinders the driving of the monopile.

The verticality is important for the installation of the wind turbine on top of the monopile.There is a certain tolerance in the inclination of the monopile based on the turbine manufacturer which should be complied during the monopile installation.

1.5. Future developments and challenges for future monopile installation

The future wind turbines are becoming larger and larger in terms of diameter and subsequently increasing the weight of the monopile. As mentioned in Section 1.2, larger turbines and deeper waters will have a significant effect on the size of the future monopiles.

Currently, jack-up vessels are used widely as they are not significantly affected by waves and have a smooth installation without any motion in the gripper frame. However, jack-up vessels have certain limitations in their operation for future turbines. The depth at which the vessel can be used to install (depends on the length of the jack-up legs) and the weight it can lift (depends on the load carrying capacity of legs and crane) is limited based on the size of the jack-up vessel. Bigger jack-up vessel is needed for the future monopiles, which is more expensive than the smaller jack-up vessels. They are also prone to earthquake loads.

Van Oord decided to look into the possibility of using a floating vessel. Floating vessels can operate at deeper waters as they are uncoupled with the seabed and also less vulnerable to earthquake loading. Floating vessels can lift higher loads by ballasting the hull of the vessel, if the crane capacity allows to lift such weight. The limitation of a floating vessel is that the gripper is located on the vessel. The gripper moves with the vessel which does not provide the necessary stability to the gripper frame and affects the verticality of the monopile. This makes the weather window of the floating vessels much smaller than that of jack-up vessels with regards to wind turbine installation.

To overcome the two criteria of operating in larger weather windows (due to increased operability) and to lift larger loads, Van Oord has two solutions. They are:

- To use a floating vessel with a motion compensated gripper on the vessel
- To have a gripper on the seabed in which the gripper and vessel motions are uncoupled.

In this thesis, an optimized design for a gripper on the seabed is investigated.

1.6. Objective of the thesis

The main goal of this thesis is an optimal design of a seabed gripper structure for the installation of a monopile foundation, to ensure the verticality of the monopile during installation and in addition is easy to install, remove and reuse.

The focus of the research is the structure/frame of the seabed monopile gripper and its interaction with the soil, such that it can easily be installed, removed and reused. But, the design of the hydraulic arms and the rollers present in the gripper frame are not included in this research; optimising the geometry and structural integrity of the gripper frame is included in this research. The working principal of the hydraulic system with the rollers is adopted from the previous projects within Van Oord.

1.7. Methodology and Outline of the thesis

This section describes the steps that are involved in this thesis. The steps and the methodology involved is shown below and referenced to the corresponding chapters.

First, a literature study is done to identify the different concepts that are currently in practice, with regards to substructures and foundations. Based on findings from the literature (Chapter-2) and adapting to the requirements from Van Oord (Chapter-3), the feasible concepts are proposed (Chapter-4). Conceptual designs for these proposed concepts are made and their advantages and disadvantages are identified. A Multi Criteria Analysis (MCA) is conducted to distinguish the most optimal concept and to select the most promising one, which is explained in detail in Chapter-4.

Secondly, the preliminary design of each concept is laid out in Chapter-5. The loads acting on the monopile is found first to identify the magnitude of load that is transferred from the monopile to the seabed gripper. Next, the gripper frame is designed. In this thesis, only the position and the placement of the gripper arms and rollers are designed, not the complete design of the hydraulics and rollers involved in the gripper arms. An optimal arrangement is done such that the monopile wall does not deform from the force given from the rollers. The preliminary design of the selected concepts consists of member sizing and arrangement and calculations for the expected environmental loads acting on the seabed gripper concepts. The environmental loads acting on the monopile and the seabed gripper are calculated using the

equivalent stick model approach. Then, their respective foundation reactions are found based on these loads. These reactions are used to design the foundation of each respective concepts.

Afterwards, a Finite Element Method analysis is carried out in ANSYS, a numerical software package, to find out the response of the structure to these loads. This is shown in Chapter-6. The seabed gripper structure is optimized based on the stresses induced due to the loads acting on it and its response. Once the seabed gripper structure is designed, the next step is to look at how each of the optimal designs are interacting with the soil. This can be found in Chapter-7. The seabed gripper foundation which has the least interaction with the monopile and vice versa is selected.

Next, fatigue analysis is done to identify the number of installations and removals the seabed gripper can be used for and optimise it based on the required number of cycles. The design of the seabed gripper is optimised based on the response from the fatigue loads as shown in Chapter-8. A case study of the entire operation (i.e: time and cost involved) involved in the installation, removal and reuse is done for the final design of the seabed gripper. The best design is related back to the MCA with the main considerations being economic and time value. Thereby, outlining the final design which is presented in Chapter-9.

Finally, this thesis is concluded by summarising the final design of the seabed gripper, the important points from each chapter and the necessary recommendations for future research as discussed in Chapter-10.

2

State-of-the-Art of different concepts

For the initial phase of the thesis, the first step is to come up with some concepts to hold the gripper frame in position underwater which is also easy to install, remove and reuse. The concepts include both the support structure and the foundations. To understand the different support structures and foundations, a literature study has been done for different concepts that are currently in practice in the offshore industry both in oil & gas and wind. First, the different support structures is discussed in section 2.1 followed by different foundations in section 2.2. In these two sections, the different support structures and foundations are discussed in general along with the changes that can be adopted to design a seabed gripper.

2.1. Support structures in offshore industry

Offshore structures are either permanent or temporary depending on the purpose they serve[33]. Permanent structures are intended to stay on a location for many years. For example, in the oil and gas industry, an offshore structure typically designed for around 40 years to ensure maximum extraction of the fossil fuels beneath the seabed. On the other hand, temporary structures are intended to perform a specific task during a limited period of time. These structures are moved from one location to next and perform similar activity at each location[33]. A traditional and typical example of this is the offshore drilling jack up rig. However, more recently the offshore wind sector have required a wide array of temporary structures due to the repetitive nature of installing many wind turbines in close vicinity at a wind-farm. In this thesis, the seabed gripper template falls under this temporary structures category.

The offshore support structures are classified into two categories, namely, **Bottom Founded Structures (BFS)**, **Floating Structures (FS)** and **Hybrid Structures (HS)**. Bottom founded structures are fixed on the seabed, while the floating structures are connected to the seabed through mooring lines and the hybrid structures are a combination of both the bottom founded and floating structures. The main purpose of this thesis is to have a gripper on the seabed, which means a bottom founded structure.

Bottom founded structures can be categorized into five basic types based on their structural configuration:

- Monopile structure
- Tripod structure
- Jacket structure

- Gravity based structure
- Tripile structure

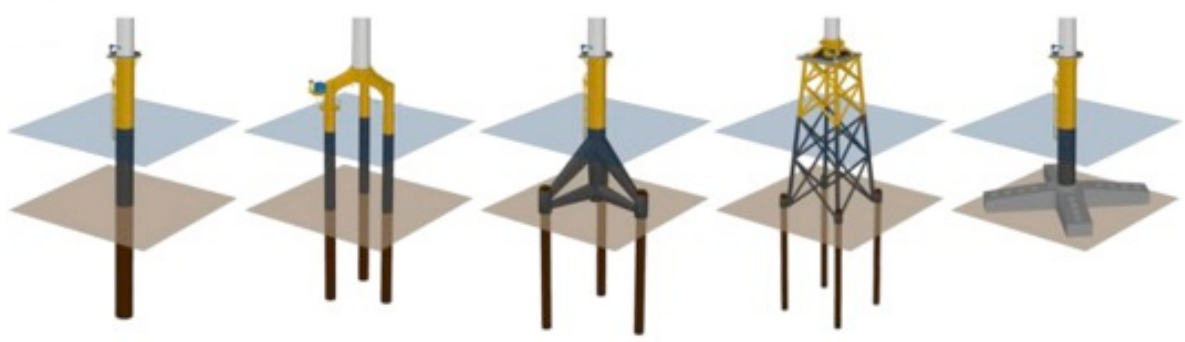

Figure 2.1: Example of bottom founded structures. From left to right: Monopile, Tripile, Tripod, Jacket and Gravity base [57]

In the following subsections, the various substructures both modern and traditional choices are outlined. As the thesis is about installing a monopile using a seabed gripper structure, a general overview of the monopile is given. This is to understand the different components involved in the monopile structure, that need to be consider while designing the seabed gripper structure.

2.1.1. Monopile

A monopile is a large tubular structure consisting of numerous circular shells (cans) that are welded together. A monopile is mostly used as a foundation for wind turbines. Typically, a monopile extends from the base of the wind turbine tower, underneath the water and then deep into the seabed [60]. It is considered as both the sub-structure and the foundation. To connect the wind turbine tower to the monopile, a transition piece is used in between them. Transition piece is used to connect monopile with tower and serves as an access for maintenance, for cable connection, corrosion protection, etc. An illustration of a monopile with a transition piece and scour protection is shown in figure2.2

The tower and the transition piece are typically connected by bolts and the transition piece is connected to the monopile by grouting the void space between the shells or by using bolted connection[42]. However, there is a new connection called slip joint which was successfully installed by Van Oord in April 2020 [1]. Slip joint connection is done by sliding the transition piece over the monopile as shown in figure 2.3, like sliding one coffee cup over the other. The capacity of the connection is achieved by clamping and friction between the transition piece and the monopile, without the need of grout connection. The same can also be done for tower over the transition piece. Originally, the main idea behind the slip joint is to neglect the transition piece and directly connect the monopile with the tower. Now, it is used to split the heavy weight of the MP. This new connection will lead a way to easy and cheaper installation of the tower over the monopile. The other advantage of the slip joint is that the strength of the connection increases over time. During operation, the tower and transition piece will settle more over the monopile due to its self weight [1].

In the future, there is a high chance of slip joint being used in the majority of the wind farms. When using slip joint connection, the length of the monopile is reduced which is one of the advantages of using slip joint to reduce material and fabrication cost [1]. This is because

Figure 2.2: Monopile with transition piece and scour protection [61]

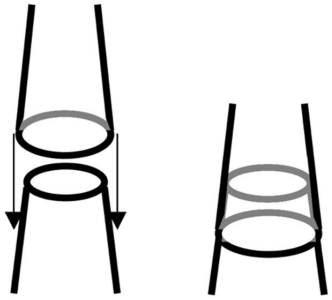

Figure 2.3: Illustration of slip joint connection [59]

the slip joint can be used underwater and will lead to an optimized design of the monopile and transition piece or monopile and tower in terms of length and weight. This may lead to difficulty in the installation of the monopile using a gripper on the vessel. When the hammer needs to pass the gripper frame, the frame is opened and the monopile is hammered to desired depth without the use of the gripper. At this point of opening, due to reduced length of the monopile, the capacity of the monopile to stand by itself may not be achieved. In this case, the use of seabed gripper structure will be more beneficial and accurate.

The vertical loads are transferred to the soil through wall or skin friction and tip resistance. The overturning moment of the monopile is resisted by the horizontal resistance from the soil [60]. The diameter and thickness of the monopile depend on the water depth, lateral loads and seabed conditions to provide enough stiffness. The monopiles are generally installed in the soil by hammering at the top of the monopile. In some cases, vibratory hammers are used instead since the noise emissions are lower. For rocky soil, drilling is needed to penetrate the monopile in the soil before hammering. There may be plugging of piles based on the soil condition the monopile is installed in. During penetration of the monopile, plugging happens when the inner friction of the monopile is large enough to prevent further soil intrusion. If plugging happens only the outside wall friction is taken to contribute to resisting the vertical loads.

Scour protection

Due to the currents acting on the monopile, the soil on the seabed gets eroded. The erosion makes a big hole around the wall of the monopile over time. Erosion is reduced by placing scour layer around the monopile. Scour layers consist of stones and rocks laid around the monopile. There are typically two layers of scour protection around the monopile. The first layer is called the filter layer which consists of small stones and the second layer is the armour layer with large stones or rocks [1]. The diameter of the surface area of the laid filter and armour layers are generally around 3 and 5 times the diameter of the monopile respectively [1].

Normally the scour protection is installed first and the monopile is installed afterwards [1]. This is to install the scour layer easily without the interference of the monopile and also to save time while the monopile is fabricated. However, the installation of the monopile depends on the size of the stones used in the armour layer of the scour protection. If the design of the scour protection tends to have big rocks as its armour layer, the monopile can get damaged in the installation procedure. This is because, while hammering the monopile, the wall of the monopile may deform when hitting the rocks of the armour layer. Depending on the armour rock size, the armour layer may be installed after the installation of the monopile.

The scour protection will play a role in the design of the seabed gripper, as the foundation of the seabed gripper maybe difficult to install in the armour layer. It will be better to have the foot print of the seabed gripper to be within the filter and armour layer area. Apart from the gravity base foundation, which will be placed on the armour layer, other foundations will be difficult to install. As the foundations need to pass through the armour layer which maybe hard and also damage the walls of the foundation because of the big rocks in the armour layer.

Monopile structure

Advantages	Disadvantages
Simple and quick fabrication process	Limitations due to heavy installation equipments (hammers)
Proven Concept	Large scour protection required
No seabed preparation required	Flexible water depths
Lower price per ton of steel	Limited to large water depths
	Difficult to remove after design life

Table 2.1: Monopile - Advantages and Disadvantages [43]

2.1.2. Jacket structure

Jacket structures were among the first to be implemented in the oil and gas industry and are still widely used to this day. By definition,

”Jacket type substructure is a substructure, made of a tubular space frame, providing support for a superstructure with all or some of the foundation-piles inserted through the legs and connected to the legs at the top of the structure”[33][34].

”Tower type substructure is a substructure, made of a tubular space frame, providing support for a superstructure with all or a number of the foundation piles inserted through and connected to sleeves around the legs at the base of the structure”[33][34].

The schematic representation of both jacket type and tower type substructure are shown in figure 2.4. In practice, both the jacket type and tower type are usually called as Jacket structure. Normally, the structure has three or four legs, however, they can have more depending on the design. The legs are connected by tubular braces to have a proper load transfer which makes the structure stiffer. All the members of the structure are tubular and they are welded together. Sometimes these tubular members are connected via plates at the joints to reduce peak stresses and hence, the lifespan of the structure in terms of fatigue failure. The fabrication of a jacket structure is complex and consumes more time as there are large number of connections between all of the tubular members.

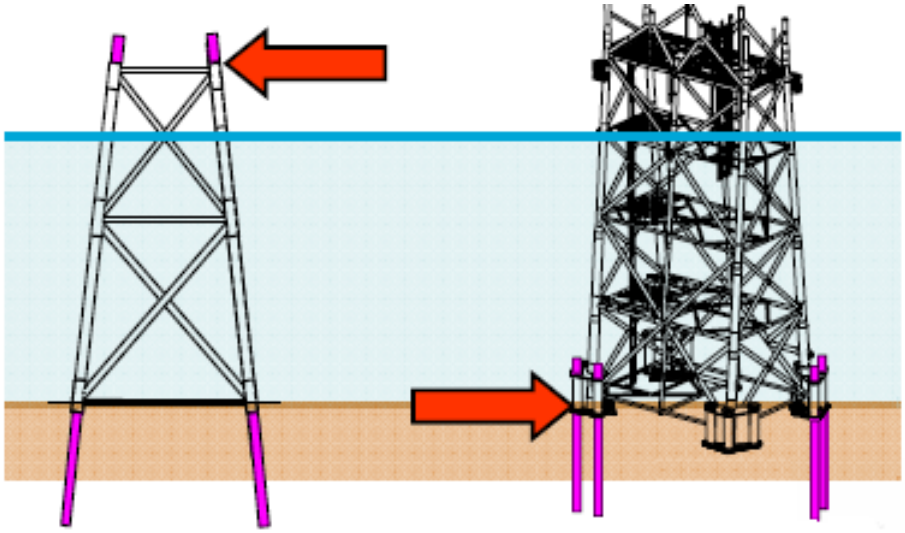

Figure 2.4: Schematic representation of a jacket type (left) and tower type (right) substructure[34]

The bracing connecting the main legs have different configurations based on the needs of the design. The typical configurations that are used in practice are shown in figure 2.5.

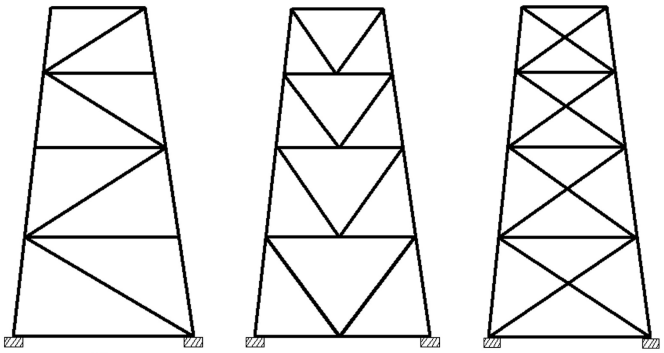

Figure 2.5: Different types of bracing. From left to right: Diagonal bracing, K bracing, X bracing [43]

Depending on the function of the jacket structure, each leg is either loaded in tension or compression. Usually piles are used as the foundation for the jacket structure which transfers the loading to the seabed. Nowadays, suction buckets and also other techniques are used as foundations for a jacket structure.

There are two methods of jacket pile installation, post piling and pre-piling. Post-piling method is the traditional way used in the oil and gas industry. For jacket type substructure, the structure is placed on the seabed and the pile is inserted inside the jacket's main legs and is hammered. The connection between the leg and the pile is done by concrete grouting and welding the top of the pile and jacket leg with the help of shim plates [34]. As the top of the jacket structure is above water it will be easy to weld between the pile and the jacket leg. For tower type substructure as seen from figure 2.4, the jacket legs are attached to pile sleeve at the bottom. The piles are inserted into the pile sleeve and hammered. The pile sleeve with the pile is grouted to ensure proper load transfer from the jacket to the pile and to the soil.

For pre-piling method, the piles are installed first with the help of piling template. The jacket structure is then placed over the installed piles on the seabed. This method can only be adopted to tower type structure. The piles must be vertical to allow the jacket to be installed after the piles. The jacket leg with the pile sleeve and the pile is connected by grouted connection.

Pre-piling method is widely used in the offshore wind industry. This is due to the number of repeated installations of the wind turbines. It is economical to install the piles by first using smaller vessels and the jacket structure is then installed using a bigger vessel at a later stage.

In this thesis, the gripper support structure should be easy to remove and reuse. As a result, it will not be feasible to use grouted connection between the jacket legs and the pile, as they need some time to set to have full loading capacity. Also the connection needs to be removed after the support structure served its purpose. Therefore, a new type of connection is needed which is easy to install and remove providing full loading capacity.

Typically, the legs of jacket structure are connected by bracing in all the sides. It will be difficult to remove the jacket structure after the installation of the monopile as all the sides are closed. To remove the jacket structure, it should be lifted above the monopile, which is difficult to lift and may damage the wall of the monopile. For this purpose, one side of the jacket structure can be left open to have easy installation and removal. This will be a new type of jacket structure, as there is no jacket structure which has been designed for one side open. This will be a challenge in the designing phase of the jacket structure.

Jacket structure

Advantages	Disadvantages
Light weight and stiff structure	Complexity of fabrication
Better global response comapred to monopiles	Large number of joints required comapred to other lattices structures
Economically viable on transistional water depths	Logistical issues due to templates (prepilling case)
No scour protection required	
Structural redundancy	
Low soil dependency	
Good response to wave loads	

Table 2.2: Jacket structure - Advantages and Disadvantages [43]

2.1.3. Tripod structure

Offshore tripods are structures with three legs made of shell structures as shown in figure 2.6. The thickness of the legs is small compared to the diameter of the leg, relative to other offshore structures. The three legs are connected to a main tubular member at the center. There are fewer members in the tripod structure than that of a typical jacket structure. However, the tripod typically have much larger member diameters. Like the jacket structure, the force acting on the tripod, load each leg in either tension or compression. The foundation of the tripod use piles, suction buckets or other forms of foundations (later discussed) which are effective in transferring the axial loads to the seabed. The legs are well spread out, which increases the moment carrying capacity of the structure [24].

As mentioned for jacket structure, one side of the tripod structure can be left open for easy installation and removal of the tripod structure.

Figure 2.6: Tripod substructure to support offshore wind turbine

Tripod structure

Advantages	Disadvantages
Light weight and stiff structure	Complexity of fabrication
Better global response comapred to monopiles	Limitaions of transportation due to width
No seabed preparation required	Slow fabrication process
No scour protection required	Impractical in shallow waters
	Main joint susceptible to fatigue

Table 2.3: Tripod structure - Advantages and Disadvantages [43]

2.1.4. Gravity based structure

Gravity based structure (GBS) stabilize the substructure by providing a huge self-weight at the base of the substructure (whether a tripod, jacket or monopile). An example of a gravity based structure is shown in figure 2.4 [63]. This solution is most suitable for shallow water

depths. The foundation is usually prepared onshore and a remade of reinforced concrete, steel or composite material. The sea bed requires preparation before the GBS can be sunk. The GBS is sunk by ballasting foundation with water, sand or gravel. Perhaps the main advantage of a GBS is the material and construction costs are generally low. Since this thesis focuses on a temporary works solution for supporting a monopile while it is driven, it is important to note the installation time. A GBS is installed on the seabed relatively quickly compared to other concepts, however, it is quite dependant on the sea condition. Rough conditions cause instabilities and therefore there is usually a small weather window for installing gravity based structure.

Table 2.4: Gravity based structure - Troll A platform [63]

Gravity based structure work to balance the overturning moment through their enormous self-weight where the load is transferred through the foundation's base line. The dead load must be large enough to prevent uplifting, sliding and tilting. This means that the soil at the site is of key consideration. For a generalised temporary works solution, this foundation may have too many limitations attached to it, however, it certainly has some attractive benefits too, as seen in table 2.5. However, as the scour layer will be placed already, the GBS can be placed over it. This will increase the bearing capacity of the soil, so that the GBS can be installed.

Gravity Based Structures

Advantages	Disadvantages
Reduced fatigue sensitivity compared to other concepts	Limitations of transportation and installation due to high self weight
Low environmental impact due to the absence of piling during the installation	High production cost
Low levels of corrosion protection	Challenging logistical requirements
The structure can be floated	Require seabed preparation for some sites
Long life time	Not suitable for soft seabed surfaces

Table 2.5: Gravity based foundation - Advantages and Disadvantages [43]

2.1.5. Tripile

A tripile is a new structure that has been interpreted from the monopile concept. A tripile has three individual piles installed which are connected together using a transition piece with three inserts. A tripile structure is used as a sub structure for wind turbines yet is often considered as both the substructure and the foundation (much like a monopile). The length of the three individual piles is changed according to the site conditions. This makes this solution applicable to overcome different water depths and uneven seabed profiles[43]. The installation of the transition piece requires a high degree of accuracy to fit inside the pile [43]. Sometimes a piling template is adopted to increase the accuracy of installation. The figure 2.7 shows the complex transition piece that will be inserted into the three piles. The connection between the transition piece and legs is done by grouting.

As mentioned for jacket structure, one side of the tripile structure can be left open for easy installation and removal of the tripile structure.

Figure 2.7: Transition piece of the tripile substructure[58]

Tripile structure

Advantages	Disadvantages
No bolted or welded connection between piles and transition piece	Complexity of transistion piece manufacturing
Easily adjustable to water depths	Complexity of transistion piece installation
Loads transferred by the grout alone	
Compact construction relatively cost-effective	
All connections above water surface	
Less dependency on weather conditions	

Table 2.6: Tripile structure - Advantages and Disadvantages [43]

2.2. Foundations in offshore industry

The offshore structures can be described based on the type of foundations used in the construction. These foundations consist of:

- Pile foundation
- Gravity base foundation
- Suction bucket foundation

The soil conditions found in offshore sites have a wide range of soil particles from clay to boulders. The choice of foundations depends on the soil conditions and therefore a good site investigation is required. The investigations are mainly based on cone penetration test (CPT), soundings and drilling to collect samples and laboratory sample testing. The North Sea seabed consists of mainly of highly over consolidated soils combined with some sand deposits in the top layers. [41]. Over consolidated soils refer to a soil that has experienced large stress than the current stress.

The choice of foundation is related to the magnitude of overturning moment with respect to the seabed, which is directly proportional to the water depth.

There is a variety of foundation concepts that are available for offshore structures. The selection of the most suitable foundation concept is dependent on the function of the substructure. In the case of a monopile structure, the monopile must resist an overturning moment [42] from the lateral capacity of the soil. Whereas, for a jacket substructure, an overturning moment is predominantly resisted axially by the soil. Koteras (2019), discusses the main differences between the foundation choices for a monopile. However, in this thesis, the foundation to be supported by the gripper frame is predefined as a driven monopile. A brief outline of the three foundations mentioned above will be discussed below, with respect to the seabed gripper support structure which will support the monopile while it is driven.

2.2.1. Suction bucket foundation

A suction bucket foundation (or suction caisson foundation) consists of a thin steel cylinder with an open bottom and a sealed top (figure 2.8) [42] [46]. The cylinder, which penetrates the soil, is called the skirt and the top is the lid. The installation of a suction bucket is accomplished in three steps: lowering, self-weight penetration and suction penetration. Initially, the bucket is lowered in the water until it touches the seabed (touchdown). This operation should be done in a very controlled manner so that the bucket lands vertically on the seabed. Penetration initiates due to the weight of the bucket. Afterwards, the suction penetration starts, which involves the pumping of the water trapped in the bucket. In this way, the under pressure in the bucket is enabled, resulting in the development of an earthward force pushing the caisson into the soil. Once the final penetration depth is reached, the pump is closed by a valve, sealing the foundation with the soil [42].

As water is pumped from the caisson, a flow is induced around the skirt (Figure 2.9). This flow is related to the development of pore pressure around the foundation, resulting in the drained soil response [42]. Water flows in the soil towards the inside of the bucket. The upward flow inside the bucket creates a hydraulic gradient that reduces the vertical effective stress leading to the reduction in friction. Evidently, it concluded that the successful installation of the suction buckets occurs in soils with high permeability.

Figure 2.8: Foundation bucket concept [42].

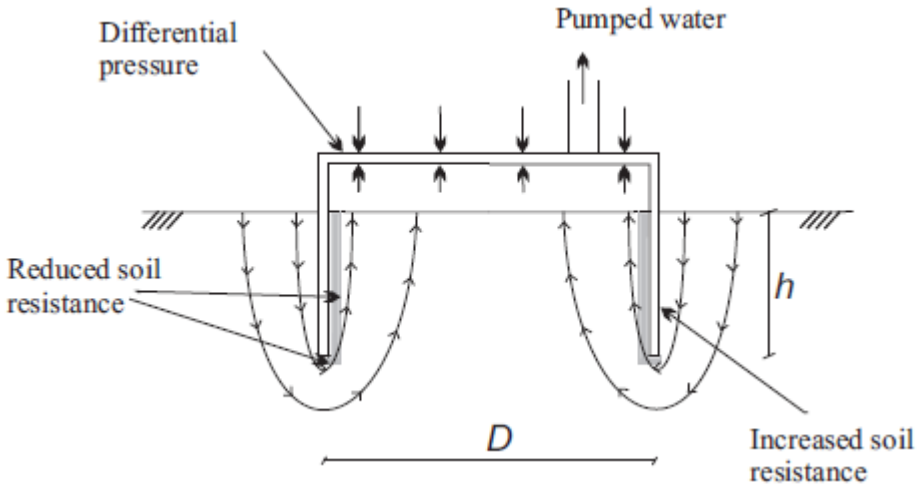

Figure 2.9: Schematic representation of the suction bucket penetration. Seepage around the skirt [42].

In this thesis, as the main goal is to have less total time for the intallation, removal and reuse of the structure, suction bucket has an advantage over the pile foundation. The suction pressure will be applied simultaneously to all the buckets present in the structure. This will have less installation time unlike pile foundation, where each pile will be installed one by one based on the number of legs present in the seabed gripper structure. However, there are some limitations while installing a suction bucket which is discussed below. The advantages and the limitations need to be fully analysed and considered for the next upcoming phase of the project.

Several limitations in the installation of the suction buckets have been identified [42]. First of all, a limiting factor is the cavitation pressure. The cavitation pressure increases with water depth. ”The allowable pressure before the cavitation limit is reduced due to the pump capacity” [42]. Secondly, the induced high load difference between the inside and outside of the skirt

during suction, may lead to buckling failure. Buckling has a detrimental impact on both the installation and operation of the foundation. Other limitations are the piping failure and the seabed topography. If a critical suction is exceeded then piping channels are created at the circumference of the skirt, which breaks the sealed connection between the foundation and the soil. As a result, the pressure between the inside and outside of the bucket is identical, causing the penetration to stop. Regarding the seabed topography, if the soil consists of layers (especially clay below sand) then there is the risk of soil plug. This stops the installation before the required penetration depth is reached.

Various methods exist to properly install the suction bucket in difficult soil conditions. For soil where the penetration resistance is higher, nozzles can be used to jet water alongside the skirt tip. The water from the nozzle, causes liquefaction for sand or remolding of clay, reducing the tip resistance [42]. Cotter (2010)[53] studied the water injection at the skirt tip of the suction bucket. The water injection reduces the suction needed and the reduction is proportional to the pressure of the water jet. The injection of water did not cause any piping failure even for high injection pressure.

Another method is a repeated process of applying pressure and stopping. This is called cyclic penetration. Over-consolidated clay becomes remolded due to this process, which also reduces the friction on the skirt [42]. In sand, the soil dilates at the skirt tip due to unloading.

Another method is to add weight (i.e. sand bags) to the structure which ensures the sufficient self-weight penetration in very stiff clays. For sands, very high suction pressure can be avoided which may result in piping failure.

However, there are many hazards and mitigation measures, which are discussed in detail in ”Suction Installed Caisson - Foundation for Offshore Wind: Design Guidelines”[26]. The table 2.7 shows the several hazards (mode of failure) and the suggested mitigation methods.

Hazard	Mitigation
Piping or ratholing	Pause operations Remedial seabed works Backfilling holes Ballasting
Shallow obstructions	Tip injection Ballasting Pressure cycling / Pressure shock
Tilting	Tip injection Eccentric loading Multi-chamber design
Soil plug failure	Pause operations (no underpressure) Retrieval and reinstallation Pressure cycling

Table 2.7: Installation hazards and suggested mitigation methods [26]

Although, there are many criteria to account for to design a suction bucket, they have many advantageous characteristics. The main ones are low cost, less installation time and that they are reusable. Shchucheng Jin (2014) [19] investigated the group effect of the multi-bucket foundation, which proves that the ultimate bearing capacity of a four bucket foundation is nearly 2.4 times than the single bucket foundation [19]. However, the vertical bearing capacity is not equal to the sum of the single bucket's bearing capacity [19].

For a tripod bucket foundation in clay soil, the bearing capacity is influenced by the penetration depth of the bucket and the bucket spacing [24]. The length-diameter ratio of the bucket influences the group effect of the tripod bucket foundation. The vertical bearing capacity due to the group effect is negligible[24]. With an increase in spacing between the buckets, the horizontal bearing capacity increased significantly and converged at a constant value, whereas the moment bearing capacity increased continuously [24].

Koohyar Faizi (2019)[25], investigated the behaviour of a model hybrid tripod suction bucket as shown in figure 2.10. The hybrid tripod suction bucket provides around a 25% - 100% increase in the overturning moment capacity depending on the diameter of the mats and the spacing between the buckets [25].

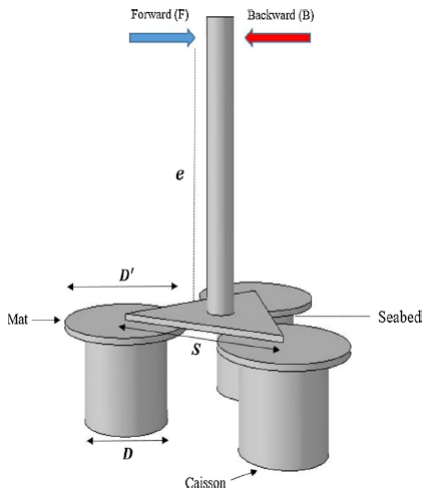

Figure 2.10: Hybrid three suction bucket with mat foundation[25].

2.2.2. Pile foundation

Piling is a type of deep foundation which is simply a slender column inserted into the soil. For offshore purposes, piles are mostly made up of steel, however, sometimes composite materials are also used. Pile foundations are used when the top layers of the soil can not provide enough bearing capacity (for example, in suction bucket). The piles can be penetrated to a certain depth where the bearing capacity is high. The loads are transferred from the pile to the soil through end bearing and skin friction. Since the diameter of the pile is less compared to suction bucket or monopile, it is not so good with resisting horizontal forces. Piles are good in taking both tension and compression force.

There are different types of installing a pile offshore and are listed below.

1. Driven piling
2. Screw piling

2.2.2.1 Driven piling

The most commonly used techniques to drive piles are impact driving and vibratory driving. There are a few new techniques that are in their developing stage such as Blue piling (impact driving) and Gentle driving of piles (vibratory driving).

Impact driving

To date, most of the offshore piles are driven by impact. Hydraulic hammers are used to deliver a series of blows to the top of the pile making the pile gradually penetrate into the soil. The installation time taken for the pile depends on the pile dimensions, soil conditions and the input energy of the hydraulic hammer. For a monopile, usually it takes hundreds or even thousands of hammer blows to install the pile properly [44]. Some of the advantages of impact driving are it is a very reliable method which has been used for many years in the offshore industry. The desired depth can be reached with impact driving except in few cases where there is boulder or very high resistance from the soil.

However, the use of impact hammers is not good for the environment, as the sound waves generated during impacting will transmit through the soil and water and disturbs marine life. To reduce this, noise mitigation techniques are used to reduce the intensity of sound waves. The different types of noise mitigation techniques are:

- Bubble curtains (Single or double)
- Hydro sound Damper
- Noise mitigation screen
- Cofferdam

The impact force induces high stresses within the pile which causes more fatigue damage and leads to expensive foundation piles.

On the contrary, the new impact driving BLUE piling technology offers a low-noise pile driving solution. The principle of BLUE piling is that," a column of water is pushed up by the combustion of gas mix, which then falls back down by force of gravity and strikes the monopile"[62]. The fatigue damage of the pile is also reduced because the impact time is long and spread out, causing the reduction of peak stresses during hammering. However, BLUE piling technology is in its developing stage, which may be seen in the future installation.

Vibratory driving

The vibratory driving is implemented by the use of vibratory hammer. The working principles of vibratory driving is to impart longitudinal vibratory motions on the pile to reduce the soil resistance to penetration [47]. Based on the broad experience from the past, vibratory driving offers outstanding options to install driven piles (particularly into wet granular soils) [35]. In the correct soil conditions, vibratory driving has various advantages over impact hammers, as mentioned by Saleem (2011)[48]:

- Three to four times faster installation than the impact hammering
- The vibratory hammers needs less energy and time to install the piles which directly leads to lower costs.
- The vibratory process can be adopted for installation, removal and reinstall piles.

- Low noise emission. The noise created during the installation is less compared to the impact hammering. Approximately 15 - 20 dB of noise level is reduced when using a vibratory hammer and can be higher based on pile and soil condition.

On the contrary, vibratory driving have few disadvantages. The most importantly, the reliability of the bearing capacity obtained from vibrodriven piles.

A comparative study between the impact driving and vibratory driving has been done by Deep Foundation Institute (DFI) and the summary is listed below [35].

- From a number of studies, on an average the vibrated piles has 80% of the axial capacity compared to the impact driven piles. Some tests show results as low as 50% of the capacity of impact driven piles.
- The reduction in capacity is a combination of both shaft and tip resistance.
- The axial resistance of the vibrated pile depends on the properties of the hammer used. Low frequency with low penetration piles seem to have higher axial capacity. However, to avoid refusal of pile, high frequency with high penetration is beneficial.
- Not many studies have been done to understand the lateral capacity of the vibrated piles. Data from two studies show that there is no influence on the lateral capacity of the piles. However, the results need to be applied with caution.

The new technique of Gentle driving of piles (GDP) is in the research stage and has been tested offshore for small diameter piles. The principle behind the GDP, is to simultaneously apply low-frequency and high-frequency vibrations which exerts two different modes of motion on the pile. The main aim of the research is to develop this new method for monopiles, but this can also be used for small diameter piles like jacket pile foundation.

Both the driven piles and screw piles have both advantages and disadvantages. For impact driven, it is not environmental friendly, but is used in most of the pile foundation. Vibratory pile and screw pile are silent when compared to the impact driven pile. But the installation of piles using vibration will reduce the strength of the soil around the pile.

The type of piling can be adopted based on the soil condition of the project site. For example, for very hard soil impact driving can be adopted, as the vibratory and screw piles are difficult to install in hard soils. For soils less than hard soils, helical piles can be adopted as they are easy to install in these type soil.

2.2.2.2 Screw piling

Screw or helical piles are piles with one or more helix shaped bearing plates welded to the central shaft as shown in figure 2.11. The diameter of the shaft is small compared to the diameter of helix.

Helical piles are one of the oldest foundations used in the offshore environment. The first recorded use of helical piles dates back to 1836 by Alexander Mitchell. He used the helical pile for moorings and later applied it to Maplin Sands lighthouse in England in 1838 [49]. The lighthouse operated for more than 90 years until it collapsed in 1931. The foundation was undermined due to scour leading to failure. After the pioneering work from Mitchell, helical piles were used for a large varieties of offshore and onshore structures. The use of offshore helical piles is not widely used nowadays. However, the characteristics of the helical piles tend to be suitable for the multi-legged offshore wind turbine application [12]. For the multi-legged structure, the load carrying capacity is mainly through tension and compression, where the helical piles are better at carrying these loads compared to normal piles.

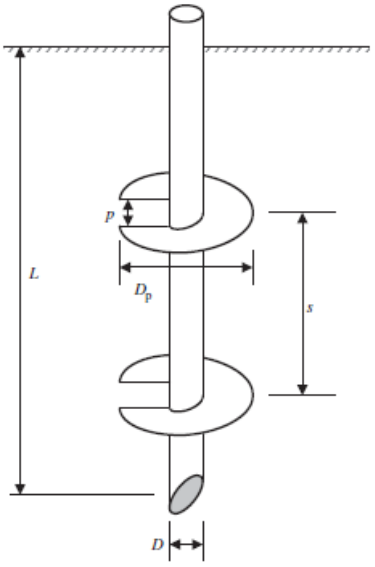

Figure 2.11: Geometrical parameter of a helical pile[12].

Helical piles are effective at transferring axial loads from the structure to the soil. The load carrying capacity is determined by the bearing capacity of the plates and the shaft skin friction. For the loading condition of offshore wind turbines, both the helix diameter and its overall length are substantially larger compared to those used onshore [12]. For lateral capacity, the diameter of the main shaft near the soil surface is increased by using a winged sleeve or a skirted collar, where the vertical plates provide additional lateral resistance [12].

For onshore applications, modular type helical piles are used, where an extra shaft is attached to the main shaft with or without a helix based on the load carrying capacity needed [14]. Modular foundation systems are also being developed for the offshore application of helical piles [12].

Helical piles are installed by screwing, rotating or torquing into the soil while applying little vertical force at the top of the pile. The helical pile is easily removed by unscrewing. The torque motor used to screw the pile is relatively quiet compared to the impact piling. The measurement of the torque during installation is used to find the pile capacity from the relation given by Hoyt and Clemence (1989) [50].

Existing industrial guidelines for the installation of screw piles show that the piles should be installed in a pitch-matched manner to avoid disturbance in the soil to increase the in-service performance of the helical pile [14]. Pitch-matched manner refers to the rate of vertical advancement of the pile per rotation, that depends on the distance between the helix leading edge and end of the helix [52]. Pitch-matched installation results in an advancement ratio (AR) of 1, given as the ratio of vertical displacement per rotation by the geometric pitch of the plate [52].

In a recent study, October 2020, the in-service performance of a single screw pile has been investigated using Discrete Element Method in sand of different relative densities [51]. The study compares the pitch-matched (AR=1) and over-flighting (AR<1), to assess the in-service capacities both in tension and compression. Some of the key factors from the study are shown below, which are useful for the design and installation of the screw piles.

- With over-flighting, the installation force required is reduced up to 96%, which makes it

possible to install the helical pile under its self-weight.

- The installation torque is less affected by AR. However, by over-flighting, it is possible to reduce the installation torque up to 35%.
- Over-flighting reduces the compression capacity of the helical pile upto 39%.
- Over-flighting increases the tensile capacity and stiffness of the helical pile upto 120% in loose soil and 60% in other densities
- The verification of the capacity of a single helix pile with relation to installation torque maybe unsafe for large pile geometries

3

Design requirements for the seabed gripper

The main requirement is to have a gripper template on the seabed, to support the installation of the monopile at the maximum installation weather condition of the vessel. As seen in section 1.1.1, the rapid growth in the offshore wind industry influences the design of the future projects. When the wind turbine size increases, the self weight and the load acting on the turbine will increase, which subsequently influences the design of the monopile. So, Van Oord provided certain boundary conditions and parameters, for which the seabed gripper needs to be designed. The conditions are shown in Table 3.1

Description	Values	Unit
Diameter of monopile at mud line	7 - 11	m
Length of monopile	max 110	m
Weight of monopile	max 3000	tonnes
Water depth	55	m
H_s	2.5	m
T	5.6 - 7.2	sec
V_{wind}	20	m/s
Inclination of monopile	1	deg

Table 3.1: Initial parameters and conditions

For the above mentioned diameter of the monopile, hammers are being developed by the suppliers like Menck and IHC [1]. Hence, some reasonable assumptions have been made for the properties of the hammer. The assumptions are listed in table 3.2.

Assumptions	Values	Unit
Diameter of hammer	8.5	m
Length of hammer	25	m
Weight of hammer	max 1000	tonnes

Table 3.2: Assumed hammer properties

The starting points that are considered are listed below:

- The seabed gripper template should be easy to install, removed and reused.

- It should be suitable for most types of soil conditions.
- The planning of the transport and installation of the seabed gripper needs to be done and compared with the conventional method that is in practice, to have an overview of the total transport time and cost associated.
- The most optimal solution is to have a concept with lowest cost over its complete lifetime.
- An impact load between the monopile and the gripper frame is considered. This happens when the monopile is slewed and lowered into the gripper frame.
- Fatigue analysis needs to be done to assess the lifetime of the structure, as the structure should be durable for multiple wind farms.

During hammering of the monopile, the hammering load and vibration from the monopile to the gripper structure is ignored in this thesis. This is because the monopile is only 1 degree inclined, so most of these loads will be directly transferred to the soil.

For the design of the foundation of the seabed gripper, sand layer with an angle of internal friction of 25 deg is taken as the base condition. It is also assumed that there is only one type of soil for the entire depth of the foundation which is sand.

4

Concept Generation and Selection

Note: As this chapter deals only with the conceptual design, the figures and their dimensions shown here is not final, they are just an illustration of how the considered concepts looks like. After selecting the concepts in this chapter, their detailed designing and final configurations will be discussed in the further chapters.

From the literature review, different concepts have been studied and understood. With these information and considering the scope of this thesis and requirements from Van Oord, several concepts have been generated. These concepts are modified from the concepts discussed in the literature based on the purpose of the structure. The generated concepts are listed below and explained.

1. Tripod structure with suction bucket
2. Jacket structure with helical piles
3. Steel structure with mudmats
4. Jacket pile template with vibratory driven piles

4.1. Tripod structure with suction bucket

The First concept considered is a tripod structure as a superstructure, with suction buckets as the foundation. The figure 4.1 shows the configuration of this concept. Each main leg connects the gripper frame to the suction bucket which acts as a main member to transfer load from the gripper to the foundation. The gripper frame has an open side to have easy installation of the monopile and to remove the template after installation of the monopile. An additional frame (stiffener frame) is provided to increase the stiffness of the whole structure.

This template can be installed by lifting from the vessel and placing it on the seabed. The suction buckets are connected to pumps on-board the vessel and will be operated from the vessel. After the installation of the suction bucket, the monopile will be slewed inside the gripper frame. The gripper frame will provide sufficient force needed to make the monopile vertical within its tolerance till the end of the installation. Then the monopile is hammered and after the installation, the template is removed. The template can be easily removed by lifting it sideways and up. Some of the advantages and disadvantages of this structure are listed below.

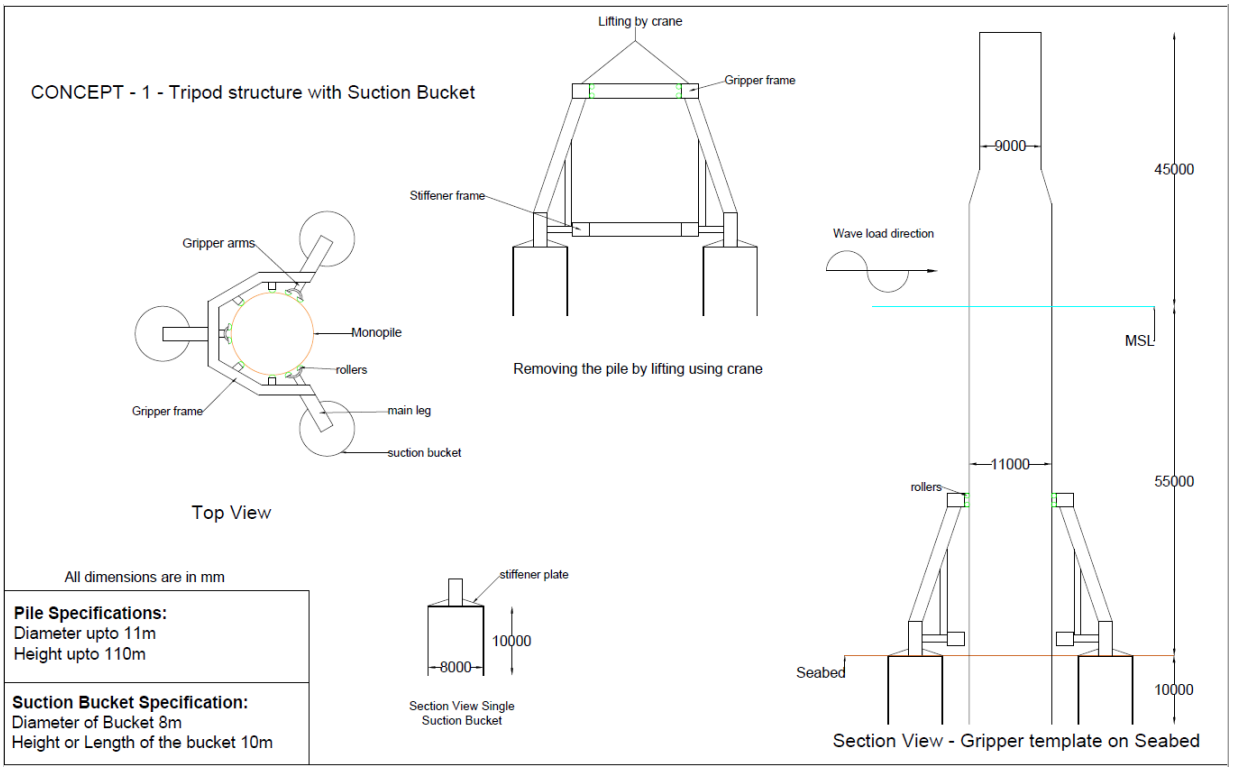

Figure 4.1: Tripod structure with suction bucket

Advantages:

- Stiff structure;
- No seabed preparation;
- Suction bucket are easy to install and remove;
- Provides more lateral loading capacity;
- If the whole structure can be floated, there is no space needed on deck to store and transport the structure;
- Horizontal level of the whole structure can be adjusted by adjusting the penetration depth of the suction bucket.

Disadvantages:

- Not suitable for hard soils, clay and armour layer of scour protection;
- If there are mixed soil layers of sand and clay, then the installation will be challenging[26].

4.2. Jacket structure with helical piles

The second concept considered is a 4 legged Jacket structure as superstructure with helical piles as the foundation. The helical piles can be easily switched between normal hammered piles or vibratory driven piles based on the need. The figure 4.2 shows the schematic representation of the concept. The jacket structure has two bays. The top bay has a K bracing to connect the gripper frame to the main legs of the jacket. The bottom frame has a X bracing to provide

stiffness and have proper load transfer. Mudmats are attached to each legs at the bottom, so that the structure does not settle inside the top weak soil layer due to its own weight.

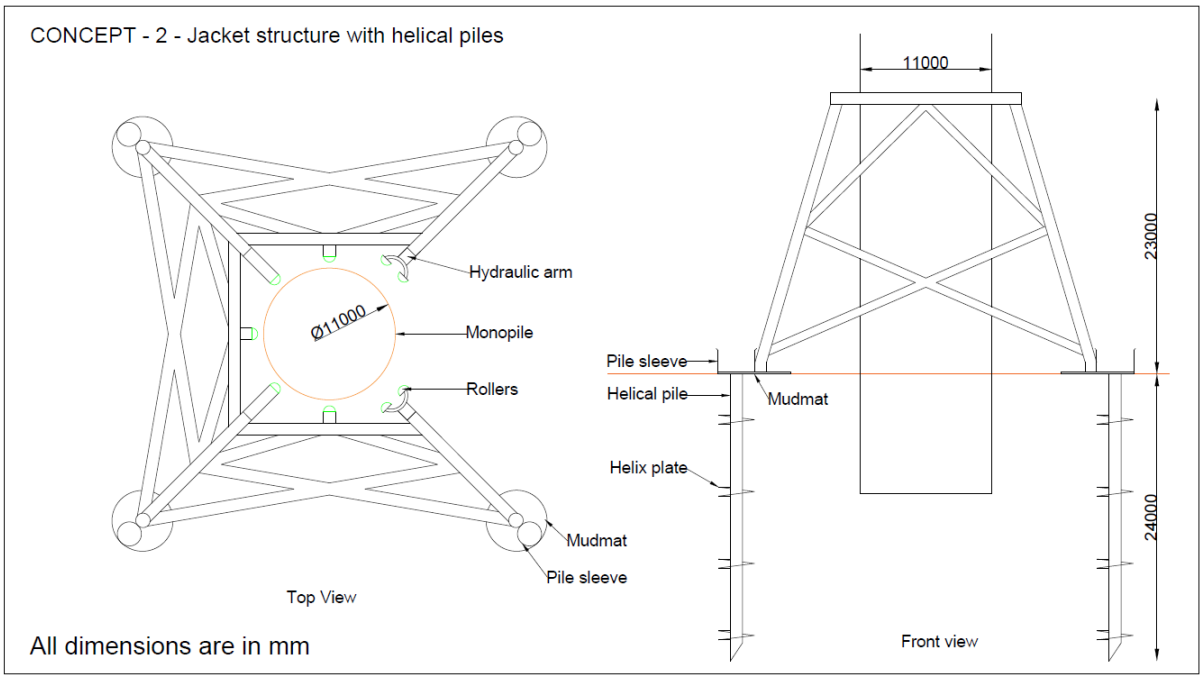

Figure 4.2: Jacket structure with helical piles

Usually a normal jacket structure has bracing connected between their main legs. This structure has only three sides with bracing and an opening on one side for easy installation and removal. The jacket structure is placed on the seabed and the helical piles are lifted and lowered inside the pile sleeve and screwed to desired depth. The piles can be removed by screwing in the opposite direction(i.e: unscrewing) and the structure can be removed by lifting sideways and up. Some of the advantages and disadvantages of this structure are listed below.

Advantages:

- Light weight and stiff structure;
- The spacing of the legs are designed so that, they are away from the armour layer;
- Helical piles can withstand more tension and compression force than a normal pile, which is the governing force acting due to moment (push-pull loading);
- Easy to install by applying small vertical force or self-weight and screwing the piles;
- Modular type of helical piles can be used based on site specific condition.(i.e: if more load carrying capacity is needed, extension pile, with or without helices can be attached to the top of the pre-existing helical pile);
- Provides immediate load carrying capacity, which is vital in our case;
- Suitable for very soft to very stiff clay and from loose to very dense sand [14];
- Very less soil disturbance.

Disadvantages:

- Not good with gravels or cobble deposits (i.e.: It can be used up to a maximum soil grain size of 60% of the helical pitch [14];
  - This can affect our installation, if the filter layer has a bigger grain size based on its design;
  - This can lead to installing the scour layer after the installation of the monopile or reducing the grain size of the filter layer;
- There should be a minimum weight of the equipment. ½ tonnes per 1356 N-m torque needed for the installation [14].

4.3. Steel structure with mudmats

The third concept is a steel structure with mudmats. This is a type of gravity based structure. The figure 4.3 shows the arrangements of this concept. This concept has 6 steel frames with mudmats attached to it at the bottom. The six steel frames are only interconnected by means of the gripper frame and the stiffener frame. The top layer will be weaker and is difficult to provide enough stability to the structure for the conditions provided in 3.1. So the mudmats are integrated with the helical (or rammed) pile foundation. For stronger soils, the use of mudmats will be sufficient, no need of integrating with any other foundation.

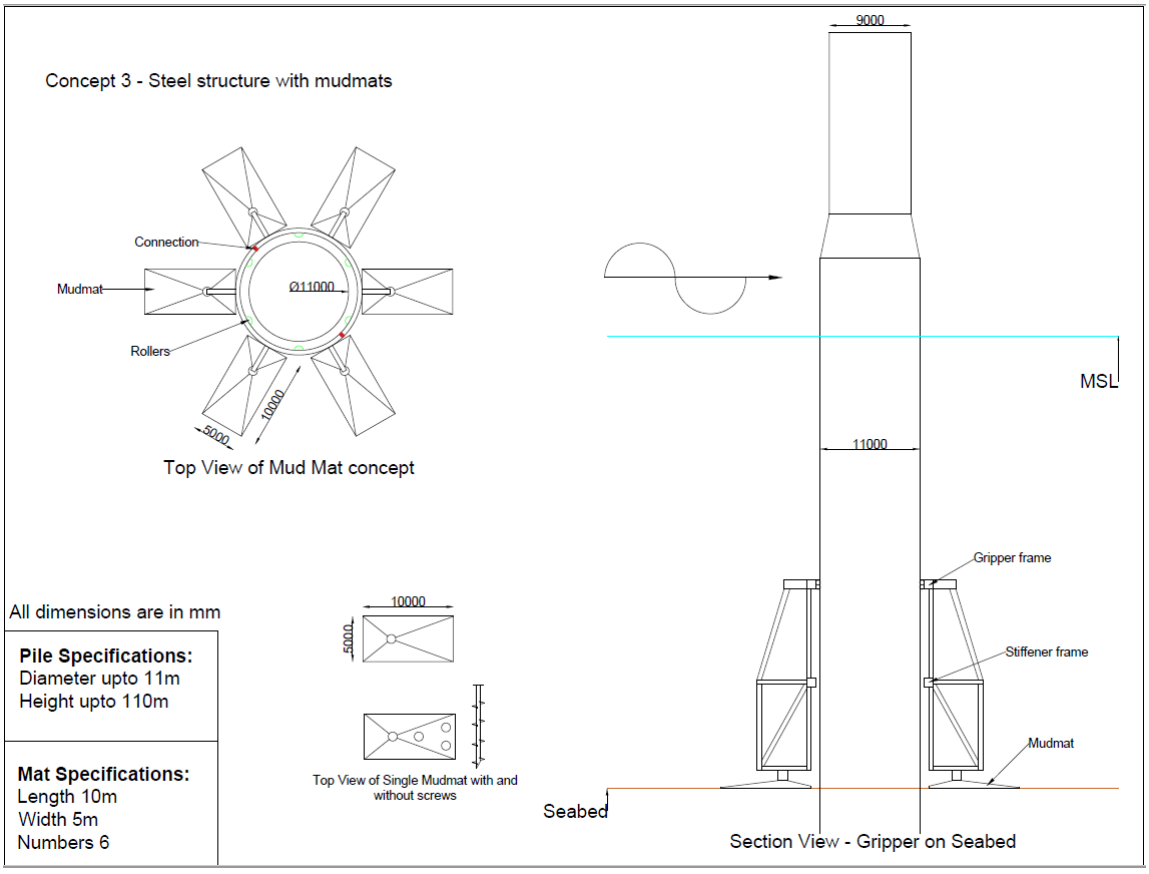

Figure 4.3: Steel structure with mudmats

The structure is installed by lifting from the vessel and placing it on the seabed. For weak soil, the helical piles are screwed in each mudmats, otherwise it is an easy installation. The

monopile can be lowered into the gripper frame and hammered. There are two connection points in both the gripper and the stiffener frame which comprises of bolted connections. For the removal of the gripper structure, the connection point should be removed first and then lifting the structure as two parts.

Advantages:

- Easy to install for hard soil conditions;
- Can be placed over scour layer; if wanted the scour layer can be used to make the seabed a bit even;

Disadvantages:

- Can't be used for weak top layer soil;
  - The weak layer can be removed and replaced with denser soil;
  - Replacing of weak layer will be more expensive depending on the thickness;
- The integrated pile foundation will take more time to install.

4.4. Jacket pile template with vibratory driven piles

The fourth concept is a monopile pile template with vibratory driven piles. The figure 4.4 shows the schematic representation of this concept. The monopile template is a bit of a modification of jacket pile template. It is a three legged structure with two frames and one side is open for easy installation and removal of the structure. Each pile sleeves have a pile with vibratory hammer on top of it. The pile sleeves are closed initially at the bottom so that the piles inside does not slip through it. Mudmats are attached to the bottom of the pile sleeves to prevent the settlement of the structure from its self weight.

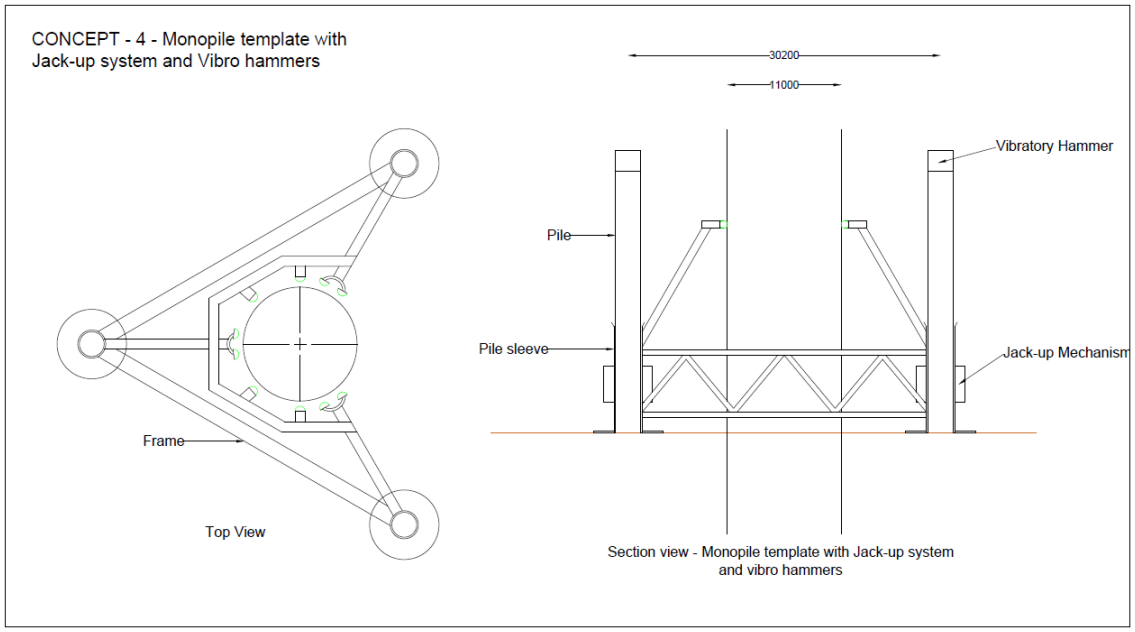

Figure 4.4: Monopile template with vibratory driven piles

The monopile template along with the three pile arrangements are lifted and placed on the seabed. The hammers are controlled from the vessel. The bottom of the sleeves are opened

and the piles are installed by the vibratory hammers. After driving the piles, the monopile is lowered into the gripper frame and hammered. After the installation of the monopile, the piles are removed with the help of a jack-up mechanism and vibrating the pile again. Due to the vibration of the pile, the friction between the soil and the pile reduces. This supports the lifting by the jack-up mechanism and the bottom of the sleeves are closed. If the design of the the jack-up mechanism is hard as the pile will be vibrating while lifting, it can be replaced by lifting by crane.

Advantages:

- Easy to install the piles using vibro-hammer;
- Good for sand type soils.

Disadvantages:

- Not so good with clay.
  - It needs high amplitude vibrator;
  - Instead hammering is recommended for clay;
- The axial resistance of vibratory pile is less than the hammered pile [35]. (It is around 80% of the capacity of hammered pile)
  - To increase the axial resistance, vibratory hammers with low frequency and low penetration velocity can be used
  - Additional penetration needs to be done to make the axial resistance equal to the hammered pile.
- Lateral capacity seems to be equal but as there is not many data on this, it should be considered cautiously;
- For the Design, 40% reduction factor from the capacity of hammered pile should be taken for cohesive and dense sands and for loose sands, lower reduction factor must be justified[35].

4.5. Multi Criteria Analysis

With the aforementioned concepts that are considered for this thesis, the multi-criteria analysis method is adopted to select the optimal concepts, to proceed further for design. There are four major topics that are covered in the multi-criteria analysis and they are described below with the explanation of why the points are awarded for each criteria for each concepts.

1. Installation & Removal
   - This comprises of the time taken and different operations needed to install and remove the structure.
   - As a whole new structure is being installed to assist the installation of a monopile, the new structure should be easy to install and remove and the time taken should be less. This directly represents the time associated and its cost, which is the major factor at the end of the project. Therefore, it is given 50% of the total weight.
   - For concept 1, suction bucket is easy to install by giving suction pressure and remove by reverse suction. However for the installation, it takes time to install depending on the type of soil. Therefore, it is given 0.9 out of 1.

- For concept 2, helical piles are also easy to install and remove by screwing and unscrewing. However, all the helical piles needs to be lifted and installed separately, unlike the suction bucket, where all the buckets are installed simultaneously as it is fixed to the structure. Hence, it is awarded 0.8 out 1.
- For concept 3, mudmats are one of the easy method to install by lifting and placing on the seabed or scour protection. However, to remove the frame as seen in figure 4.3, screws needs to be removed underwater and the structure becomes two components, which will lifted and placed on vessel and bolted again on board the vessel for next installation. Thus, it is given less point of 0.7 out of 1, only because of removal.
- For Concept 4, installing the piles are easier by vibration, but for removing my jack-up system or by crane will take time. So, it is awarded 0.75 out of 1.

2. Types of soil

- This covers the different types of soil condition that the structure can be installed in. This structure is going to installed for multiple wind farms and different locations. There will be all kinds of soil that will be present on site. So it must be preferable to install the structure in mostly all types of soil conditions.
- For concept 1, suction bucket are not suitable for very hard soils and has difficulty in installing in different layers of soil mainly consisting of clay. Hence it is awarded 0.75 out of 1.
- For concept 2, helical piles are not suitable for very hard and big granular soils. Therefore, it is awarded 0.8 out of 1.
- For concept 3, mudmats are suitable for all kinds of soil except very weak top layers. Thus, it is awarded 0.9 out of 1.
- For concept 4, vibratory piles are not suitable for very hard soils and there if difficulty in installing in clay soil. So, it is awarded 0.8 out of 1.

3. Complexity

- This includes the difficulty in operating the structure and its components. The more complex the structure, the more complexity in fabrication and operation of the structure. Which therefore, increases the cost.
- For concept 1, applying suction pressure to install the bucket need to be closely monitored throughout the installation process. It requires more attention for layered soil consisting of clay layers.
- For concept 2, there are complications in installing in clay soil and needs attention while installing. Therefore, it is awarded, 0.9 out of 1.
- For concept 3, removing the bolts underwater to split the structure for easy removal is a complex operation. Thus, it is given 0.6 out of 1.
- For concept 4, the self installing mechanism and removal using the vibratory hammer is difficult to fabricate and operate. Also, removing the piles using jack-up system while vibrating requires a complex design. So, it is given 0.5 out of 1.

The table-4.1 shows the points given for these four topics, for each concepts and their total. The concepts with most points will be taken for further design.

	Installation & Removal	Types of Soil	Complexity	Total
Tripod with Suction Bucket	0.9	0.75	0.8	83.5
Jacket structure with Helical Piles	0.8	0.8	0.9	82
Mudmats with 6 legs (without piles)	0.7	0.9	0.6	74
Jacket pile template with vibro pile	0.75	0.8	0.5	71.5
Weight	50	30	20	100

Table 4.1: Multi-Criteria Analysis for the generated concepts

From the table above, it is evident that the concepts tripod with suction bucket and jacket with helical piles are better, out of these aforementioned concepts. In the upcoming chapters, the detailed designing and the soil-structure interaction are done for these two concepts and will be discussed in detail.

4.6. Discussion

The selected two concepts can be split into two on the basis of super-structure and foundation. The Jacket structure can be implemented with both Suction Bucket and Helical pile foundation and same applies for Tripod structure.

During the FEM analysis the super structure will be designed, analyzed and optimised accordingly. The difficulty in design and fabrication will be determined in this stage.

During the soil-structure interaction phase, the type of foundation which is best suited for this project can be identified.

Then a most optimal final concept will be proposed combining the super-structure with the foundation considering some series of factor like cost associated , time taken for installation and removal, foundations interaction with the monopile and durability of the structure.

5

Preliminary design of Selected concepts

5.1. Loads acting on the Monopile an Hammer

Initially, to start the preliminary design of the concepts, the loads acting on the monopile and hammer are calculated. This load will be transferred from the monopile to the gripper frame as a horizontal load. The loads are calculated based on the conditions given in table 3.1. The figure 5.1 shows the schematic representation of the loads acting on the monopile.

First, the wind load is calculated followed by the hydrodynamic loading and load due to the inclination of the monopile. In most of the sites, the top layer of the soil are weaker with clay or silt or loose sand. Therefore, it will be conservative to find the self-weight penetration of the monopile for the base soil condition. This conservative approach is adopted to find the self-weight penetration. The monopile is taken as unplugged and the vertical resistance is provided from the shaft friction(Q_s) and the tip resistance(Q_t) of the monopile. The self-weight penetration stops at a depth where the self-weight of the monopile equals the total resistance of the soil.

$$\begin{aligned} S.W\ of\ MP - Buoyancy\ weight &= Total\ resistance \\ 29430 - 1893.8 &= Q_s + Q_t\ kN \end{aligned} \tag{5.1}$$

The shaft friction and tip resistance are calculated using the equations 5.2, 5.3 respectively.

$$\begin{aligned} Shaft\ friction\ (Q_s) &= f_s A_{shaft} \\ &= 158.965\ z^2\ kN \end{aligned} \tag{5.2}$$

where,

f_s - unit skin friction capacity = βp_0

β - shaft friction factor = tan(25°) (Reasonable low first estimate)

p_0 - effective vertical stress = $\gamma' z$

γ' - effective unit weight of soil = 10 kN/m^3

A_{shaft} - area of pile shaft for unplugged pile = $\pi(D_o + D_i)z$

D_o, D_i - outer and inner diameter of monopile respectively

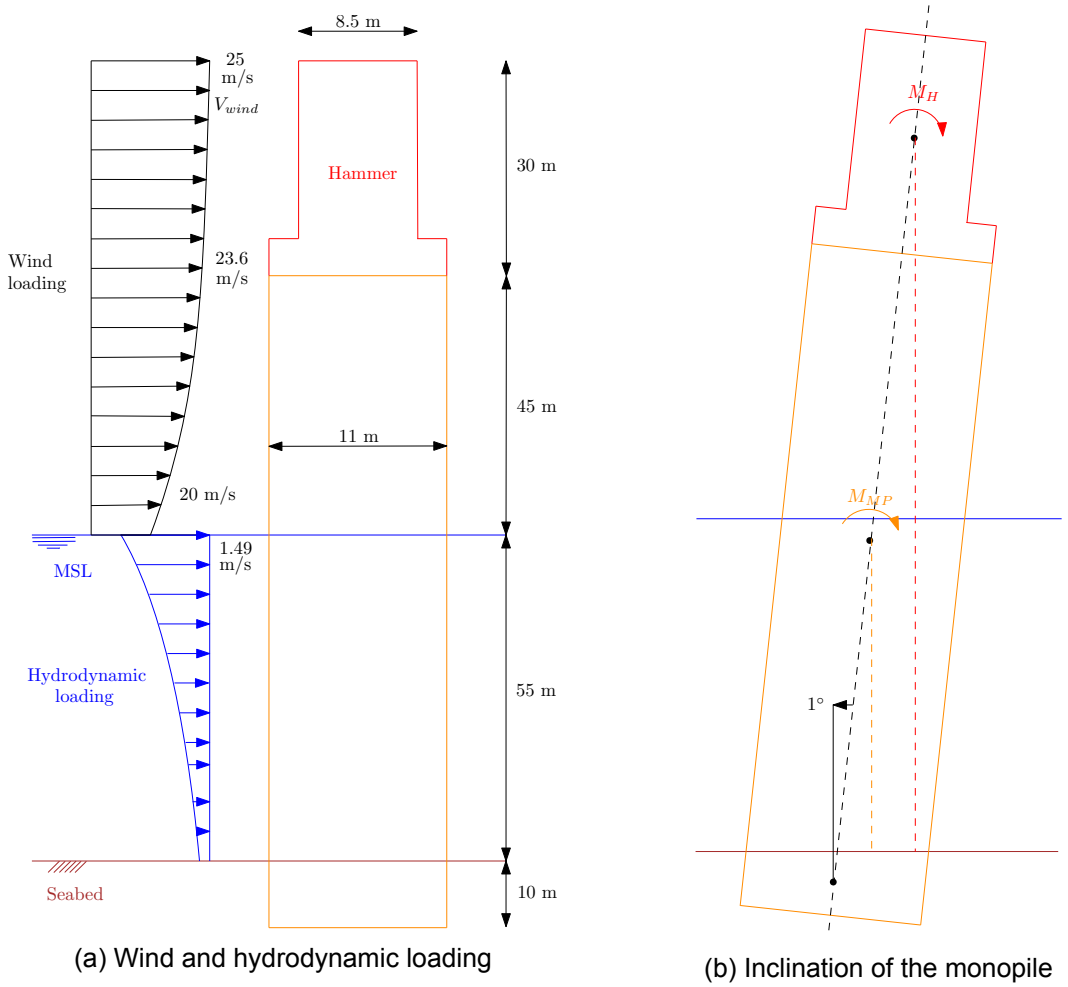

(a) Wind and hydrodynamic loading

(b) Inclination of the monopile

Figure 5.1: Loads acting on the monopile

z - penetrated depth of monopile

$$Tip\ resistance(Q_t) = qA_{tip} = 2045.2\ z\ kN \tag{5.3}$$

where,

f_s - unit end bearing capacity = $N_q p_0$

N_q - end bearing capacity factor = 40

A_{tip} - Area of tip = $\pi(D_0 - t)t$

t - thickness of monopile

z - depth

The equations 5.2 and 5.3 are substituted in equation 5.1 and solved for the penetration depth. The self-weight penetration of the monopile is found as 9.6 m. The total length of the monopile above the water level is:

$$MP\ above\ MSL = Total\ length\ of\ MP - water\ depth - S.W\ penetration$$
$$= 110m - 55m - 9.6m = 45.4m \tag{5.4}$$

The velocity of the wind at certain height is calculated using the equation 5.5

$$v_w(h) = v_{10}\left[\frac{h}{h_{10}}\right]^a \tag{5.5}$$

where,

v_w(h) - velocity of the wind (m/s), at height h

v_{10} - velocity of the wind (m/s), at height h_{10} = 10 meters

a - Hellmann exponent

The velocities are calculated per meter from MSL till 45.4 m for monopile and from 45.4 m to 75.4 m for the hammer. These velocities are substituted in the drag part of the Morison equation 5.6, to find the force per meter acting on the monopile and hammer.

$$f = \frac{1}{2}\rho_{air} C_d\ D\ v_w(h)|v_w(h)| \tag{5.6}$$

where,

ρ_{air} - density of air

C_d - drag coefficient = 0.7 for cylindrical smooth surface

D - diameter of monopile or hammer accordingly

The total wind force is calculated as the integration of the individual forces along the structures. Likewise, the total moment is calculated as the integration of the individual forces multiplied by the corresponding distance from the seabed. The total force and moment due to wind is given in table 5.1 and the calculations are shown in A.2

Description	Values	Unit
$F_{wind,MP}$	130	kN
$F_{wind,Hammer}$	72	kN
F_{wind}	202	kN
$M_{wind,MP}$	10091	kNm
$M_{wind,Hammer}$	8304	kNm
M_{wind}	18395	kNm

Table 5.1: Wind loading on hammer and monopile

For hydrodynamic loading, linear wave theory is combined with wheeler stretching to find the horizontal velocity (5.7) and acceleration (5.8) of the wave particle at desired depths. This is valid because the wave height is small during operation compared to the water depth, which results in deep water condition (d/λ = 1.12 > 0.5).

$$u_x = \omega a \frac{cosh(k(d+z'))}{sinhkd} cos(kx - \omega t) \tag{5.7}$$

$$\dot{u}_x = \omega^2 a \frac{cosh(k(d+z'))}{sinhkd} sin(kx - \omega t) \tag{5.8}$$

where,

ω - angular frequency

a - wave amplitude

k - wave number

d - water depth

z' - true depth from wheeler stretching (depth below the wave crest)

t - time

The loads are calculated as a function of time. The maximum load acting on the monopile occurs at 4.36 sec of the total time period of 5.6 sec of the wave. Wheeler stretching method stretches the water column linearly into a height equivalent to the mean water depth. The true depth is found by equation 5.9 and substituted in equations 5.7 and 5.8 to find the horizontal velocity and acceleration of the wave particle.

$$z' = d\frac{d+z}{d+\zeta} - d \tag{5.9}$$

where,

ζ - z-value at the instantaneous water surface

A current velocity of 1 m/s is assumed to be act on the entire water column. The current velocity is added with the horizontal velocity of the wave particle. This added velocities and accelerations are used in the Morison equation 5.10 to find the force per meter due to drag and inertia. These total force per meter for the entire depth are summed up to get the total hydrodynamic force acting on the monopile. The drag and inertia coefficient used here is 1 and 2 respectively. The Morison equation is valid for cylinder diameter that is relatively smaller than the wave length. For large diameter monopiles, when installed in shallow water and small wave length, the validity of the equation can be compromised.

Monopile has an impact on the wave field called diffraction. To include this effect, MacCamy–Fuchs correction factor is introduced which reduces the inertia co-efficient for large d/λ. However, it is conservative not to apply the MacCamy–Fuchs correction factor in the equation.

$$F = \underbrace{\frac{1}{2}\rho_w C_d D u_x |u_x|}_{F_d} + \underbrace{\frac{\pi}{4}\rho_w C_m D^2 \dot{u}_x}_{F_I} \tag{5.10}$$

where,

F - total force per unit monopile length

ρ_w - density of water

C_d - drag coefficient = 1

C_m - inertia coefficient = 2

D - diameter of monopile

The moment acting on the monopile is the total force per meter times the distance from the seabed. The combination of drag and inertia forces are the largest at 4.36^{th} sec of the wave period. The final value of the force and moment with respect to seabed at 4.36^{th} sec are shown in table 5.2 and the calculation is shown in A.3.

Description	Values	Unit
F_{wave}	5997	kN
M_{wave}	278767	kNm

Table 5.2: Hydrodynamic loading on monopile (@4.36^{th} sec)

The next step is to find the moment due to the inclination of the monopile. The COG of monopile and hammer is assumed to act at half of their length respectively. From table 3.1, it is known that the initial inclination of the monopile is 1 deg. So the moment due to the inclination is,

$$M_I = weight * gravity * vertical\ distance\ from\ COG\ to\ seabed\ * tan(1^{\circ}) = 60146\ kNm \tag{5.11}$$

A factor of safety of 1.1 and 1.35 are adopted for permanent load and environmental load respectively. The total base shear and moment acting on the monopile and hammer at the seabed is

$$F_{SB} = F_{wind} * 1.35 + F_{wave} * 1.35 = 8368\ kN \tag{5.12}$$

$$M_O = M_{wind} * 1.35 + M_{wave} * 1.35 + M_I * 1.1 = 467574\ kNm \tag{5.13}$$

5.2. Gripper components arrangement

The components and the functionality of the gripper fame can be found in section 1.4. In the scope of this thesis, the hydraulic arms and rollers are not designed. Only the position of the gripper arm and the number of rollers per arm are proposed.

The total base shear and moment acting on the monopile will be transferred on the gripper. The height were the gripper frame should be placed on the template is be dependent on the gripper arm and roller arrangement. From the previous projects within the company, it is known that a single roller in a gripper arm should give a maximum opposing force of 2100 kN [1]. If it exceeds that limit the monopile wall will deform. The gripper frame arrangement is shown in figure 5.2.

The gripper has two types of roller arrangements. One with 4 rollers arranged in the vertical direction and other with a combination of two 4 roller arrangement which is connected together with a horizontal spacing between them. It is shown in figure 5.3. Each arms are placed at 45° angle between each other. If the arms are placed closer to each other, then the rollers between the arms interacts with each other, which leads to the deformation of the monopile wall. So an optimal angle of 45° is chosen to give an opposing force without causing any deformation. Each 4 and 8 roller arms can only give a maximum opposing force of 8400 kN and 16800 kN respectively.

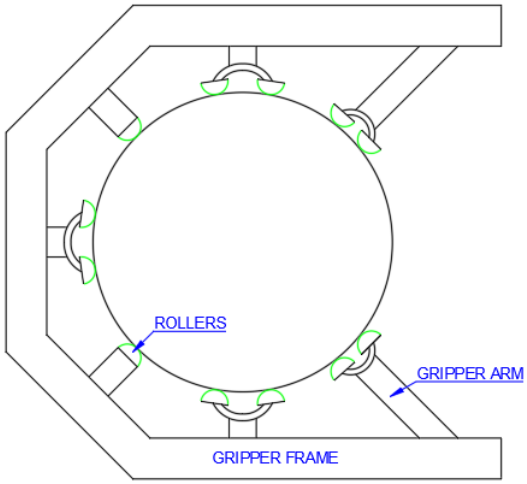

Figure 5.2: Gripper frame arrangement with arms and rollers

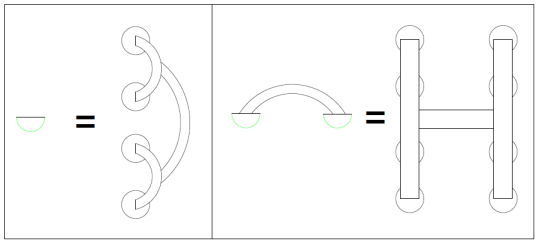

Figure 5.3: Roller configuration

For the calculation of the force that is transferred from the monopile to the gripper, the point of rotation of monopile is taken as half the height of self weight penetration. So the total force at gripper is,

$$F_{Gripper} = F_{SB} + \left[\frac{M_O}{h + (\frac{S.W.P}{2})}\right] \tag{5.14}$$

where,

h - height where the gripper frame is present

SWP - self-weight penetration = 9.6m

To find the height 'h', the critical loading direction needs to be identified. This is were the gripper can give the least opposing force if the loads acts in that critical direction. This least opposing force can be substituted in the equation 5.14, to find the height 'h' at which the gripper frame can be placed. The different loading directions are shown in figure 5.4.

The figure 5.4 shows the maximum capacity of the gripper in each loading direction. The values shown, are for each gripper arms giving 100% of its capacity as opposing force, which is not the real case. It is purely based on the design of the hydraulics and rollers and it's associated factors. For condition 1, both the gripper arms will take 50% of the load acting in that direction. But for condition 2, the gripper arm in-line with the loading direction will take more load than the arm at an angle. For example, if the in-line arm takes 70% of the total load

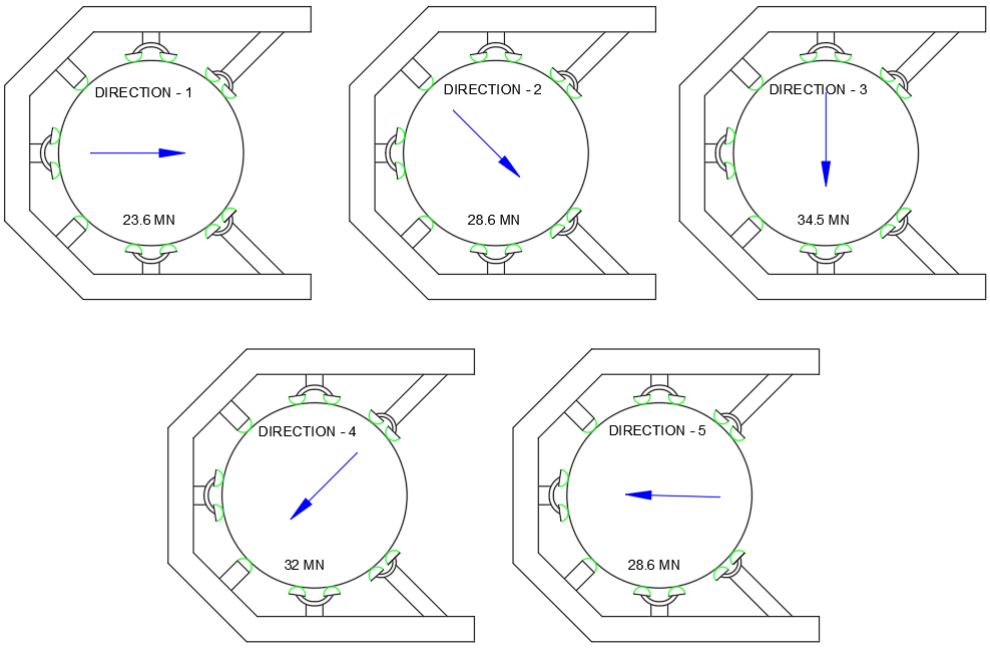

Figure 5.4: Different gripper loading directions

and the arm at an angle takes 30% of the total load, then the total capacity in that direction will reduce to 24MN. In the end, load distribution between the gripper arm plays a role.

Although the total capacity depends on the load distribution between the gripper arms, still condition 1 is the critical loading direction. When the load acts in that direction, only two 8 roller gripper arm which is 45° to the loading direction can give opposing force. The total opposing force given in condition 1 is,

$$F_{Gripper} = 2 * 16800 * cos(45^{\circ}) = 23.6\ MN \tag{5.15}$$

The equation 5.15 shows the maximum capacity of the gripper at the critical loading direction 1.

Substituting the value from equation 5.15 in equation 5.14, the height is found as 25.66 m. But the final height is taken as 26.5 m from the seabed to be conservative. Substituting this final height of 26.5m in equation 5.14 with the base shear (eq.5.12) and overturning moment (eq.5.13) acting on the monopile w.r.t seabed, the actual load transferred from the monopile to the gripper can be found. This is shown in equation below.

$$F_{Gripper} = 8368 + \left[\frac{467574}{26.5 + 4.8}\right] kN = 23211.8\ kN \tag{5.16}$$

The selected two concepts will be designed for this 26.5m height and the gripper force will be used in later stage for the design.

5.3. Preliminary design of the support structure

The preliminary design of both the concepts are done according to ” Hand book of Bottom Founded Offshore Structures, Part I & II”[32][33]. The steps involved in the design are:

1. Initial member sizing and arrangements

2. Calculating the total weight of the structure
3. Hydrodynamic loads acting on the structure
4. Determining the foundation reaction
5. Design of the foundation

5.4. Jacket structure with helical piles

It is ensured that the base of the structure goes beyond the armour layer of the scour protection. This makes the installation of the pile easier, as armour layer has big stone or rocks.

5.4.1. Initial member sizing and arrangements

Reasonable dimensions are assumed for the initial member sizing with a D/t ratio of 40 as shown in table 5.3 and figure 5.5. Lengths shown in table are for one leg and one side of the frame for bays.

Jacket leg			**Top bay**		
L	27.655	m	L	38.6	m
Dia	2	m	Dia	1	m
t	0.05	m	t	0.025	m
Bottom bay			**Gripper frame**		
L	54.26	m	L	50.3	m
Dia	1	m	Dia	2	m
t	0.025	m	t	0.05	m

Table 5.3: Dimension of the members

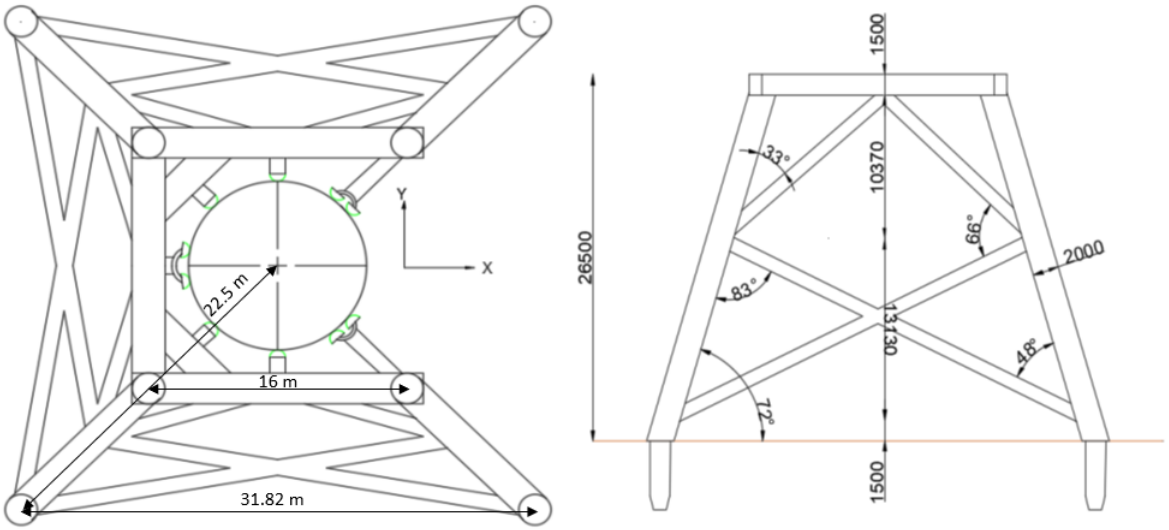

Figure 5.5: Initial dimensions and sizing of jacket structure

As the structure is just 26.5 m high, it will be optimal to have two bays. For fabrication purposes, the bays are often chosen geometrically equal.(i.e. Each bay i has dimensions:

$dim_{(i+1)} = m * dim_i$. The height of the bays is calculated using the formulas given below,

$$m = \left[\frac{b_N}{b_0}\right]^{1/N} \tag{5.17}$$

$$h_1 = h\left[\frac{m-1}{m^N - 1}\right] \tag{5.18}$$

where,

h - total height of the structure = 26.5 m

b_N - width of the structure at seabed = 31.82 m

b_0 - width of the structure at gripper frame = 16 m

N - Number of bays = 2

h_1 - height of first bay (top bay)

5.4.2. Total weight of the jacket structure

In the next step, the net weight of the whole structure is calculated. The bracings are taken as non-flooded members. The gripper frame along with the hydraulic arrangement are considered as a top side for this phase. As the hydraulics are not designed here, a reasonable self weight of 200 tonnes (i.e. 35 tonnes for each 8 roller arms and 23.75 tonnes for each 4 roller arms) is assumed for the hydraulic arm including the rollers.

$$Net\ weight = Dry\ weight - Buoyancy\ weight \tag{5.19}$$

Weight of the jacket structure		
Dry Weight	836	ton
Buoyancy Weight	286	ton
Net Weight	550	ton

Table 5.4: Weight of the jacket structure

5.4.3. Hydrodynamic load acting on the jacket structure

As the initial dimensions and sizing are performed, next step is to find the load acting on the structure due to waves and current. An equivalent stick model approach is used to find the equivalent diameter of the structure over its height which correctly matches the drag and inertia loads. The detailed approach is shown in this Handout [36] and the equivalent diameters are calculated for the height of the structure. These diameters for drag and inertia are substituted in the Morison equation (5.10) to find the loads acting over the height of the structure. In figure 5.6, the loads acting per meter are converted into points loads at the nodes. These loads are multiplied by a factor of safety of 1.35. The force and moment at each nodes and the total base shear and overturning moment with respect to seabed is shown in table 5.5.

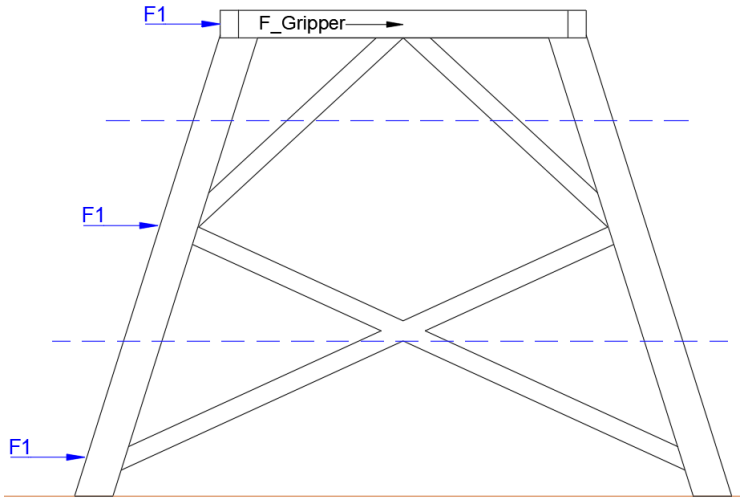

Figure 5.6: Loads acting on the nodes

Force at Nodes	Values	Unit
F1	340	kN
F2	314.4	kN
F3	141.5	kN
M1	9007	kNm
M2	6192	kNm
M3	212	kNm
F_{SB}	**796**	**kN**
M_{SB}	**15411**	**kNm**

Table 5.5: Loads on nodes and the total load w.r.t seabed

5.4.4. Determining the foundation pile reaction

Next step is to find the reactions of each leg. Based on these reaction forces, the foundation piles can be designed. The schematic of the loading and its respective reactions are shown in figure 5.7.

The total vertical load acting on the structure is its self weight.

$$F_G = Self\ weight * g * 1.1 = 5935\ kN \tag{5.20}$$

Total base shear at seabed is sum of the hydrodynamic loads acting on the jacket structure and load from the monopile on the gripper as shown in figure 5.6.

$$\begin{aligned} F_B &= F_{Gripper} + F_{SB} \\ &= 23196 + 796 = 23992\ kN \end{aligned} \tag{5.21}$$

The overturning moment with respect to seabed comprises of three parts.

- Due to the load from monopile on the gripper(topside),
- Due to hydrodynamic load,

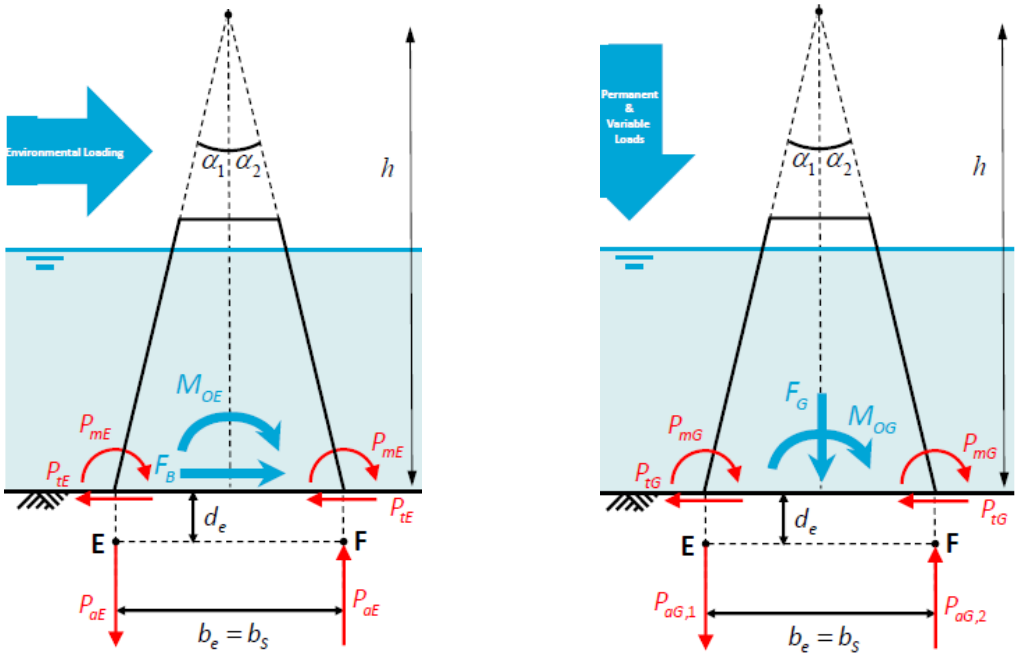

(a) Environmental Loading

(b) Permanent Loading

Figure 5.7: Schematic of the pile reactions for one side of the jacket.[34]

- Due to eccentricity, as the structure is not symmetrical in axis.

The eccentricity is calculated in the x axis taking the center of the monopile as the origin. The eccentricity of the jacket and the topside (gripper frame) for both dry and submerged condition is shown in table 5.6.

	Dry condition (m)	Submerged (m)
$e(x)_{Jacket}$	-2.09	1.36
$e(x)_{Gripper}$	-2.28	-2.16

Table 5.6: Eccentricity for Jacket structure

From the above table, it is seen that the eccentricity of the jacket structure changed from -2.09 m to 1.36 m. This is because the bracings are not flooded and they provide some flotation, which makes the structure lighter under water. The eccentricity can be made to zero by ballasting the members accordingly, if the capacity of the crane allows to lift such weight. To find the pile reaction, the eccentricity while the structure is submerged is used. Moment due to eccentricity is the net weight of jacket and gripper multiplied with their respective eccentricity and factor of safety of 1.1.

$$\begin{aligned} M_{eccentricity} &= (W_{Jacket} * e(x)_{Jacket} + W_{Gripper} * e(x)_{Gripper}) * 9.81 * 1.1 \\ &= (171.7 * 1.36 + 378.2 * -2.16) * 9.81 * 1.1 \\ &= -6948\ kNm \end{aligned} \tag{5.22}$$

All the three moments are added to account for the worst case scenario of all loads and

moment acts in the same direction. The total overturning moment is,

$$\begin{aligned} M_O &= M_t + M_{hydro} + M_{eccentricity} \\ &= 23196 * 26.5 + 15411 + 6948 = 637053\ kNm \end{aligned} \tag{5.23}$$

With these final loads (F_G,F_B and M_O), the pile reactions can be found. Diagonal loading direction is taken as the base condition. It is assumed that only two legs will carry load (one leg with compression and one leg with tension loading) and is shown in figure 5.8. Other two legs will be carrying either tension or compression based on the distribution of load within the structure and the self-weight of the structure. However, at this stage, it is assumed that, those two legs does not carry any loads. In this case, the piles are installed vertically.

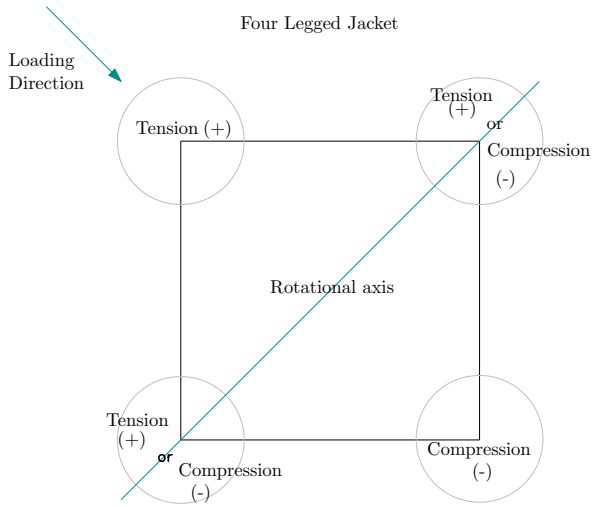

Figure 5.8: Loading direction and rotation axis

Reaction forces due to environmental loads for vertical piles are,

$$P_{tE} = \frac{F_B}{4} = 6017\ kN \tag{5.24}$$

$$P_{mE} = P_{tE} * d_e = 27076.5\ kNm \tag{5.25}$$

$$P_{aE} = \frac{(F_B * d_e) + M_{OE}}{b_e} = 16436\ kN \tag{5.26}$$

where,

P_{tE} - transverse reaction due to environmental loads

P_{mE} - moment reaction due to environmental loads

d_e - effective depth (3 * Diameter of the pile)

b_e - distance between two legs = 45 m

M_{OE} - Moment due to environmental loads ($M_t + M_{hydro}$)

The effective depth d_e depends on the diameter of the pile adopted and will change accordingly. The effective depth represents the first inflection point where the pile moment is equal to zero. In reality the pile behaviour is non-linear. However, the soil reaction above the highest

inflection point is linear by approximation [34]. The dimensions of the adopted helical piles are shown in table 5.11.

Reaction forces due to permanent and vertical loads for vertical piles are,

$$P_{aG1} = \frac{M_{OG}}{b_e} - \frac{F_G}{4} = -1343.7\ kN \tag{5.27}$$

$$P_{aG2} = \frac{M_{OG}}{b_e} + \frac{F_G}{4} = 1623.3\ kN \tag{5.28}$$

$$P_{tG} = 0\ ;\ P_{mG} = 0 \tag{5.29}$$

where,

P_{aG1} - axial reaction due to vertical load in left pile

P_{aG2} - axial reaction due to vertical load in right pile

M_{OG} - Moment due to permanent and vertical loads ($M_{eccentricity}$)

P_{tG} - transverse reaction due to Permanent and vertical loads (0 for vertical piles)

P_{mG} - moment reaction due to Permanent and vertical loads (0 for vertical piles)

The combined pile reactions for vertical piles are,

$$P_t = P_{tE} = 6017\ kN \tag{5.30}$$

$$P_m = P_{mE} = 27076.5\ kNm \tag{5.31}$$

$$P_{a1} = P_{aE} + P_{aG1} = 15092.4\ kN\ (Tension\ pile) \tag{5.32}$$

$$P_{a2} = P_{aE} + P_{aG2} = 18059.4\ kN\ (Compression\ pile) \tag{5.33}$$

where,

P_t - combined transverse reaction (For simplification, it is assumed the impact of the lateral pile response to the moment transfer = 0)

P_m - combined moment reaction

P_{a1} - combined axial reaction in left pile (Tension)

P_{aG2} - combined axial reaction in right pile (compression)

5.4.5. Design of the helical piles

With these combined pile reactions, the piles can be designed. The design of the helical pile is done according to the book “Helical Piles: A practical guide to Design and Installation” by Howard A.Perko [14]. The schematic representation of the helical pile and its parameters are shown in figure 5.11.

There are two types of load transfer mechanism in the helical piles, the independent plate and envelope friction (cylindrical shear). These are shown in the figure 5.10 for tensile loading condition. The minimum of these two mechanisms will be compared with the design load carrying capacity.

The worst case scenario is envelope friction or cylindrical shear loading capacity for both compression and tensile loading. The components in the cylindrical shear are the adhesion along the shaft (shaft friction), shear stress along the cylinder (envelope friction) and the bearing capacity of the bottom helix (in compression loading) or top helix (in tensile loading). The

Description	Value	Unit
L	24	m
D_p	4	m
D_s	1.5	m
S/D_p	2.25	-
S	10	m
p	0.75	m
Numbers	3	-

Table 5.7: Dimension of helical pile

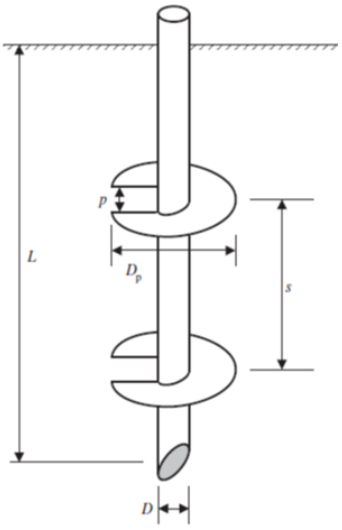

Figure 5.9: Parameters of helical pile [12]

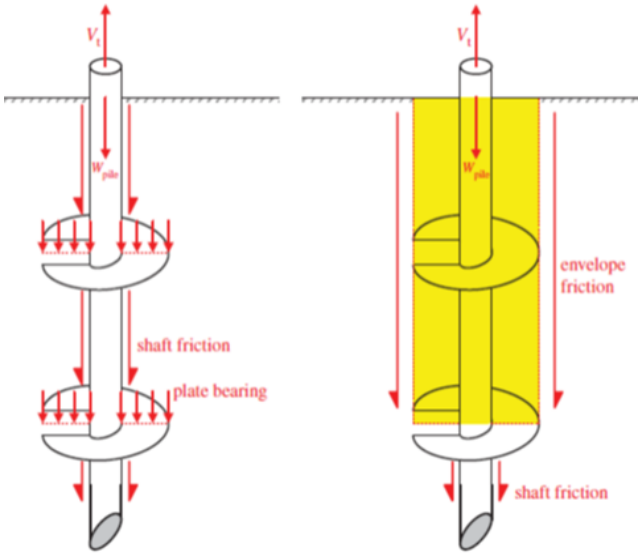

Figure 5.10: Two type of loading mechanism of helical pile for tensile loading [12]

ultimate bearing capacity for cylindrical shear method for compression is given by the equation 5.34.

$$P_u(Compression) = \underbrace{q_{ult}A_1}_{\text{bearing capacity}} + \underbrace{T(n-1)s\pi D_{avg}}_{\text{envelope friction}} + \underbrace{\alpha H(\pi d)}_{\text{shaft friction}} \tag{5.34}$$

where,

q_{ult} - ultimate bearing pressure

A_1 - area of the bottom helix including shaft area (plugged pile)

T - soil shear strength

(n-1)s - length of the soil between the helices

α - adhesion between soil and the shaft = $\beta p_o = tan(25°)\ \gamma' z$

H - length of the shaft above the top helix

d - diameter of the pile shaft = D_s

$$T = (0.09e^{(0.08\Phi)})(\gamma_s z - \gamma_w h_w) tan\Phi \tag{5.35}$$

where,

Φ - angle of internal friction for sand = 25°

γ_s - saturated unit weight of soil = 20 kN/m^3

γ_w - unit weight of water ≈ 10 kN/m^3

h_w - height of water above depth z

$$q_{ult} = q'(N'_q - 1) \tag{5.36}$$

where,

N'_q - bearing capacity factor = 23 (from figure 4.4 in [14])

q' - effective overburden stress at the bearing depth

This equation of q_{ult} with respect to q' will result in the calculated ultimate bearing pressure increasing without bound, as q' increases steadily with depth. This leads to an over prediction of bearing capacity in many cases. To avoid this, the effective overburden stress q' is replaced by product of the effective unit weight of soil and two times the average helix diameter as shown in equation 5.37

$$\begin{aligned} q_{ult} &= 2D_{avg}\gamma'(N'_q - 1) \\ &= 1760\ kN/m^3 \end{aligned} \tag{5.37}$$

where,

γ' - effective unit weight of soil = 10 kN/m^3

In this helical design, the three helices are at 9 m, 19 m and 29 m with a 10 m spacing between them. In compression force, the length of shaft above the top helix counts for the shaft friction and the remaining lengths accounts for the envelope friction. The shaft and the envelope friction depends on the depth z. These are calculated for each meter and added at the end to get the total shaft and envelope friction. The ultimate bearing capacity is,

$$\begin{aligned} P_u(Compression) &= 22116.8 + 12713.5 + 604.3 \\ &= 35434.6\ kN \end{aligned} \tag{5.38}$$

The detailed calculation can be found in Appendix - B.

A factor of safety of 1.5 is taken for both individual bearing and cylindrical shear method to calculate the ultimate bearing capacity of the helical pile [14]. From equation 5.33, the design compression load needed is 18059.4 kN, which is below the capacity available $35434.6/1.5 = 23623.05\ kN$ (Unity check is 0.764 <= 1). It is safe in compression loading condition.

The ultimate bearing capacity for cylindrical shear method for tension is given by the equation 5.39. It is the same as the compression loading condition except the area of bottom helix(A_1) is replaced by area of top helix(A_T). For the tensile loading, the shaft below the bottom helix counts for shaft friction and the remaining lengths for envelope friction as shown in figure 5.10. The total uplift capacity is,

$$\begin{aligned} P_u(Tension) &= \underbrace{q_{ult}A_1}_{\text{bearing capacity}} + \underbrace{T(n-1)s\pi D_{avg}}_{\text{envelope friction}} + \underbrace{\alpha H(\pi d)}_{\text{shaft friction}} + S.W\ of\ the\ pile \\ &= 19006.6 + 9839.55 + 1032.8 + 696.79 \\ &= 30575.76\ kN \end{aligned} \tag{5.39}$$

where,

A_T - area of the top helix excluding shaft area

The detailed calculation can be found in Appendix - B.

To calculate the self weight of the helical pile, a thickness of 0.06 m is taken for both pile and the helices. A factor of safety of 2 is taken for the tensile loading [14]. From equation 5.32, the design tension load needed is $15092.4kN$, which is below the capacity available $30575.76/2 = 15287.88\ kN$ (Unity check is 0.987 <= 1). Its safe in tension loading condition.

5.5. Tripod structure with suction bucket

The steps involved in the preliminary design of the tripod structure is similar to the jacket structure. In this concept, the legs are near to the armour layer of the scour protection and the suction bucket can't be installed on the armour layer because the stones or rocks are bigger in size. Therefore, the armour layer needs to be placed after the installation of the monopile.

5.5.1. Initial member sizing and arrangements

The assumed dimensions for the initial member sizing with a D/t ratio of 40 is shown in table 5.10 and figure 5.12.

5.5.2. Total weight of the tripod structure

As discussed previously, the gripper frame is considered as topside. The net weight of the structure including suction bucket is given in table 5.9.

5.5.3. Hydrodynamic load acting on the tripod structure

The loads due to hydrodynamic are calculated using stick model and adopting wheeler stretching. The force and moment at each nodes and the total base shear and overturning moment with respect to seabed is shown in table 5.10 and figure 5.13.

5.5.4. Determining the foundation bucket reaction

Next step is to find the reaction forces of each leg. the total vertical load acting on the structure is its self weight.

$$F_G = Self\ weight * g * 1.1 = 24690.24\ kN \tag{5.40}$$

Main Leg			Horizontal brace		
L	65.366	m	L	15.156	m
Dia	2.800	m	Dia	0.8	m
t	0.070	m	t	0.020	m
Vertical brace			**Gripper frame**		
L	26.130	m	L	46.45	m
Dia	0.8	m	Dia	2.95	m
t	0.020	m	t	0.07	m
Stiffener frame			**Suction bucket**		
L	46.45	m	D	9	m
Dia	1.50	m	L	18	m
t	0.04	m	t	0.15	m

Table 5.8: Dimension of the members

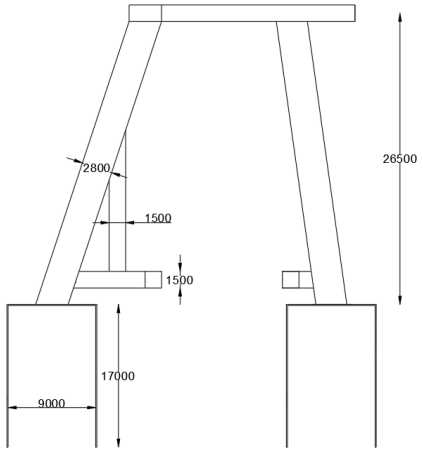

Figure 5.11: Front view of the tripod structure

Weight of the jacket structure		
Dry Weight	2772.9	ton
Buoyancy Weight	484.9	ton
Net Weight	2288	ton

Table 5.9: Weight of the tripod structure

Total base shear at seabed is sum of the hydrodynamic loads acting on the tripod structure and load from the monopile on the gripper as shown in figure5.13.

$$F_B = 23196 + 558.7 = 23754.7\ kN \tag{5.41}$$

The overturning moment with respect to seabed comprises of three parts.

- Due to the load from monopile on the gripper(topside),
- Due to hydrodynamic load,
- Due to eccentricity, as the structure is not symmetrical in axis.

The eccentricity is calculated in the x axis taking the center of the monopile as the origin(In figure 5.12, the plus in the center of the monopile is the origin). The eccentricity of the tripod and the topside (gripper frame) for both dry and submerged condition is shown in table 5.11.

To find the pile reaction the eccentricity while the structure is submerged is used. Moment due to eccentricity is the net weight of tripod and gripper multiplied with their respective eccentricity and factor of safety of 1.1.

$$\begin{aligned} M_{eccentricity} &= (W_{Tripod} * e(x)_{Tripod} + W_{Gripper} * e(x)_{Gripper}) * 9.81 * 1.1 \\ &= (1878.34 * -0.045 + 409.7 * -0.32) * 9.81 * 1.1 \\ &= -1510\ kNm \end{aligned} \tag{5.42}$$

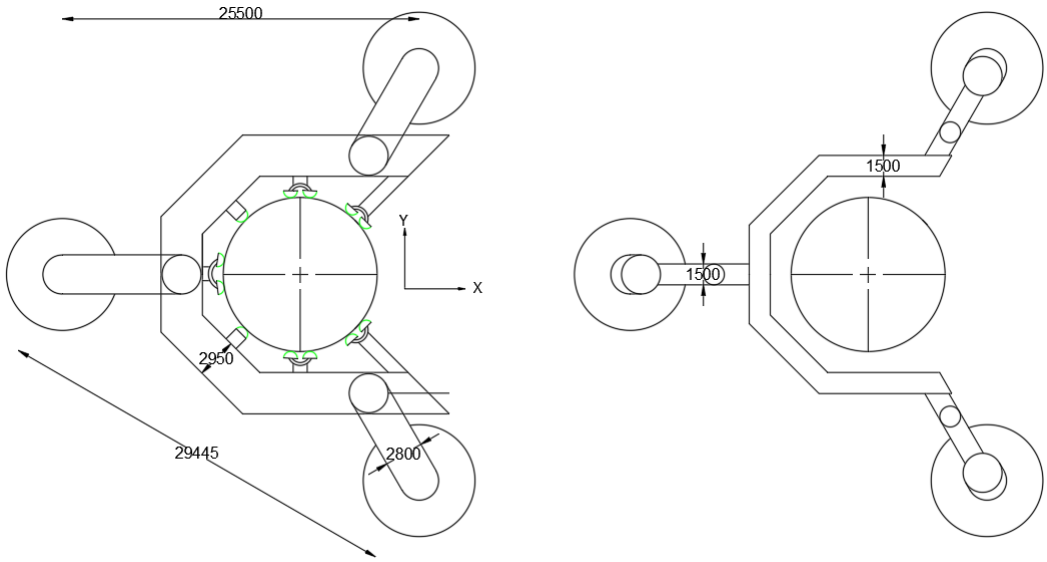

Figure 5.12: Top view of the tripod (Left: Gripper frame, Right: Stiffener frame)

Force at Nodes	Values	Unit
F1	142.6	kN
F2	209.4	kN
F3	206.8	kN
M1	3672	kNm
M2	2852.6	kNm
M3	465.2	kNm
F_{SB}	**558.7**	**kN**
M_{SB}	**6989.8**	**kNm**

Table 5.10: Loads on the nodes and total load w.r.t seabed

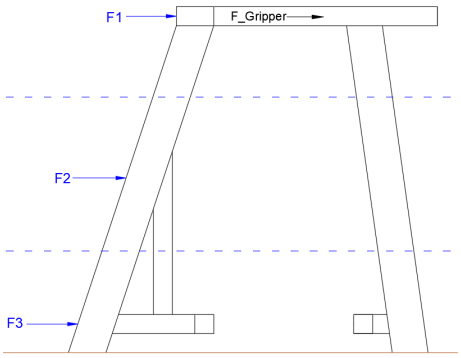

Figure 5.13: Loads acting on the nodes

All the three moments are added to account for the worst case scenario of all loads and moment acts in the same direction. The total overturning moment is,

$$\begin{aligned} M_O &= M_t + M_{hydro} + M_{eccentricity} \\ &= 23196 * 26.5 + 6989.8 + 1510 = 623201.5\ kNm \end{aligned} \tag{5.43}$$

With these final loads (F_G,F_B and M_O), the pile reactions can be found. The considered loading direction is shown in figure 5.14. It is assumed that only two legs will carry load (one leg with compression and one leg with tension loading).

The connection point between the main leg and the suction bucket is taken as fixed condition. Reaction forces due to environmental loads for suction bucket are,

$$P_{tE} = \frac{F_B}{3} = 7918.3\ kN \tag{5.44}$$

$$P_{mE} = 0 \tag{5.45}$$

	Dry condition (m)	Submerged (m)
$e(x)_{tripod}$	-0.02	-0.045
$e(x)_{Gripper}$	-0.3	-0.32

Table 5.11: Eccentricity for Tripod structure

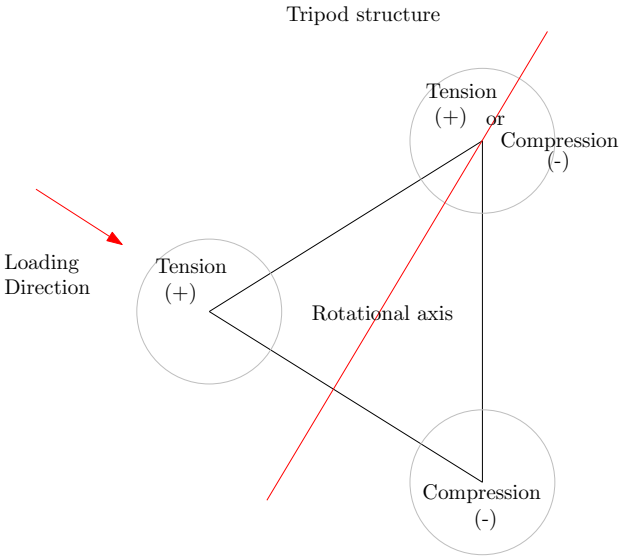

Figure 5.14: Loading direction and rotation axis

$$P_{aE} = \frac{M_{OE}}{b_e} = 21113.7\ kN \tag{5.46}$$

where,

b_e - width between two legs = 29.45 m

Reaction forces due to permanent and vertical loads for suction bucket are,

$$P_{aG1} = \frac{M_{OG}}{b_e} - \frac{F_G}{3} = -7873.9\ kN \tag{5.47}$$

$$P_{aG2} = \frac{M_{OG}}{b_e} + \frac{F_G}{3} = 7976.46\ kN \tag{5.48}$$

$$P_{tG} = 0\ ;\ P_{mG} = 0 \tag{5.49}$$

The combined pile reactions for suction bucket are,

$$P_t = P_{tE} = 7918.3\ kN \tag{5.50}$$

$$P_{a1} = P_{aE} + P_{aG1} = 13239.75\ kN\ (Tension) \tag{5.51}$$

$$P_{a2} = P_{aE} + P_{aG2} = 29090.12\ kN\ (Compression) \tag{5.52}$$

5.5.5. Design of the suction bucket

The design of the suction bucket is based on ”Suction Installed Caisson Foundations for Offshore Wind: Design Guidelines” [26]. The properties of the sand are same as the ones used for designing helical piles. As it is assumed that the loads act at the connection point between the main leg and the suction bucket (Load Reference Point - Red), they are converted to the base and side of the suction bucket(Blue). Here the external friction and lateral pressure on the skirt will play a role. The following expression can be made from the figure 5.15.

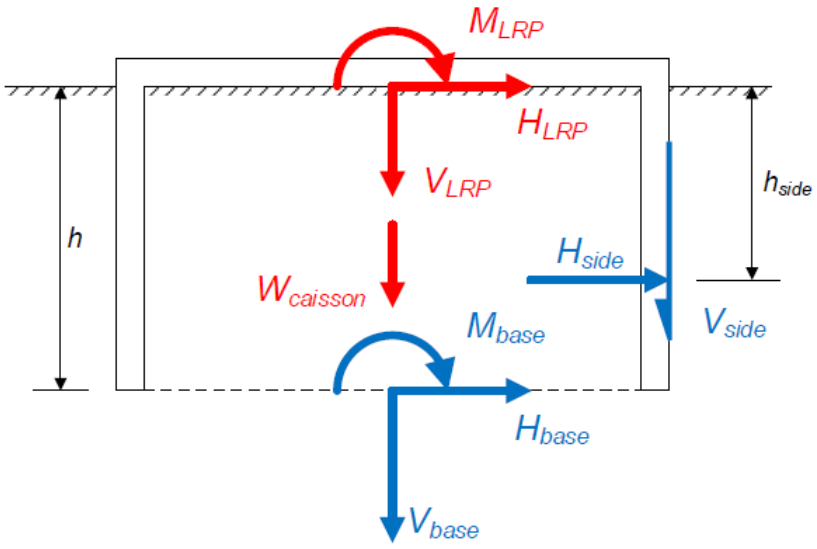

Figure 5.15: Load - capacity conversion [26]

[1]

The dimension of the suction bucket is shown in table 5.12

Description	Value	unit
D_o	9	m
L	18	m
t	0.15	m

Table 5.12: Dimension of suction bucket

$$V_{LRP} + W_{caisson} = V_{base} + V_{side} \tag{5.53}$$

where,

$W_{caisson}$ - includes soil trapped in it (i.e: including $\frac{\pi D_i^2 h\gamma'}{4}$)

$$H_{LRP} = H_{base} + H_{side} \tag{5.54}$$

$$M_{LRP} = M_{base} - h_{side}H_{side} - hH_{base} \tag{5.55}$$

The vertical compression loading capacity from the side of the caisson is,

$$V_{side} = (\pi Dh)\frac{\gamma' h}{2} K tan\delta = 33604.7kN \tag{5.56}$$

[1]Suction caisson = Suction bucket

where,

$Ktan\delta$ - friction factor used in pile capacity analysis

The horizontal loading capacity from the side of the caisson is,

$$H_{side} = \frac{\gamma' h^2 D}{2}(K_p - K_a) = 30006\ kN \tag{5.57}$$

where,

K_a, K_p - active and passive earth pressure coefficients = $K_p = \frac{1}{K_a} = \frac{1+sin\phi'}{1-sin\phi'}$

ϕ' - angle of internal friction of sand

A_{eff} - area of the base of the footing

The horizontal load act at an effective depth and is given in the equation below.

$$h_{side} = \frac{2h}{3} \tag{5.58}$$

The bearing capacity at the skirt tip level is,

$$V_{base} = A_{eff}\left(\frac{1}{2}\gamma' B_{eff} N_\gamma s_\gamma d_\gamma i_\gamma + \gamma' h N_q s_q d_q i_q\right) \tag{5.59}$$

where,

N_q, N_γ - conventional bearing capacity factor

$$N_q = tan^2\left(\frac{\pi}{4} + \frac{\phi'}{2}\right)e^{\pi tan\phi'} = 10.66 \tag{5.60}$$

$$N_\gamma = 1.5(N_q - 1)tan\phi' = 6.76 \tag{5.61}$$

s_q, s_γ - shape factors

$$s_q = 1 + i_q\left(\frac{B'}{L'}\right)sin\phi' = 1.21 \tag{5.62}$$

$$s_\gamma = 1 - 0.4 i_\gamma\left(\frac{B'}{L'}\right) = 0.8 \tag{5.63}$$

d_q - depth factor

$$d_q = 1 + 1.2\left(\frac{h}{B'}\right)tan\phi'(1 - sin\phi')^2 = 1.37 \tag{5.64}$$

i_q, i_γ -load inclination factor

$$i_q = 1 - 0.5\left(\frac{H_{base}}{V_{base}}\right)^5 = 1 \tag{5.65}$$

$$i_\gamma = 1 - 0.7\left(\frac{H_{base}}{V_{base}}\right)^5 = 1 \tag{5.66}$$

The A_{eff} changes if the suction bucket is considered as either plugged or unplugged. Taking the worst case scenario of unplugged condition, the V_{base} is,

$$V_{base} = 14315.16\ kN \tag{5.67}$$

The total compression capacity of the suction bucket in unplugged condition is,

$$V_{compression} = 33604.75 + 14315.16 = 47919.9\ kN \tag{5.68}$$

A factor of safety of 1.5 is taken for the compression loading [64]. From equation 5.51, the design compression load is 29395, which is below the capacity available 47919.9 / 1.5 = 31946.6 (Unity check is 0.92 <= 1). Hence, it is safe in tensile loading condition.

For the vertical tensile loading, there are two cases: 1. rapid (undrained loading) and slow (drained) loading.

For rapid loading, tensile capacity may be very high and invariably controlled by cavitation under the footing base or caisson lid [26]. It is assumed that there is full communication of free water into the void. The ultimate load is calculated as smaller of the following, For cavitation at footing base:

$$V_{ult,t} = \frac{\pi D^2}{4}\gamma' h + \pi D \frac{\gamma' h^2}{2} K tan\delta = 32810\ kN \tag{5.69}$$

For cavitation below caisson lid:

$$V_{ult,t} = 2\pi D \frac{\gamma' h^2}{2} K tan\delta = 42717.9\ kN \tag{5.70}$$

For slow loading, the tensile resistance is only from friction on the sides and is the same as equation 5.70.

As the support structure is used for a short term purpose, it is considered as rapid loading and the tensile capacity should meet equation 5.69. A factor of safety of 2 is taken for the tensile loading [64]. From equation 5.51, the design tensile load 12934.85, which is below the capacity available 32810 / 2 = 16405 (Unity check is 0.788 <= 1). Hence, it is safe in tensile loading condition.

6

Finite Element Analysis of the selected concepts

The next step is to see how the structures responds to the loads in different loading conditions. For this, Finite Element Analysis (FEA) is done using the software ANSYS Parametric Design Language (APDL).

6.1. Jacket structure with helical piles

At the beginning, the structure is analysed without including the foundation and the soil. The legs at the bottom are assumed as fixed. This is done to understand the response of the structure. In later stage, soil model is included and the final optimisation of the members will be done.

6.1.1. Modelling

Some of the input parameters used for modelling are,

- The center line of the members are used to create the model.
- The material model is taken as Linear - Elastic - Isotropic with a young's modulus of 210000 N/mm^2 and Poisson ratio of 0.3.
- The members are modelled as 3D beams (BEAM 188) and the soil springs as COMBIN39 (non-linear springs)
- The section of the members are given the size same as the initial dimensions.

Using a K bracing for the top bay was not optimal because the load transfer was not efficient. So, the top bay is changed to X bracing and the load transfer was better compared to K bracing.

The created model in ANSYS with the new X bracing is shown in figure 6.1.

In the front view, it is seen that the joints (connection) at 1,2,3,4 have some gap between the members. This is to have easy and proper welding of members during the fabrication of the structure. The loads were applied for each load conditions and solved and the response of the structure is noted.

After solving the model, the forces and moments acting in each member is taken from ANSYS and checked according to the NORSOK Standard [37]. A figure plotted with von mises stress for condition 2 is shown in figure 6.2

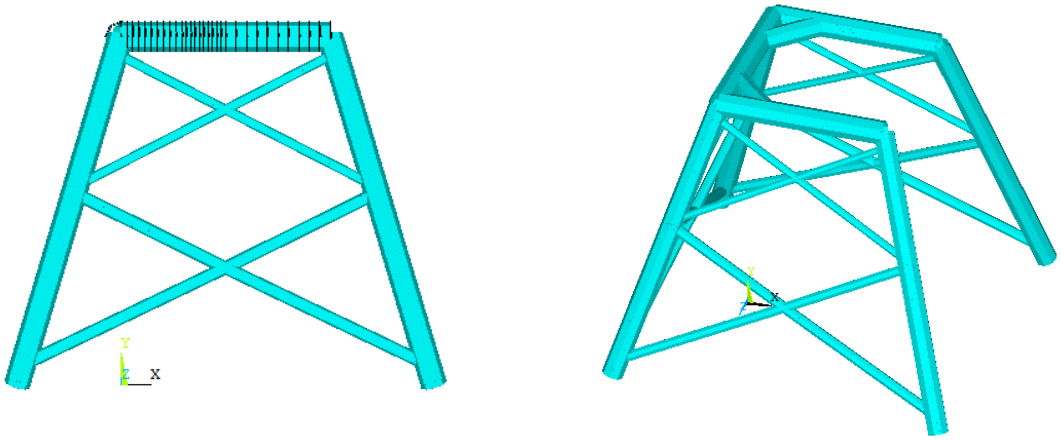

(a) Front View (b) Oblique View

Figure 6.1: ANSYS model of the jacket structure

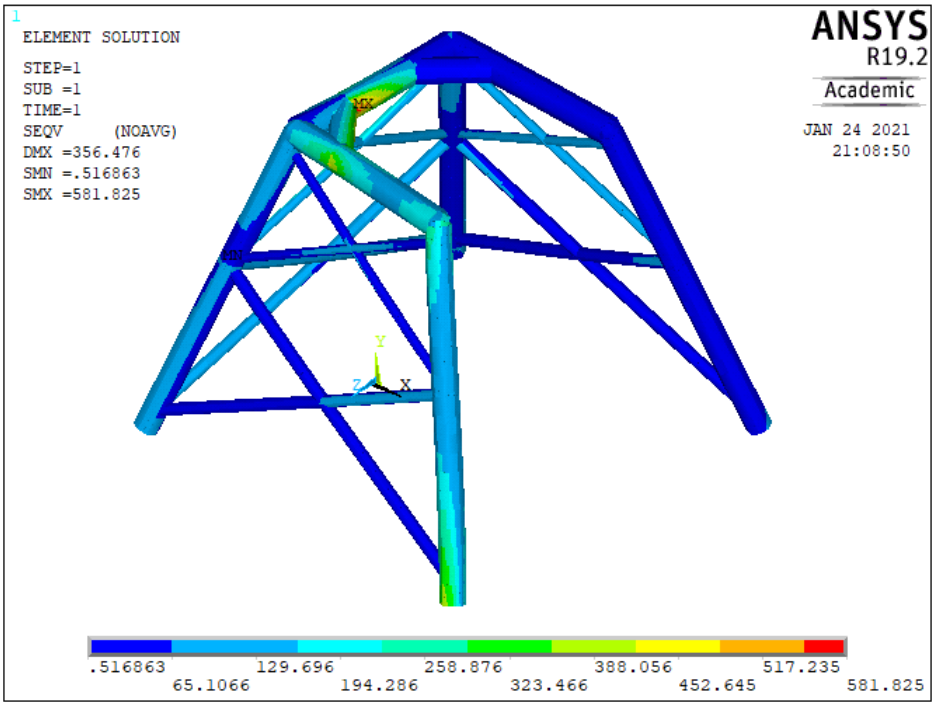

Figure 6.2: von mises stress for condition 2

The critical loading condition is condition 2 (from figure 5.4) where the stresses in the members are high as it is concentrated more on a single frame. This condition will govern the member design of the entire structure. As the response of the structure is understood, the soil model is included in the structure. The nonlinear p-y curve for the helical pile is created according to DNVGL - RP - C212[4] and the steps are shown from equations 6.1 till 6.4.

$$p = A\, p_u tanh\left(\frac{k\, X}{A\, p_u} y\right) \tag{6.1}$$

where,

p_u - static ultimate lateral resistance (min of these two)

$$= (C_1X + C_2D)\gamma'X$$
$$= C_3D\gamma'X \quad (6.2)$$

C_1, C_2, C_3 - coefficients depend on friction angle and is shown in figure 6.3

y - deflection

A - factor to account for static or cyclic loading

$$A = 3 - 0.8\frac{X}{D} - for\ static\ loading \quad (6.3)$$

D - shaft diameter of the pile

X - depth below the spoil surface

k - initial modulus of subgrade

$$k = 2.21 + 0.0584D_r + 0.0166D_r^2 \quad (6.4)$$

D_r - relative density = 20% for loose soil

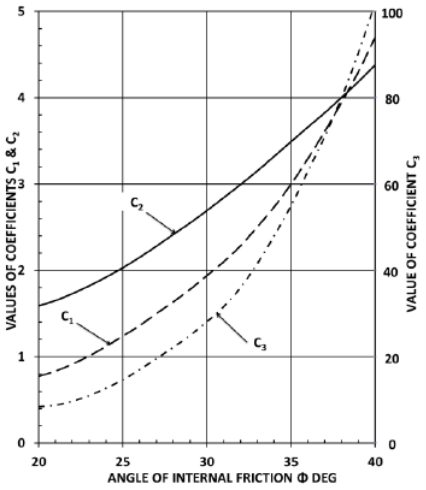

Figure 6.3: Coefficients C1, C2, C3 [4]

The p-y curves per 0.5 m are generated and the values are imported in ANSYS. p-y curve at 10 m depth is shown in figure 6.4 to show an illustration of the curve.These forces are applied to the soil model as nonlinear springs in X and Z direction(i.e: for each 0.5 m depth of the pile the respective force and displacement is taken). The end of the pile is restricted in vertical direction (Y axis) for both displacement (U_y) and rotation (ROT_y). The figure 6.5 shows the model of the jacket structure with pile.

The results from this soil model is used to get the forces ($F_x, F_y, F_z, M_x, M_y, M_z$) acting within each member from ANSYS. These values are for the local axis of the member and the axis is shown in figure 6.6. In the figure, X,Y,Z are global axis, x,y,z are local axis and I is the start point of the beam and J is the end point of the beam. With these forces the critical members are checked for safety. The grades of the steel are chosen according to EN 10025-4 [8], where the yield strength of the steel is decreasing for increasing thickness and is shown in figure6.1

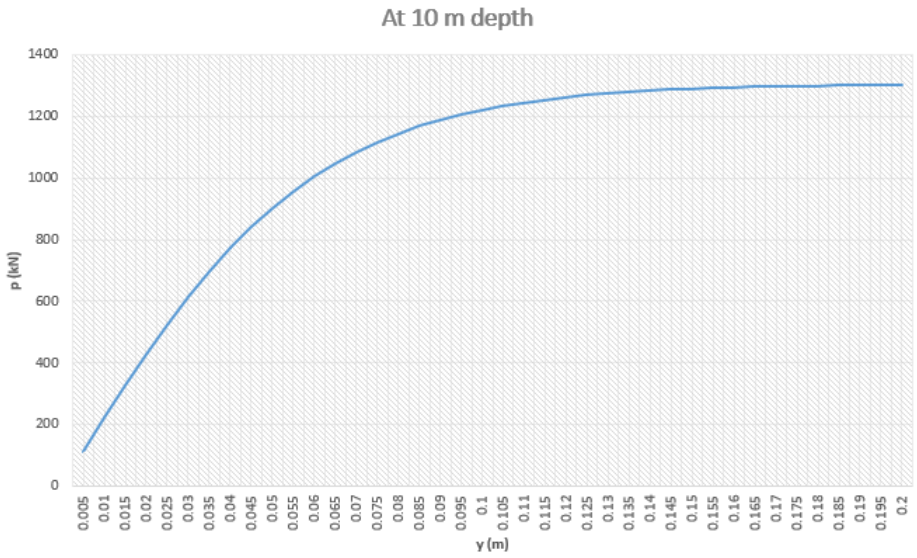

Figure 6.4: p-y curve at 10 m depth

6.1.2. Design check using NORSOK 10025 -4

The different checks performed using NORSOK code are,

Axial tension

$$N_{Sd} \leq N_{t,Rd} = \frac{Af_y}{\gamma_m} \tag{6.5}$$

where,

N_{Sd} - design axial force (tension positive) [F_x, input from ansys]

f_y - characteristic yield strength

A - cross sectional area - $\frac{\pi}{4}(D_o^2 - D_i^2)$

γ_M - material factor = 1.15

Axial compression

$$N_{Sd} \leq N_{c,Rd} = \frac{Af_c}{\gamma_m} \tag{6.6}$$

where,

N_{Sd} - design axial force (compression positive) [F_x, input from ANSYS]

γ_M - material factor = 1.15

f_c - characteristic axial compression strength

$$\begin{aligned} f_c &= [1 - 0.28\lambda'^2]f_{cl} \qquad for\ \lambda' \leq 1.34 \\ f_c &= \frac{0.9}{\lambda'^2}f_{cl} \qquad for\ \lambda' > 1.34 \end{aligned} \tag{6.7}$$

where,

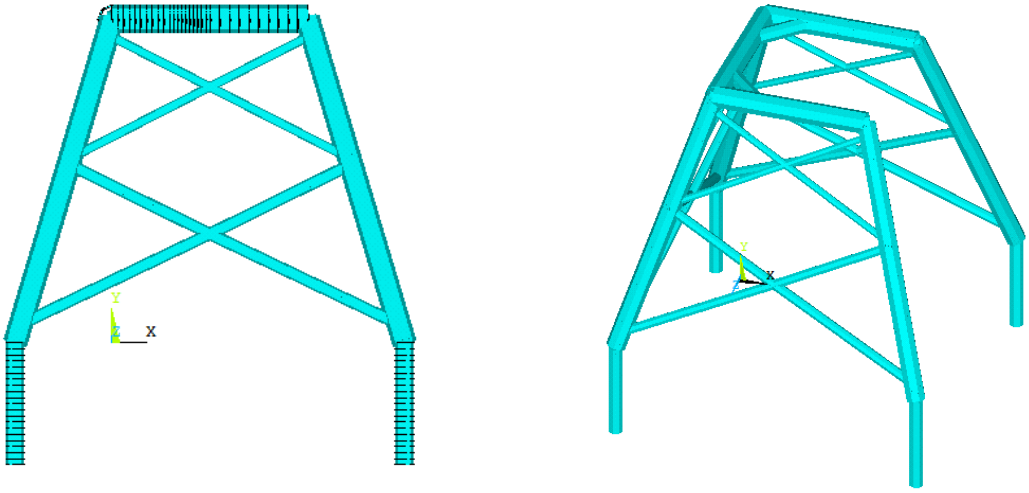

(a) Front View (b) Oblique View

Figure 6.5: ANSYS model of the jacket structure including pile

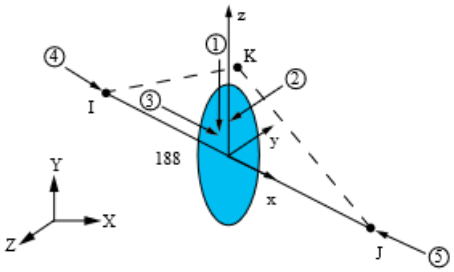

Figure 6.6: Local axis of the beam

λ' - column slenderness parameter

$$\lambda' = \sqrt{\frac{f_{cl}}{f_e}} = \frac{kl}{\pi i}\sqrt{\frac{f_c l}{E}} \tag{6.8}$$

where,

i - radius of gyration - $\frac{\sqrt{D_o^2+D_i^2}}{4}$

E - Young's modulus of elasticity = 21000 N/mm^2

k - effective length factor

f_{cl} - characteristic local buckling strength

l - longer unbraced length in y or z direction - For jacket legs the whole length is used for the check to be conservative. For other members, the true length is used.

Designation		Minimum yield strength R_{eH} [a] MPa						Tensile strength R_m [a] MPa					Minimum percentage elongation after fracture [b] % $L_0 = 5{,}65\sqrt{S_0}$
		Nominal thickness mm						Nominal thickness mm					
Steel name	Steel number	≤ 16	> 16 ≤ 40	> 40 ≤ 63	> 63 ≤ 80	> 80 ≤ 100	> 100 ≤ 150	≤ 40	> 40 ≤ 63	> 63 ≤ 80	> 80 ≤ 100	> 100 ≤ 150	
S275M S275ML	1.8818 1.8819	275	265	255	245	245	240	370 to 530	360 to 520	350 to 510	350 to 510	350 to 510	24
S355M S355ML	1.8823 1.8834	355	345	335	325	325	320	470 to 630	450 to 610	440 to 600	440 to 600	430 to 590	22
S420M S420ML	1.8825 1.8836	420	400	390	380	370	365	520 to 680	500 to 660	480 to 640	470 to 630	460 to 620	19
S460M S460ML	1.8827 1.8838	460	440	430	410	400	385	540 to 720	530 to 710	510 to 690	500 to 680	490 to 660	17
S500M S500ML	1.8829 1.8839	500	480	460	450	450	450	580 to 760	580 to 760	580 to 760	560 to 750	560 to 750	15

[a] For plate, strip and wide flats with widths ≥ 600 mm the direction transverse (t) to the rolling direction applies. For all other products the values apply for the direction parallel (l) to the rolling direction.

[b] For product thickness < 3 mm for which test pieces with a gauge length of $L_0 = 80$ mm shall be tested, the values shall be agreed upon at the time of the order.

Table 6.1: Yield strength table according to EN 10025-4[8]

$$f_{cl} = f_y \qquad for \qquad \frac{f_y}{f_{cle}} \leq 0.17$$
$$f_{cl} = \left(1.047 - 0.274\frac{f_y}{f_{cle}}\right) f_y \qquad for \qquad 0.17 < \frac{f_y}{F_{cle}} \leq 1.911 \tag{6.9}$$
$$f_{cl} = f_{cle} \qquad for \qquad \frac{f_y}{f_{cle}} > 1.911$$

$$f_{cle} = 2C_e E\frac{t}{D} \tag{6.10}$$

where,

C_e - critical elastic buckling coefficient = 0.3

t - wall thickness

D - outside diameter

Bending

$$M_{Sd} \leq M_{Rd} = \frac{f_m W}{\gamma_M} \tag{6.11}$$

where,

M_{Sd} - design bending moment = $\sqrt{M_y^2 + M_z^2}$ (input from ANSYS)

f_m - characteristic bending strength

$$f_m = \frac{Z}{W} f_y \qquad for \qquad \frac{f_y D}{Et} \leq 0.0517$$
$$f_m = \left(1.13 - 2.58\left(\frac{f_y D}{Et}\right)\right)\frac{Z}{W} f_y \qquad for \qquad 0.0517 < \frac{f_y D}{Et} \leq 0.1034 \tag{6.12}$$
$$f_m = \left(0.94 - 0.76\left(\frac{f_y D}{Et}\right)\right)\frac{Z}{W} f_y \qquad for \qquad 0.1034 < \frac{f_y D}{Et} \leq 120$$

where,

W - elastic section modulus

$$W = \frac{\pi}{32}\frac{[D^4 - (D - 2t)^4]}{D} \tag{6.13}$$

Z - plastic section modulus

$$Z = \frac{1}{6}[D^3 - (D - 2t)^3] \tag{6.14}$$

Shear

$$V_{Sd} \leq V_{Rd} = \frac{A f_y}{2\sqrt{3}\gamma_M} \tag{6.15}$$

where,

V_{Sd} - design shear force = $\sqrt{F_y^2 + F_z^2}$ (input from ANSYS)

Tubular member subjected to shear from torsional moment should be designed to statisfy the following condition,

$$M_{T,Sd} \leq M_{T,Rd} = \frac{2 I_p f_y}{D\sqrt{3}\gamma_M} \tag{6.16}$$

where,

$M_{T,Sd}$ - design torsional moment = M_x (input from ANSYS)

I_p - polar moment of inertia

$$I_p = \frac{\pi}{32}[D^4 - (D - 2t)^4] \tag{6.17}$$

Hydrostatic pressure

$$\sigma_{p,Sd} \leq f_{h,Rd} = \frac{f_h}{\gamma_M} \tag{6.18}$$

where,

f_h - characteristic hoop buckling strength

$\sigma_{p,Sd}$ - design hoop stress due to hydrostatic pressure

$$\sigma_{p,Sd} = \frac{p_{Sd} D}{2t} \tag{6.19}$$

p_{Sd} - design hydrostatic pressure = $\rho_w g d = \frac{1025*9.81*55}{10^6} = 0.553\ N/mm^2$

$$\begin{aligned} f_h &= f_y && for && f_{he} > 2.44 f_y \\ f_h &= 0.7 f_y \left[\frac{f_{he}}{f_y}\right]^{0.4} && for && 2.44 f_y \geq f_{he} > 0.55 f_y \\ f_h &= f_{he} && for && f_{he} \leq 0.55 f_y \end{aligned} \tag{6.20}$$

$$f_{he} = 2 C_h E \frac{t}{D} \tag{6.21}$$

$$\begin{aligned} C_h &= 0.44\frac{t}{D} && for && \mu \geq 1.6\frac{D}{t} \\ C_h &= 0.44\frac{t}{D} + 0.21\frac{\frac{D}{t})^3}{\mu^4} && for && 0.825\frac{D}{t} \leq \mu < 1.6\frac{D}{t} \\ C_h &= \frac{0.737}{(\mu - 0.579)} && for && 1.5\frac{D}{t} \leq \mu < 0.825\frac{D}{t} \\ C_h &= 0.8 && for && \mu < 1.6\frac{D}{t} \end{aligned} \tag{6.22}$$

$$\mu = \frac{L}{D}\sqrt{\frac{2D}{t}} \tag{6.23}$$

where,

L - Length of tubular between stiffening rings,diaphragms or end connections

μ - geometric parameter

Material factor

The material factor γ_M is given as,

$$\begin{aligned} \gamma_M &= 1.15 && for && \lambda_s' < 0.5 \\ \gamma_M &= 0.85 + 0.6\lambda_s' && for && 0.5 \leq \lambda_s' \leq 1.0 \\ \gamma_M &= 1.45 && for && \lambda_s' > 1.0 \end{aligned} \tag{6.24}$$

where,

$$\lambda_s' = \frac{|\sigma_{c,Sd}|}{f_{cl}}\lambda_c + \left(\frac{\sigma_{p,Sd}}{f_h}\right)^2 \lambda_h \tag{6.25}$$

$$\lambda_c = \sqrt{\frac{f_y}{f_{cle}}}; \qquad \lambda_h = \sqrt{\frac{f_y}{f_{he}}} \tag{6.26}$$

$$\sigma_{c,Sd} = \frac{N_{Sd}}{A} + \frac{\sqrt{M_{y,Sd}^2 + M_{z,Sd}^2}}{W}$$

N_{Sd} is negative if in tension. The material factor for the above equations are calculated based on equation 6.24.

Tubular members subjected to combined loads without hydrostatic pressure are,

Axial tension and bending

$$\left(\frac{N_{Sd}}{N_{t,Rd}}\right)^{1.75} + \frac{\sqrt{M_{y,Sd}^2 + M_{z,Sd}^2}}{M_{Rd}} \leq 1.0 \tag{6.27}$$

Axial compression and bending

$$\frac{N_{Sd}}{N_{c,Rd}} + \frac{1}{M_{Rd}}\left[\left[\frac{C_{my}M_{y,Sd}}{1-\frac{N_{Sd}}{N_{Ey}}}\right]^2 + \left[\frac{C_{mz}M_{z,Sd}}{1-\frac{N_{Sd}}{N_{Ez}}}\right]^2\right]^{0.5} \leq 1.0 \tag{6.28}$$

$$\left(\frac{N_{Sd}}{N_{cl,Rd}}\right)^{1.75} + \frac{\sqrt{M_{y,Sd}^2 + M_{z,Sd}^2}}{M_{Rd}} \leq 1.0 \tag{6.29}$$

where,

C_{my} - moment reduction factor corresponds to y axes - c) from table 6.7 for all members

C_{mz} - moment reduction factor corresponds to z axes- c) from table 6.7 for all members

k_y - effective length corresponds to y axes - 1 for legs, 0.8 for X brace, 0.7 for gripper frame members - from table 6.7

k_z - effective length corresponds to z axes - 1 for legs, 0.8 for X brace, 0.7 for gripper frame members - from table 6.7

N_{Ey} - Euler buckling strength corresponds to y axes

N_{Ez} - Euler buckling strength corresponds to z axes

$N_{cl,rd}$ - design axial local buckling resistance

$$N_{cl,Rd} = \frac{f_{cl}A}{\gamma_M} \tag{6.30}$$

$$N_{Ey} = \frac{\pi^2 EA}{\left[\frac{kl}{i}\right]_y^2} \quad ; \quad N_{Ez} = \frac{\pi^2 EA}{\left[\frac{kl}{i}\right]_z^2} \tag{6.31}$$

Interaction shear and bending moment

$$\begin{aligned} &\frac{M_{Sd}}{M_{Rd}} \leq \sqrt{1.4 - \frac{V_{Sd}}{V_{Rd}}} \qquad for \qquad \frac{V_{Sd}}{V_{Rd}} \geq 0.4 \\ &\frac{M_{Sd}}{M_{Rd}} \leq 1.0 \qquad\qquad\qquad for \qquad \frac{V_{Sd}}{V_{Rd}} < 0.4 \end{aligned} \tag{6.32}$$

Structural element	k	C_m [1]
Superstructure legs		
- Braced	1.0	(a)
- Portal (unbraced)	k[2]	(a)
Jacket legs and piling		
- Grouted composite section	1.0	(c)
- Ungrouted jacket legs	1.0	(c)
- Ungrouted piling between shim points	1.0	(b)
Jacket braces		
- Primary diagonals and horizontals	0.7	(b) or (c)
- K-braces[3]	0.7	(c)
- Longer segment length of X-braces[3]	0.8	(c)
Secondary horizontals	0.7	(c)

Notes:
1. C_m values for the cases defined in Table 6-2 are as follows:
   (a) 0.85
   (b) for members with no transverse loading,
   $C_m = 0.6 - 0.4\ M_{1,Sd}/M_{2,Sd}$,
   where $M_{1,Sd}/M_{2,Sd}$ is the ratio of smaller to larger moments at the ends of that portion of the member unbraced in the plane of bending under consideration. $M_{1,Sd}/M_{2,Sd}$ is positive when the number is bent in reverse curvature, negative when bent in single curvature.
   (c) for members with transverse loading,
   $C_m = 1.0 - 0.4\ N_{Sd}/N_E$, or 0.85, whichever is less, and $N_E = N_{Ey}$ or N_{Ez} as appropriate.
2. Use effective length alignment chart in Clause 12.
3. At least one pair of members framing into the a K- or X-joint shall be in tension if the joint is not braced out-of-plane. For X-braces, when all members are in compression, the k-factor should be determined using the procedures given in Clause 12.
4. The effective length and C_m factors given in Table 6-2 do not apply to cantilever members and the member ends are assumed to be rotationally restrained in both planes of bending.

Figure 6.7: Effective length and moment reduction factor[37]

Interaction shear, bending moment and torsional moment

$$\frac{M_{Sd}}{M_{Red,Rd}} \leq 1.0\sqrt{1.4 - \frac{V_{Sd}}{V_{Rd}}} \qquad for \qquad \frac{V_{Sd}}{V_{Rd}} \geq 0.4$$
$$\frac{M_{Sd}}{M_{Red,Rd}} \leq 1.0 \qquad for \qquad \frac{V_{Sd}}{V_{Rd}} < 0.4 \tag{6.33}$$

$$M_{Red,Rd} = \frac{W f_{m,Red}}{\gamma_M}; \qquad f_{m,Red} = f_m\sqrt{1 - 3\left(\frac{\tau_{T,Sd}}{f_d}\right)^2} \tag{6.34}$$

$$\tau_{T,Sd} = \frac{M_{T,Sd}}{2\pi R^2 t}; \qquad f_d = \frac{f_y}{\gamma_M} \tag{6.35}$$

Tubular members subjected to combined loads with hydrostatic pressure are given below. The equation in this section are not applicable if the equation 6.18 fails. There are two methods given in the code. Method A assumes that the capped end compressive force due to external hydrostatic pressure are not included in the structural analysis[37]. Method B assumes that such forces are included in the analysis [37].s

In this model, such forces are not included. So, method A is followed in this combined check.

Axial tension, bending and hydrostatic pressure

(a) $\sigma_{a,Sd} \geq \sigma_{q,Sd}$ - net axial tension condition

$$\frac{\sigma_{a,Sd} - \sigma_{q,Sd}}{f_{th,Rd}} + \frac{\sqrt{\sigma_{my,Sd}^2 + \sigma_{my,Sd}^2}}{f_{mh,Rd}} \leq 1.0 \tag{6.36}$$

where,

$\sigma_{a,Sd}$ - design axial stress (tension positive) = $\frac{F_x}{A}$

$\sigma_{q,Sd}$ - axial compression stress due to eternal hydrostatic pressure = 0.5 $\sigma_{p,Sd}$

$\sigma_{my,Sd}$ - design in-plane bending stress = $\frac{M_y y}{I_{yy}} = \frac{M_y D}{2I_{yy}}$

$\sigma_{mz,Sd}$ - design out of plane bending stress = $\frac{M_z z}{I_{zz}} = \frac{M_z D}{2I_{zz}}$

$$f_{th,Rd} = \frac{f_y}{\gamma_M}[\sqrt{1 + 0.09B^2 - B^{2\eta}} - 0.3B] \tag{6.37}$$

$$f_{mh,Rd} = \frac{f_m}{\gamma_M}[\sqrt{1 + 0.09B^2 - B^{2\eta}} - 0.3B] \tag{6.38}$$

$$B = \frac{\sigma_{p,Sd}}{f_{h,Rd}}; \qquad B \leq 1.0; \qquad \eta = 5 - 4\frac{f_h}{f_y} \tag{6.39}$$

(b) $\sigma_{a,Sd} < \sigma_{q,Sd}$ **- net axial compression condition**

$$\frac{|\sigma_{a,Sd} - \sigma_{q,Sd}|}{f_{cl,Rd}} + \frac{\sqrt{\sigma_{my,Sd}^2 + \sigma_{my,Sd}^2}}{f_{mh,Rd}} \leq 1.0 \tag{6.40}$$

$$f_{cl,Rd} = \frac{f_{cl}}{\gamma_M}$$

When $\sigma_{c,Sd} > 0.5\frac{f_{he}}{\gamma_M}$ and $f_{cle} > 0.5 f_{he}$, then this equation should be satisfied,

$$\frac{\sigma_{c,Sd} - 0.5\frac{f_{he}}{\gamma_M}}{\frac{f_{cle}}{\gamma_M} - 0.5\frac{f_{he}}{\gamma_M}} + \left[\frac{\sigma_{p,Sd}}{\frac{f_{he}}{\gamma_M}}\right]^2 \leq 1.0 \tag{6.41}$$

$$\sigma_{c,Sd} = \sigma_{m,Sd} + \sigma_{q,Sd} - \sigma_{a,Sd} \tag{6.42}$$

Axial compression, bending and hydrostatic pressure

$$\frac{\sigma_{a,Sd}}{f_{ch,Rd}} + \frac{1}{f_{mh,Rd}}\left[\left[\frac{C_{my}\sigma_{my,Sd}}{1 - \frac{\sigma_{a,Sd}}{f_{Ey}}}\right]^2 + \left[\frac{C_{mz}\sigma_{mz,Sd}}{1 - \frac{\sigma_{a,Sd}}{f_{Ez}}}\right]^2\right]^{0.5} \leq 1.0 \tag{6.43}$$

$$\frac{\sigma_{a,Sd} + \sigma_{q,Sd}}{f_{cl,Rd}} + \frac{\sqrt{\sigma_{my,Sd}^2 + \sigma_{my,Sd}^2}}{f_{mh,Rd}} \leq 1.0 \tag{6.44}$$

where,

$\sigma_{a,Sd}$ - design axial stress (compression positive)

$f_{ch,Rd}$ - design axial compression strength in the presence of external hydrostatic pressure

$$f_{Ey} = \frac{\pi^2 E}{\left[\frac{kl}{i}\right]_y^2} \qquad ; \qquad f_{Ez} = \frac{\pi^2 E}{\left[\frac{kl}{i}\right]_z^2} \tag{6.45}$$

$$f_{ch,Rd} = \frac{f_{cl}}{2\gamma_M}\left[\xi - \frac{2\sigma_{q,Sd}}{f_{cl}} + \sqrt{\xi^2 + 1.12\lambda'^2\frac{\sigma_{q,Sd}}{f_{cl}}}\right] \quad for\ \lambda' < 1.34\sqrt{\left[1 - \frac{2\sigma_{q,Sd}}{f_{cl}}\right]^{-1}} \tag{6.46}$$

$$f_{ch,Rd} = \frac{0.9 f_{cl}}{\lambda'^2\gamma_M} \qquad for \qquad \gamma' \geq 1.34\sqrt{\left[1 - \frac{2\sigma_{q,Sd}}{f_{cl}}\right]^{-1}} \tag{6.47}$$

$$\xi = 1 - 0.28\lambda' \tag{6.48}$$

When $\sigma_{c,Sd} > 0.5\frac{f_{he}}{\gamma_M}$ and $f_{cle} > 0.5 f_{he}$, then this equation should be satisfied,

$$\frac{\sigma_{c,Sd} - 0.5\frac{f_{he}}{\gamma_M}}{\frac{f_{cle}}{\gamma_M} - 0.5\frac{f_{he}}{\gamma_M}} + \left[\frac{\sigma_{p,Sd}}{\frac{f_{he}}{\gamma_M}}\right]^2 \leq 1.0 \tag{6.49}$$

$$\sigma_{c,Sd} = \sigma_{m,Sd} + \sigma_{q,Sd} + \sigma_{a,Sd} \tag{6.50}$$

All the checks mentioned above need to be satisfied. These checks are done for all the critical members in all the loading conditions. A sample calculation of the main leg of the jacket for condition 2 which is critical is shown in figure B.1. The final optimal configuration derived from these checks is given in figures 6.8,6.9 and 6.10. In the figure, the brown circle represents the armour layer.

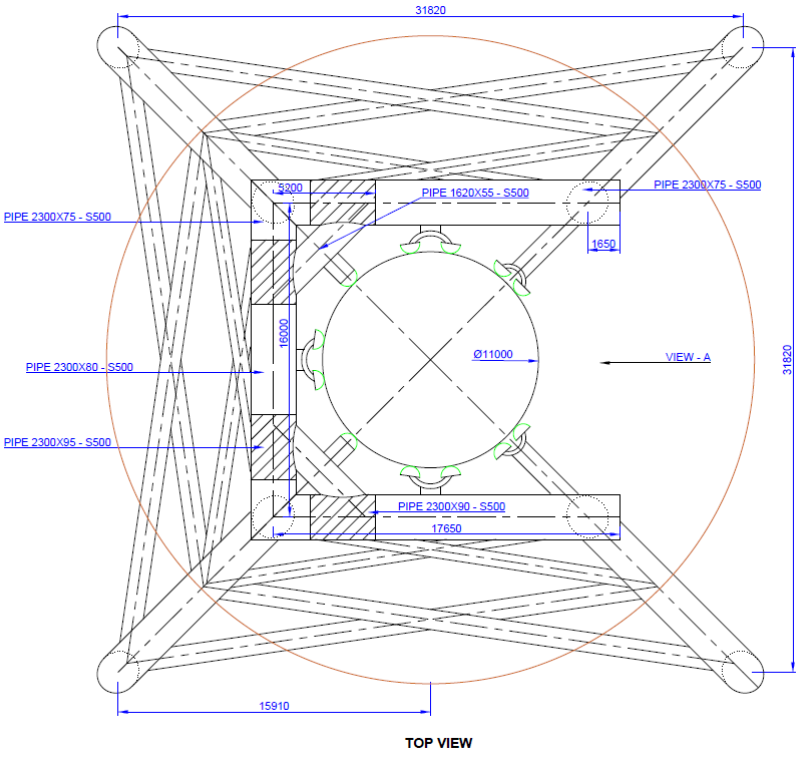

Figure 6.8: Jacket final configuration - Top View

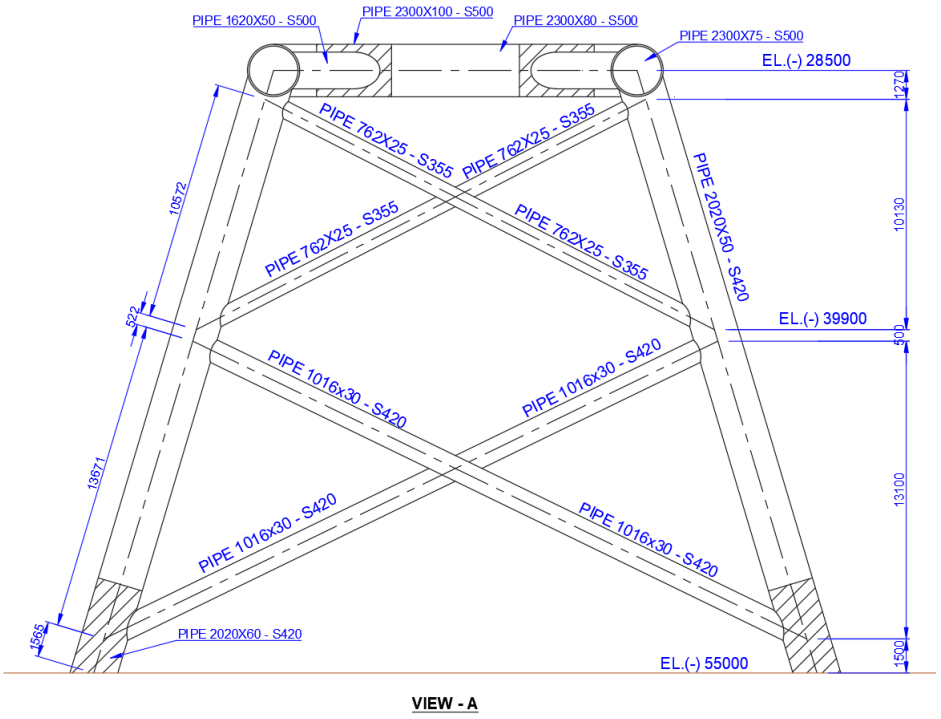

VIEW - A

Figure 6.9: Jacket final configuration - View - A

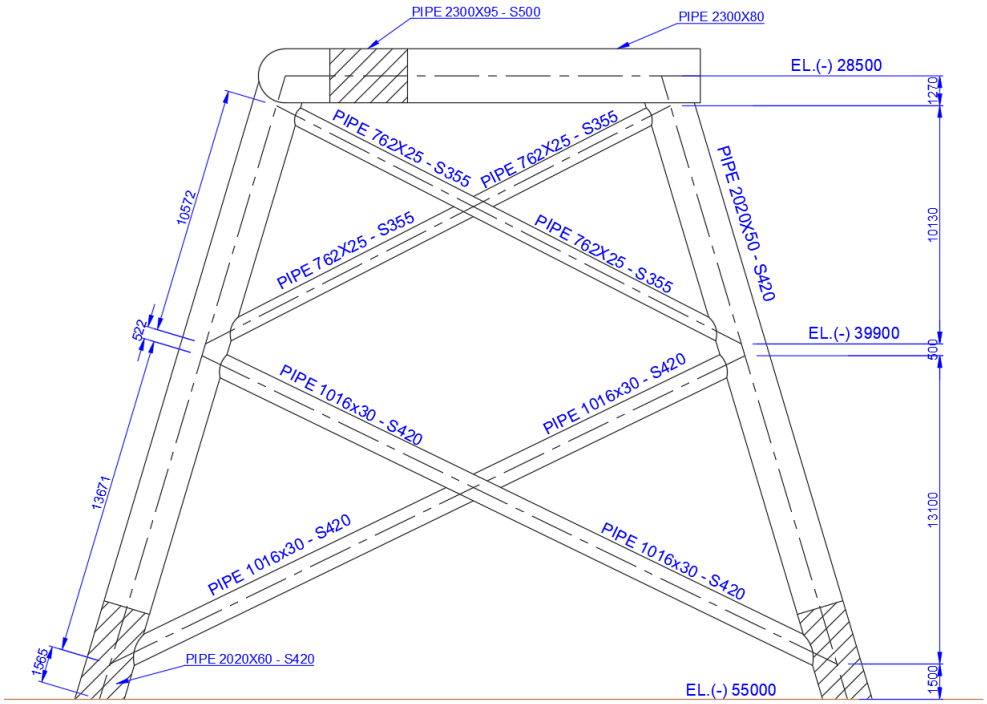

FRONT VIEW

Figure 6.10: Jacket final configuration - Front View

As seen from the figures 6.8,6.9,6.10, most of the members are designed with higher grade steel. As one side of the structure is open, the jacket couldn't distribute the loads properly throughout all the members. For example, if the loading condition is 2 applied, the stress

distribution within the structure is concentrated only on one side (can be seen in figure 6.2). The bottom right leg takes most of the loads. For conditions 1,2,3 the loads act at one frame which makes the gripper frame to open up. It causes high stress in the gripper frame due to in-plane and out-of plane bending. To resist these high stresses, increased thickness of the members are needed. Instead of increasing the thickness of the members very much, high strength steel is used. Also the increase in thickness leads to decrease in yield strength of steel as shown in table 6.1. Increasing the thickness of a member by 10mm will be costly when compared to adopting high strength steel. This reduces the amount of steel used, self-weight of the structure and the cost associated. The check done for the critical member of the gripper frame using low grade steel and high grade steel and their influence in the thickness is shown in table 6.11. From table, it is seen that for a low grade steel of S355 a thickness of 105mm is needed for the member to be safe. While using a high grade steel of S500, the thickness is reduced to 80mm.

Do =	2.3	m
Di =	2.09	m
t =	0.105	m
fy =	320	N/mm2

Tension	Nt	0.0605	<=1	SAFE
Compression	Nc	NA	<=1	NA
Moment	Mb	0.937	<=1	SAFE
Shear	Vs	0.176	<=1	SAFE
Torsion	Ts	0.283	<=1	SAFE
Hydrostatic pressure	Fh	0.012	<=1	SAFE
Tension & Moment	Nt , Mb	0.94	<=1	SAFE
Compression & Moment	Nc , Mb	NA	<=1	NA
Shear & Moment	Vs , Mb	0.937	<=1	SAFE
Shear, Moment & Torsion	Vs,Mb,Ts	0.967	<=1	SAFE
Tension,Bending & Hydrostatic	Nt,Mb,Fh	0.995	<=1	SAFE
		NA	<=1	NA
Compression, Bending & Hydrostatic	Nc,Mb,Fh	NA	<=1	NA
		NA	<=1	NA

(a) Low grade steel with increased thickness

Do =	2.3	m
Di =	2.14	m
t =	0.08	m
fy =	450	N/mm2

Tension	Nt	0.05583	<=1	SAFE
Compression	Nc	NA	<=1	NA
Moment	Mb	0.881	<=1	SAFE
Shear	Vs	0.162	<=1	SAFE
Torsion	Ts	0.255	<=1	SAFE
Hydrostatic pressure	Fh	0.014	<=1	SAFE
Tension & Moment	Nt , Mb	0.89	<=1	SAFE
Compression & Moment	Nc , Mb	NA	<=1	NA
Shear & Moment	Vs , Mb	0.881	<=1	SAFE
Shear, Moment & Torsion	Vs,Mb,Ts	0.905	<=1	SAFE
Tension,Bending & Hydrostatic	Nt,Mb,Fh	0.935	<=1	SAFE
		NA	<=1	NA
Compression, Bending & Hydrostatic	Nc,Mb,Fh	NA	<=1	NA
		NA	<=1	NA

(b) High grade steel with lower thickness

Figure 6.11: Unity checks according to NORSOK 10025-4

Even though the members are safe, the joints are always subjected to failure. This is because they are subjected to multi-axial loading. Therefore, the checks for the joints are done according to Norsok Standard N-004. The different type of simple joints and their parameters are given in figure 6.12.

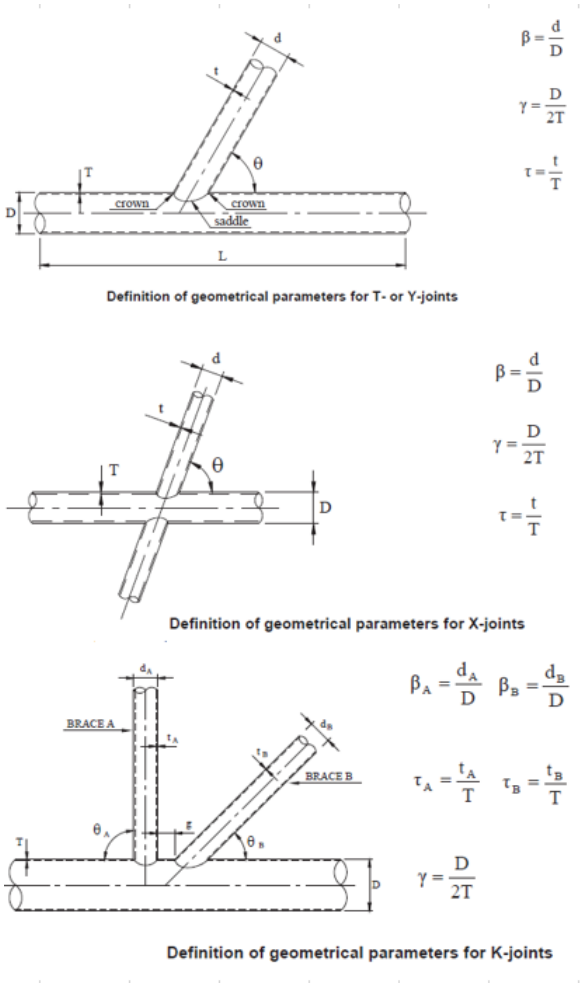

Figure 6.12: Different types of simple joints[37]

The characteristic resistance for simple tubular joints are,

$$N_{Rd} = \frac{f_y T^2}{\gamma_M sin\theta} Q_u Q_f \tag{6.51}$$

$$M_{Rd} = \frac{f_y T^2 d}{\gamma_M sin\theta} Q_u Q_f \tag{6.52}$$

where,

N_{Rd} - joint design axial resistance

M_{Rd} - joint design bending moment resistance

f_y - yield strength of the chord member

γ_M - material factor - 1.15

Q_u - strength factor

Q_f - chord action factor

The strength factor (Q_u) depends on the type of joint and the action of the brace. This is shown in figure 6.13.

Joint Classification	Brace action			
	Axial Tension	Axial Compression	In-plane Bending	Out-of-plane bending
K	$\min\begin{cases}(16+1.2\gamma)\beta^{1.2}Q_g \\ 40\beta^{1.2}Q_g\end{cases}$		$(5+0.7\gamma)\beta^{1.2}$	$2.5+(4.5+0.2\gamma)\beta^{2.6}$
Y	30β	$\min\begin{cases}2.8+(20+0.8\gamma)\beta^{1.6} \\ 2.8+36\beta^{1.6}\end{cases}$		
X	$6.4\,\gamma^{(0.6\beta^2)}$	$(2.8+(12+0.1\gamma)\beta)Q_\beta$		

Figure 6.13: Strength factor Q_u [37]

1. Q_β is a geometric factor given as,

$$\begin{aligned} Q_\beta &= \frac{0.3}{\beta(1-0.833\beta)} \qquad for \qquad \beta > 0.6 \\ Q_\beta &= 1 \qquad for \qquad \beta \le 0.6 \end{aligned} \tag{6.53}$$

2. Q_g is a gab factor given as,

$$\begin{aligned} Q_g &= 1 + 0.2\left(1 - \frac{2.8g}{D}\right)^3 \qquad for \qquad \frac{g}{D} \ge 0.0, but Q_g \ge 1.0 \\ Q_g &= 0.13 + 0.65\phi\gamma^0.5 \qquad for \qquad \frac{g}{D} \le -0.05 \end{aligned} \tag{6.54}$$

where,

$\phi \quad = \frac{t f_{y,b}}{T f_{y,c}}$

$f_{y,b}$ - yield strength of brace (or brace stub if present)

$f_{y,c}$ - yield strength of the chord (or chord can if present)

The chord action factor (Q_f) accounts for the presence of factored actions in the chord.

$$\begin{aligned} Q_f &= 1.0 + C_1\frac{\sigma_{a,Sd}}{f_y} - C_2\frac{\sigma_{my,Sd}}{1.62f_y} - C_3A^2 \\ A^2 &= \left(\frac{\sigma_{a,Sd}}{f_y}\right)^2 + \left(\frac{\sigma_{my,Sd}^2 + \sigma_{mz,Sd}^2}{1.62f_y^2}\right) \end{aligned} \tag{6.55}$$

where,

$\sigma_{a,Sd}$ - design axial stress in chord, positive in tension

$\sigma_{my,Sd}$ - yield strength of brace (or brace stub if present)

$\sigma_{mz,Sd}$ - yield strength of the chord (or chord can if present)

C_1, C_2, C_3 - coefficients depending on joint and load type as given in figure 6.14

Joint type	C_1	C_2	C_3
K joints under balanced axial loading	0.2	0.2	0.3
T/Y joints under brace axial loading	0.3	0	0.8
X joints under brace axial tension loading 1)			
$\beta \leq 0.9$	0	0	0.4
$\beta = 1.0$	0.2	0	0.2
X joints under brace axial compression loading 1)			
$\beta \leq 0.9$	0.2	0	0.5
$\beta = 1.0$	-0.2	0	0.2
All joints under brace moment loading	0.2	0	0.4

Figure 6.14: Values for C_1, C_2, C_3[37]

For a brace intersection with the chord, the chords average loads and bending moment on either side of the intersection should be used in equation 6.55.

Strength of the joint is checked by the interaction equation for axial force and bending moment and is shown below.

$$\frac{N_{Sd}}{N_{Rd}} + \left(\frac{M_{y,Sd}}{M_{y,Rd}}\right)^2 + \frac{M_{z,Sd}}{M_{z,Rd}} \leq 1.0 \tag{6.56}$$

where,

N_{Sd} - design axial force in the brace member

N_{Rd} - joint design axial resistance

$M_{y,Sd}$ - design in-plane bending moment in the brace member

$M_{y,Rd}$ - design in-plane bending resistance

$M_{z,Sd}$ - design out-of-plane bending moment in the brace member

$M_{z,Rd}$ - design out-of-plane bending resistance

The joint checks are done according to the above equations and the final strengthened joints are shown in figures 6.8, 6.9 and 6.10. From the figures, it is seen that the joints between the gripper frame members are strengthened more. As explained in the member checks, the high bending stress causes the failure of the joints. An example of a joint check for one of the joint in the gripper frame is show in table B.1.

The figures 6.8,6.9,6.10 represents the optimised designed of the jacket structure based on ULS conditions but not the final design. Fatigue analysis (Chapter-8) will be done and the the structure will be optimised accordingly. The final optimised design can be found in that chapter.

6.2. Tripod structure with suction bucket

The procedure for the tripod structure is same as followed in the analysis of the jacket structure. Therefore the changes and the results will be mentioned here. The created model of the tripod in ANSYS is shown in figure 6.15. ‘A figure plotted with von mises stress for condition 2 is shown in figure 6.16.

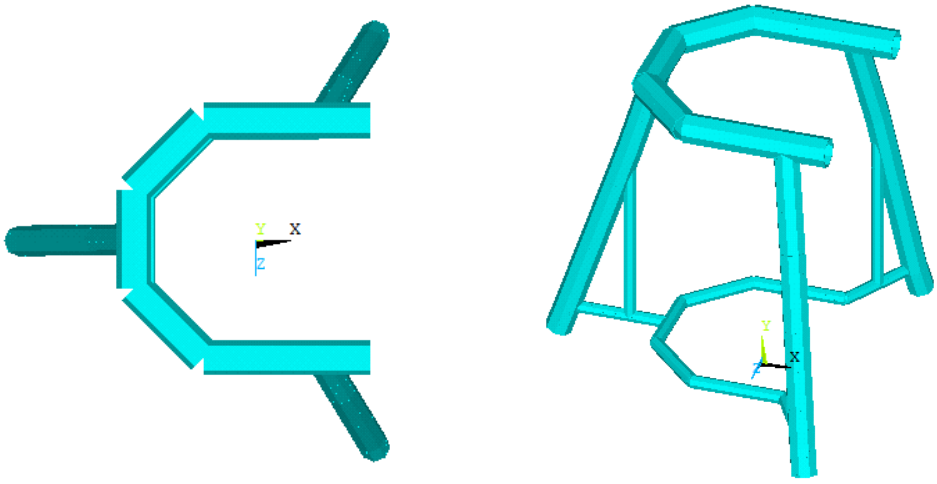

(a) Top View (b) Oblique View

Figure 6.15: ANSYS model of the tripod structure

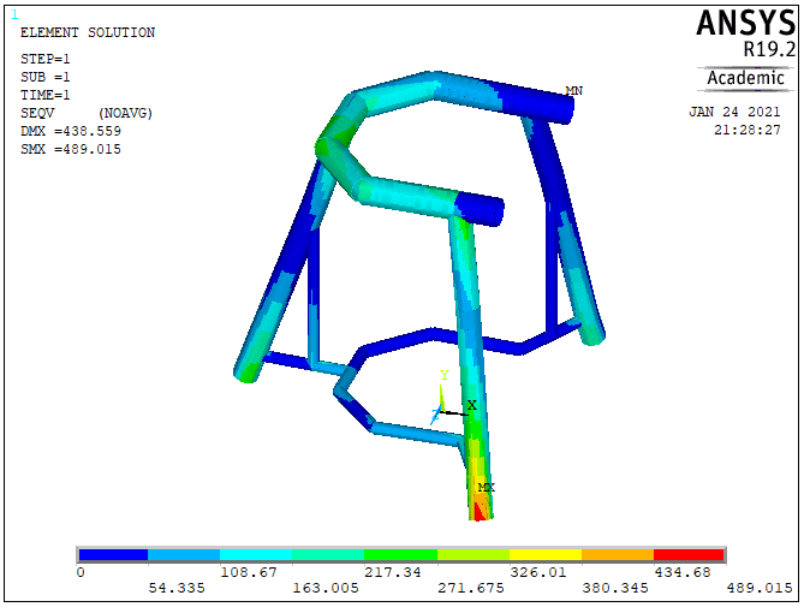

Figure 6.16: Von mises stress plot of the tripod structure for Condition 2

The p-y curve of the suction bucket per 0.5 m is calculated based on DNVGL-RP-C212 [4] and applied as a non linear soil spring in X and Z direction. The steps are shown from equations 6.1 till 6.4. The bottom of the suction is constrained in vertical Y axis for both displacement(U_y) and rotation(ROT_y). The p-y curve at 10 m depth is shown in figure 6.17.

During the check, the connection between the gripper frame and the main leg was failing due to high moments. In figure 6.16, for condition 2 loading, it can be seen that the loads acting are concentrated on one leg with compression and the other two legs are experiencing tension. As the legs and gripper frame doesn't have any support members, the moments acting on the members are high so that the thickness needs to increase more. So, in-order to avoid a large increase in thickness, a support member which connects the gripper frame and the main leg is provided. The new model with the new member and suction bucket is shown in figure 6.18.

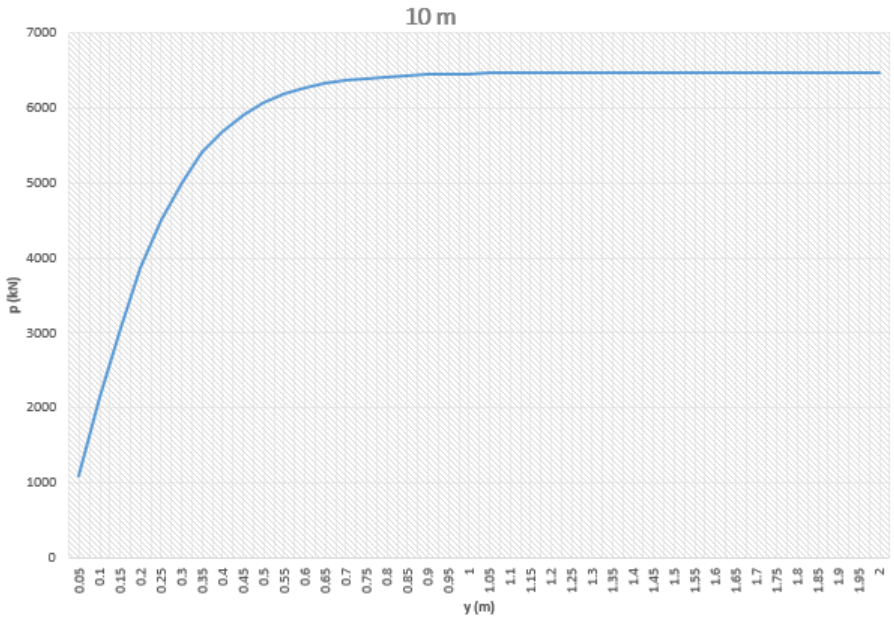

Figure 6.17: p-y curve for suction bucket at 10 m depth

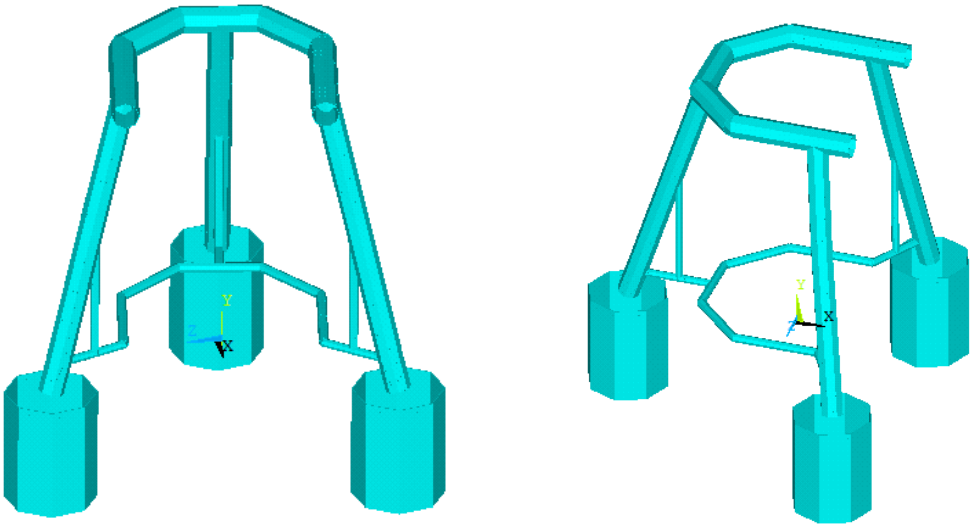

(a) Side view

(b) Oblique View

Figure 6.18: New model of the tripod structure

After the analysis is done, the members are checked based on NORSOK 10025-4 [37] which is described from equation 6.5 till 6.1.2. The joint checks are also done based on the equations from 6.51 till 6.56. The final configuration of the structure with strengthened members and joints is shown in figures 6.19,6.20 and 6.21. Although the new members help in transferring the load properly by reducing stresses on the gripper frame, the joints tend to fail. As seen in figure 6.19, the gripper frame has so many joints that need to be strengthened. For the horizontal member of the gripper frame, it has 5 tubular members welded together with different thickness. But in fabrication process it maybe be easy to have one member of the whole length with the maximum thickness(i.e: 0.11 m in this case) needed. Still the cost associated with increase in steel can be high. This really depends on the fabricator, so a conclusion can't be made at this point to choose either of these two option.

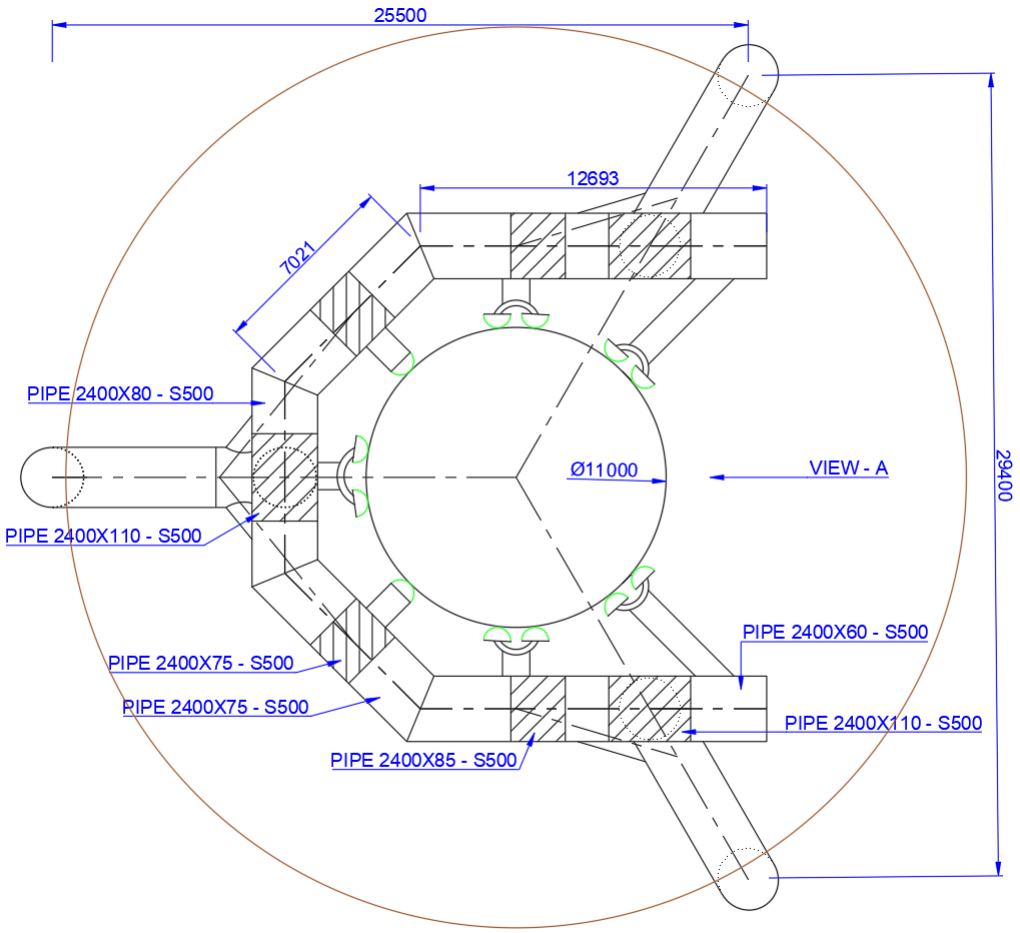

Figure 6.19: Tripod final configuration - Top view

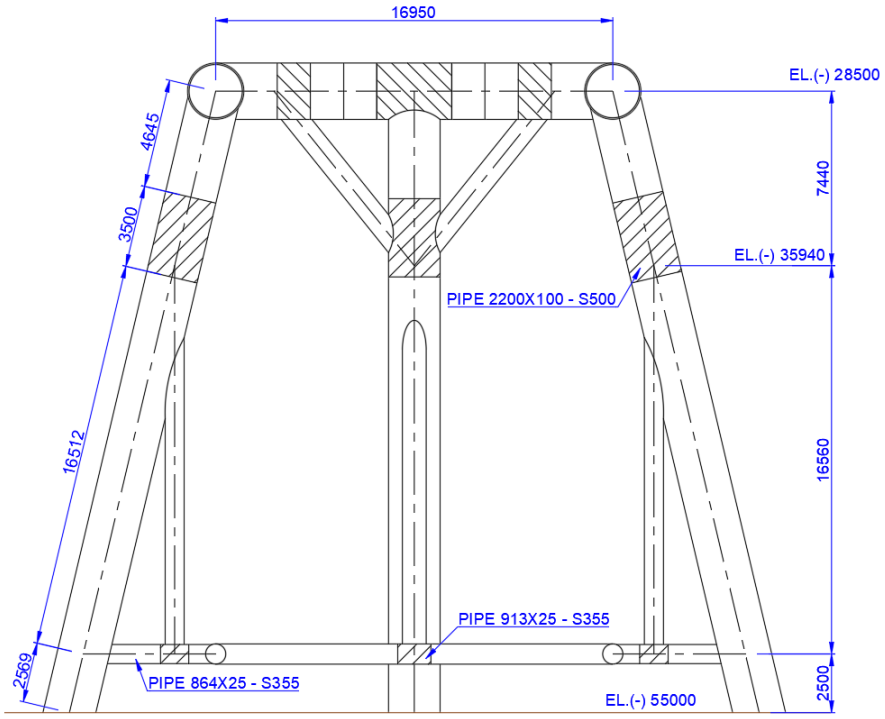

Figure 6.20: Tripod final configuration - View - A

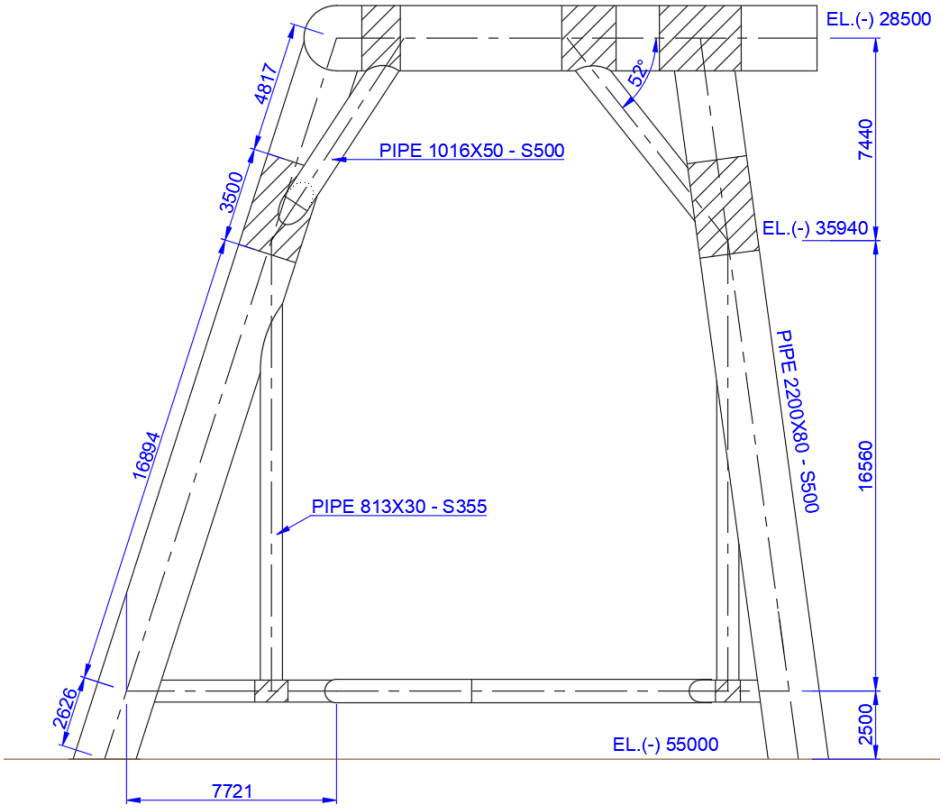

Figure 6.21: Tripod final configuration - Front view

6.3. Impact loading on the support structure

When the monopile is lowered and slewed in to the gripper frame, wave load act on the monopile which makes the monopile oscillate. During this operation the monopile may hit the side of the gripper frame which acts as impact force and induces vibrations (refer figure:6.22). In this thesis, only the impact of the force is calculated and analysed. The vibrations will be of more importance if the magnitude of the vibration is higher due to large impact force. Fenders can be provided on the gripper frame which absorb the kinetic energy thus reducing the impact force and damage.

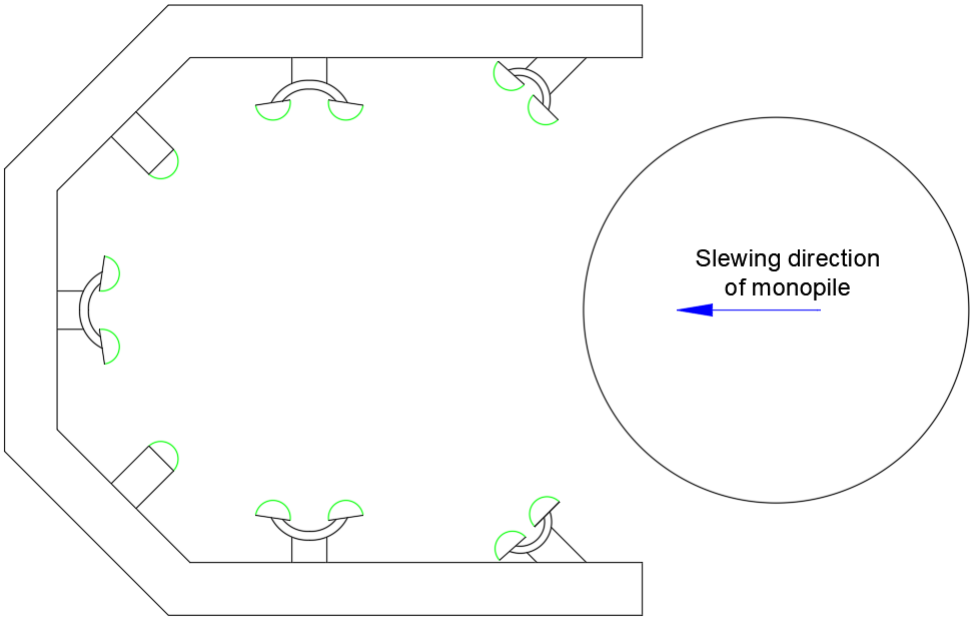

Figure 6.22: Slewing of monopile inside the gripper frame

The velocity of the water at the depth where the gripper frame is present is 0.01 m/s. The wave velocity is neglected because this velocity makes the monopile incline and the inclined monopile will be slewed and hit the support structure .The maximum operating crane velocity is taken as 0.1 m/s. The velocity of the current is neglected, as the influence of the current develops over time. In this case it is a matter of few minutes to lower and slew the monopile inside the gripper frame. Therefore, the total velocity of the monopile is equal to the velocity of the crane of 0.1 m/s.

The slewing direction is the same as the loading direction 5 as shown in figure 5.4. The global stiffness of the structure is found by the formula:

$$k = \frac{F}{d}\ kN.m \tag{6.57}$$

where,

k - global stiffness of the structure in slewing direction (kN.m)

F - Force applied in slewing direction (kN)

d - Displacement in slewing direction due to the applied load (m) (The global displacement is got from ANSYS for both the jacket and tripod structure)

With the displacement values from table 6.2, the global stiffness for the slewing direction is found for both the jacket structure and the tripod structure. The displacement and the respective stiffness is shown in table 6.2.

Concept	d (m)	k (MN/m)
Jacket	0.037	628.9
Tripod	0.105	219.1

Table 6.2: Displacement and stiffness of the structures in the slewing direction

The monopile hitting the gripper structure can be simplified as a mass hitting a spring. The gripper structure is taken as a spring because it is not fully rigid. It has certain stiffness as seen in table 6.2. The figure6.23 shows the illustration of the mass spring system.

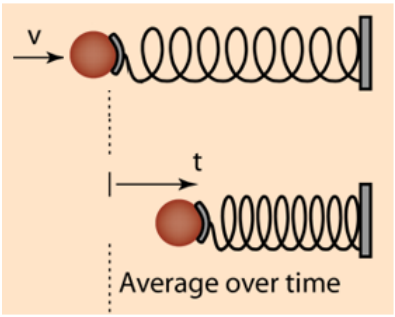

Figure 6.23: Mass spring system for impact force

In the figure 6.23, the first system shows the mass moves with a velocity(v) and hits the spring. The time at the point of contact between the mass and the spring is zero (i.e: t =0) and the initial velocity is v = 0.11 m/s (velocity of monopile).

In the second system, the mass came to rest (i.e: v = 0 m/s) in a time interval by impacting with the spring. The nature of simple harmonic motion is used to find the time interval. The time taken to bring the mass to rest is taken as the one-forth($\pi/2$) of a period of the periodic motion as seen in figure 6.24. The elastic motion would follow Hooke's law with a force constant k.

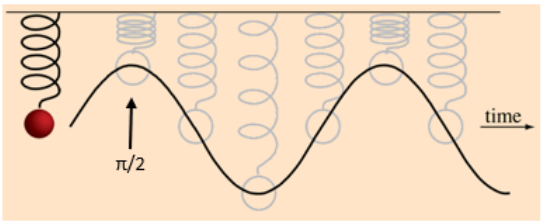

Figure 6.24: Mass spring system for impact force

The impact force of the monopile on the structure is given by,

$$F_{avg} = \frac{(m+a)v}{\Delta t} \tag{6.58}$$

where,

F_{avg} - average force of impact (N)

m - mass of the monopile (kg)

a - added mass of the monopile (inside and outside) (kg)

v - velocity of the monopile (m/s)

Δt - time taken for the monopile to come to rest, $\Delta t = \frac{\pi}{2}\sqrt{\frac{m}{k}}$ (s)

k - stiffness of the structure (N.m)

When the monopile is submerged in water, the water inside the monopile will act as a added mass along with the mass of the monopile. As the thickness of the monopile will be relatively smaller compared to the diameter of the monopile, the inner diameter is taken as the outer diameter. the added mass inside the monopile is given as,

$$a_{in} = \frac{\pi}{4}\rho_{water} D^2 l_{sub} \tag{6.59}$$

where,

a_{in} - added mass inside the monopile (kg)

ρ_{water} - density of water = 1025 (kg/m^3)

D - diameter of the monopile (m)

l_{sub} - submerged length of the monopile in water = 50m (assuming that the monopile is slewed in when it is 5m above the seabed)

The added mass outside the monopile when the monopile is translated perpendicular to the monopile vertical axis is given by,

$$a_{out} = c_a \frac{\pi}{4}\rho_{water} D^2 l_{sub} \tag{6.60}$$

where,

c_a - function of shape = 1

The total added mass acting on the structure is 9741 tonnes. After substituting in equation 6.58, it becomes as shown below and the impact force for both the jacket and the tripod is calculated.

$$\begin{aligned} F_{avg} &= \frac{2}{\pi} v \sqrt{(m+a)k} \\ &= 5.7\ MN\ (on\ jacket) \\ &= 3.36\ MN\ (on\ tripod) \end{aligned} \tag{6.61}$$

As seen from above equation the impact force for the jacket and tripod is different. This is because, the stiffness of the structure is different. When the stiffness of the structure is higher, the impact force is higher, this can be seen in the above equation. As seen in equation 6.58, impact force depends on time. When the time taken for the object to come to rest is lower the force increases. Stiffer structures tends to stop the colliding mass sooner than a less stiff structure. This explains why the impact force on the jacket structure is larger than the tripod structure.

7

Soil - Structure interaction

The type of support structure investigated in this project is new to the offshore industry. For this reason, the assessment of the soil-structure interaction is significant in this project.

In this project, a whole new support structure is installed on the seabed to install a monopile and then the support structure is removed. As there are no structures that has been installed in a manner like this, it is hard to predict the exact response of the soil and the structure.

The soil-structure interaction is discussed below based on the installation sequence of the support structure and the monopile.

7.1. Installation of the support structure

When installing and removing the support structure foundations, the footprint created by these foundations may be compared to the spud can of a jack-up leg.

The influence of the suction bucket and the helical pile maybe less than the spud cans. Because the installation of suction bucket causes some changes in the soil near to it's skirt. But studies show that the outside skirt friction is not changed during the installation of the suction bucket [27][28][29]. This means that the influence of the installation of suction bucket is very less.

For helical piles, the installation causes some degradation of the soil shear strength near the helix for clay soil. Due to the screwing of helical pile in the soil, there is a large displacement within the envelope region causing the soil to remold. This remolding causes the shear strength to change. This change has been studied for clay soil. It is shown that the shearing would occur due to the installation and it has minimal installation disturbance beyond the edge of the helices [15]. On the other hand, the installation disturbance is negligible for the soil below the bottom helix, as they do not experience shaft and helix penetration.

Some studies have been done before, where the spud cans penetrate near piles and the influence of the spud cans on the piles are observed. From these studies, it is shown that when the distance between the the spud can side and the pile foundation is over half the diameter of the spud cans, the displacement of pile's top may be neglected [38][39]. And also when the distance between the spud can and the pile increases the deflection of the pile decreases.

For this project there are four cases which are listed below.

1. Jacket structure with helical piles

- The distance between the side wall of the monopile and the side of the helix is 15 m, which is 3.75 times the diameter of the helical pile.

2. Jacket structure with suction bucket

   - The distance between the side wall of the monopile and the side of the suction bucket is 13 m, which is 1.625 times the diameter of the suction bucket.

3. Tripod with helical piles

   - The distance between the side wall of the monopile and the side of the helix is 9.5 m, which is 2.375 times the diameter of the helical pile.

4. Tripod with suction bucket

   - The distance between the side wall of the monopile and the side of the suction bucket is 7.5 m, which is 0.9375 times the diameter of the suction bucket.

For all the cases mentioned above, the distances are grater than the 0.5 times the diameter of the pile or suction bucket. This can be used as a reference at this stage that there may be negligible influence of helical pile or suction bucket on the soil around the monopile. Although, a detailed analysis would be good to understand the response clearly. This is the first stage of the installation process.

7.2. Hammering of monopile

Next the monopile is slewed into the gripper frame and hammered. The hammering of monopile produces sound wave in water, interface wave where the seafloor and water meet and seismic wave which disperses through the soil. These generated sound depends on the hammer and pile characteristics which differs per site or project.

These waves passing through the soil can change the characteristics of the soil. It is hard to predict the changes happening. In this project, only the base condition is used to design the foundation, but in reality there will be different soil conditions. Each and every soil conditions responds differently to these waves. The influence of hammering on the soil should be studied and analysed in detail.

As the support structures foundation is near to the monopile, the interface wave and the seismic wave can have an impact on the capacity of the foundations. The impact can have either a negative or a positive impact which is unknown at this point. A detailed analysis need to be done, to understand the response of the foundations to these waves due to hammering.

7.3. Removal of the support structure

After the installation of the monopile is finished, the support structure is removed. The suction buckets are removed by applying reverse suction and the helical piles are removed by unscrewing. After the removal of the foundations the soil characteristics of the volume of the soil where these foundations were installed can be different.

In practice the monopile and the transition piece is installed together first for the whole wind farm. Then the turbine and the blades are installed afterwards. The time taken between these two installation will be about few months to a year. The monopile will not be carrying the full load it is designed for between the time were the tower is installed. The soil can regain its original nature or characteristics during the time interval.

The loads acting on the monopile at the seabed will be base shear and overturning moment. The monopile rotates around a point at certain depth below the seabed based on the design and soil condition. When the monopile rotates at that point, the soil gets displaced which gives an opposing force to stop the rotation of the monopile. The influence of the monopile load on the soil depends mostly on the angle of internal friction for sand.

An example is shown in figure 7.2, how the monopile rotates at a point and the stress distribution on the surrounding soil. For sand it depends on double the angle of internal friction. The point of rotation is found to be at $d = 16m$ depth from the seabed using the simplified equations given below[65].

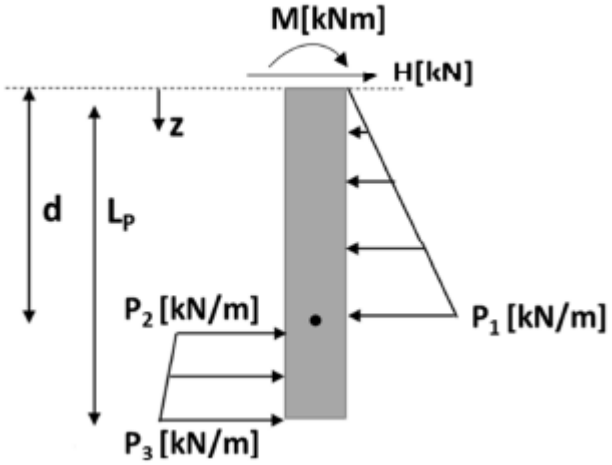

Figure 7.1: Ultimate pressure distribution in sandy soil

$$H - \left(\frac{1}{2} * P_1 * d\right) + \left(\frac{1}{2} * (P_3 - P_2) * (L_P - d)\right) + (P_2 * (L_P - d)) = 0 \quad (7.1)$$

$$M - \left(\frac{1}{2} * P_1 * d\right) + \left(\frac{1}{2} * (P_3 - P_2) * (L_P - d)\right) + (P_2 * (L_P - d)) * \quad (7.2)$$

$$\left(d + \frac{2 * (L_P - d)}{3}\right) + (P_2 * (L_P - d)) * \left(d + \frac{(L_P - d)}{2}\right) = 0 \quad (7.3)$$

The distance from the side wall of monopile and the end of the influence area (x) is given by:

$$Distance\ (X) = tan(\phi) * 16 = 7.46m \quad (7.4)$$

where,

ϕ - angle of internal friction of sand = 25^{ϕ}

If the support structures foundation is away from this area, there will be negligible interaction. In this project, for case 1, the distance is greater than the influential distance. There will be negligible interaction. For case 2, as there are overlapping at the end of the influence area, there will be interaction but not significant. For case 3,4 the distance between the monopile and the foundation is about half of the influential distance. Therefore the interaction will be more in case 3,4. Detailed analysis is needed to find the response of the monopile.

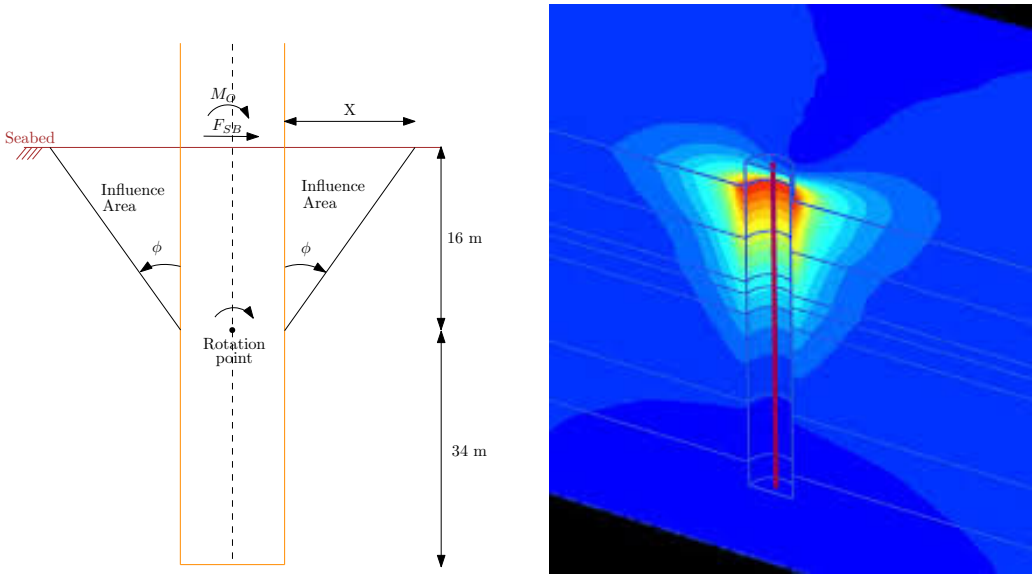

(a) Sketch of the influence line

(b) Stress distribution of a typical monopile for cyclic loading

Figure 7.2: Example of monopile influence on the soil

From the above sections, it can be seen that the jacket structure with either helical pile or suction bucket has more distance between the monopile wall and the wall of the foundation and has less interaction compared to tripod structure. Therefore, Jacket structure with either helical pile or suction bucket can be selected to proceed further in the design. However, it cannot be evidently concluded that either helical pile or suction bucket is better as detailed analysis need to be done.

A case study of the entire operation involved in the installation, removal and reuse of the structure (Chapter - 9) combined with both the foundations will be done to identify the time taken and cost associated. This way the best foundation can be selected for the seabed gripper structure and the final structure can be proposed.

8

Optimising the Design for Fatigue

In this chapter, fatigue analysis is carried out for the selected concept of jacket structure with both helical piles and suction bucket. The design is then optimised based on the response of the structure to fatigue loads. The steps involved in the fatigue analysis of the structure are:

1. Understanding the requirements
2. Fatigue loads on the structure
3. Fatigue analysis
4. Optimising the structure

8.1. Requirements for Fatigue

The requirement from Van Oord for the fatigue load is that the structure should be able to function properly for around 350 - 400 monopile installations (i.e: around 3 - 4 complete wind farms). The structure will be used for multiple wind farms, so it will be hard to adopt the environmental conditions for these multiple locations. An all year wave scatter for a North Sea location from a previous project within Van Oord is taken as the base condition for the fatigue calculation as shown in table C.1. This scatter table is taken as the sea condition for all the 350 - 400 monopile installations.

When the monopile is hammered, at certain penetration depth, the entire load acting on the monopile will be directly transferred to the soil and there is no need of any support from the seabed gripper structure. The time taken for the step by step process involved in the installation of the monopile is given as an input from Van Oord. The time period the seabed gripper structure will be subjected to fatigue load is 1 hour 45 minutes per monopile installation until the support from the structure is not needed by the monopile.

The percentage provided in the all year wave scatter is converted into the wave scatter for the fatigue loaded time period of 1 hour 45 minutes (i.e: per monopile installation) and is shown in table 8.1.

8.2. Fatigue loads on the structure

There are three major fatigue loads acting on the seabed gripper structure while installing the monopile. The seabed gripper structure is analysed only for these three loads. There are other

			sec				
	Hs \ Tz		1	2	3	4	5
			2	3	4	5	6
m	2	2.5	-	-	-	66	40
	1.5	2	-	-	-	194	2
	1	1.5	-	-	91	287	2
	0.5	1	-	-	392	137	5
	0	0.5	8	5	158	43	3

Table 8.1: Wave scatter diagram from previous project for the allowable operational weather window of $H_s = 2.5m$

forms of fatigue loading such as transport and lift point loading. These loads are assumed to be negligible in this analysis. The three major fatigue loads are:

1. Fatigue due to impact of the monopile on the gripper structure while slewing into the gripper frame (as discussed in section 6.3).
    - The vibration due to the impact is neglected; this is because certain amount of vibrations are absorbed by the dampers present in the gripper frame and also by surrounding water (hydrodynamic damping).
    - The impact load is taken as a point load and the stresses are found.
2. Fatigue due to the initial opposing force given by the gripper frame (or gripper arms) to make the monopile vertical.
    - It is assumed that the opposing force is given two times to make the monopile vertical per monopile installation.
3. Fatigue due to wave load acting on the monopile which is transferred to structure while the gripper frame is holding the monopile in position.
    - As the monopile penetrates the soil during hammering, the moment bearing capacity of the soil increases. This reduces the forcing on the gripper frame.
    - However, it is assumed that the maximum wave loading (i.e: before hammering) is transferred to the gripper frame throughout the considered time period of 1 hour 45 mins.

8.3. Fatigue analysis

For cyclic loading, joints between members are prone to fatigue failure compared to the member itself. This is because the weld inhibits a stress concentration in the form of a crack and will fail before the member fails. Therefore, the joints in the seabed gripper structure are checked for fatigue failure.

As discussed in Chapter - 6, loading condition 2 is the critical loading condition. Likewise, from figure-6.8, it can be seen that the joints in the gripper frame are the critical joints in the entire structure and subjected to high stresses. They are already strengthened by increasing the thickness of the members at the joints for ULS checks.

Initially the critical joint is checked for the fatigue loads and the structure is optimised accordingly, later the other joints are checked to make sure the entire structure is safe for the desired number of monopile installations.

The fatigue check is done based on the code DNVGL-RP-C203 - Fatigue design of offshore steel structures [7]. To find the fatigue life of the joints, the following steps are carried out:

1. Finding the number of cycles per stress range acting on the structure per monopile installation
   - Each individual wave presented in the wave scatter table will produce an individual stress range.
   - Therefore, the number of occurrences per individual waves shown in the wave scatter table is the same as the number of cycles per stress range (N) per monopile installation.
2. Calculating the different stress ranges acting on the structure.
   - The loads due to the individual waves acting on the structure is inputted as a function of time in ANSYS and analysed.
   - The internal force acting within the member of the joint is taken as an output as a function of time from ANSYS and the stresses are found based on the dimensions of the member in the joint.
   - A factor of safety need to be adopted to these stresses and there are two methods to do it.
     – First method is to calculate the Stress Concentration Factor (SCF) based on the geometry of the members and type of welds and multiply with the actual stresses. This method is adopted for tubular joints.
     – Second method is to adopt an already factored (or reduced) S-N curve from the table provided in the code based on the geometry of the members and type of welds. In this case, the actual stresses can be used directly. This method is adopted for plated joints.
   - The factored stress as a function of time has a peak and a trough. The difference between the peak and the trough for individual waves is their respective stress ranges. An example of the factored stress as a function of time for an individual wave is shown in figure-8.1.
3. Calculating the allowable number of cycles for the individual stress ranges.
   - The factored stress ranges found in the previous step are substituted in equation-8.1 and the allowable number of cycles per stress range (N_{max}) is calculated.

$$logN_{max} = log\bar{a} - m\ log\left(\Delta\sigma\left(\frac{t}{t_{ref}}\right)^{k}\right) \tag{8.1}$$

where,

N_{max} - predicted (allowable) number of cycles to failure for stress range $\Delta\sigma$

$log\bar{a}$ - intercept of the design S-N curve with the log N-axis by S-N curve (refer tables-C.1,C.2)

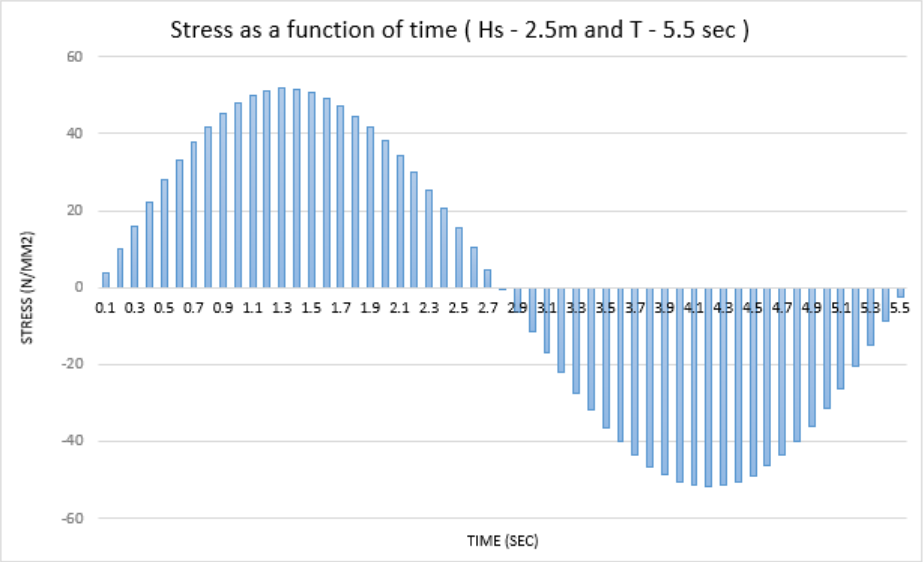

Figure 8.1: Stress as a function of time for Hs - 2.5m and T -5.5 sec

m - negative inverse slope of S-N curve (refer table-C.2)

$\Delta\sigma$ - stress range with unit [Mpa]

t - thickness through which a crack will most likely grow. $t = t_{ref}$ for t less than t_{ref}

t_{ref} - 16mm for tubular joints and 25mm for other joints

k - thickness exponent (refer tables-C.1,C.2)

- The S-N curves for air environment is adopted because the structure will be removed and placed again on the vessel and can be inspected for any damage. The S-N curve parameters for air environment are shown in table-C.1.

4. The damage per stress range is calculated by dividing the actual cycles per stress range (N) and the allowable cycles for the same stress range (N_{max}) (i.e: Number of cycles calculated in step 1 (N) divided by number of cycles calculated in step 2 (N_{max}).
5. The cumulative damage per monopile installation is found by summing the damage per stress ranges occurring per monopile installation.
6. The cumulative damage is then multiplied by the Design Fatigue Factor (DFF) to find the total fatigue damage per installation.
   - DFF depends on various parameters like inspection, etc.
   - The seabed gripper is removed and kept on-board the vessel after each monopile installation. Hence, the joints can be inspected regularly. Therefore, it is taken as 1.
7. The total damage is multiplied by the number of monopile installation (i.e: 350 -400), to find the fatigue damage for the design life of the seabed gripper structure. If it is less than 1 then the structure will be safe.

By following the above mentioned steps, fatigue check for the critical joint (as shown in figure-8.2) was performed and it was subjected to failure. The reason is that for the critical loading condition, the loads acting on the structure are concentrated on one frame and the loads are not distributed properly. Due to this, the critical joint is subjected to high stress especially stress due to out-of plane bending. To reduce this stress, the members of the gripper frame is provided with a truss members to distribute the load efficiently throughout the structure as shown in figure-8.2. In addition, the horizontal and vertical tubular member of the gripper frame is connected by an inclined tubular member as seen in figure-6.8. However, due to poor fatigue strength of the tubular joint, the inclined tubular member is replaced by curved T section as shown in figure-8.3. The horizontal plate of the T section is designed such that it occupies the corner and is welded together with the tubular members. This way, the stress acting at that joint is reduced as they are stronger than tabular joints and in addition, SCF is less for platted connections compared to tubular members.

For tubular members, SCF is calculated according to the code, which depends on angle, thickness,etc. The stresses acting on the tubular members should be multiplied with the SCF to find the stress ranges. These factored stresses are used to find the N_{max}. Here, the SN curve adopted does not have any SCF embedded in it.

For platted structure, SN curve which is already embedded with SCF is taken. In this case, the stress ranges can be directly used to find the N_{max} instead of multiplying with a SCF.

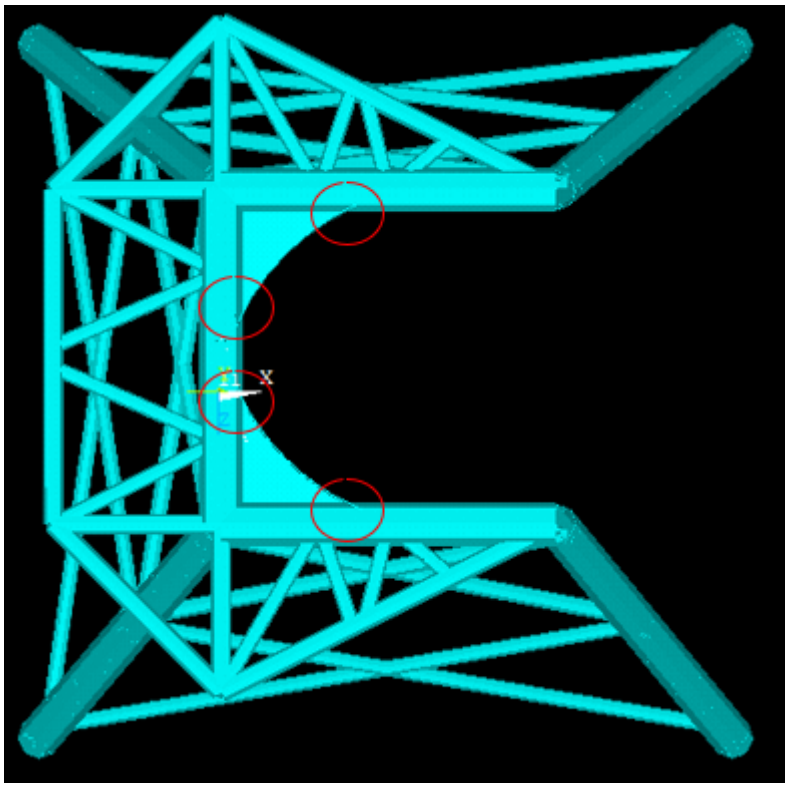

Figure 8.2: Optimised design of the jacket structure

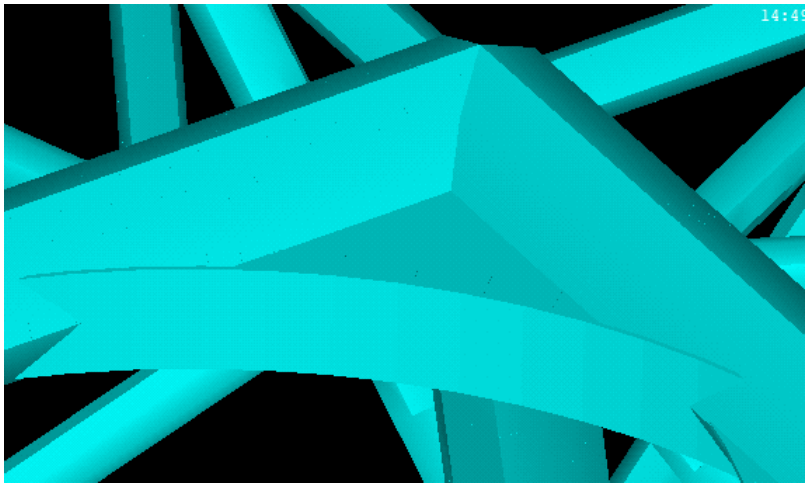

Figure 8.3: Critical joint with T section

After optimising the structure, the final value of the fatigue check of the critical joint is shown in table-8.2.

Hs	T	Δσ	N_max	N	N / N_max
0.5	2	47	4.11E+06	8	0.0000
0.5	2.5	45	4.68E+06	5	0.0000
0.5	3.5	31	1.36E+07	158	0.0000
0.5	4.5	26	2.33E+07	43	0.0000
0.5	5.5	23	3.29E+07	3	0.0000
0.5	6.5	22	4.25E+07	2	0.0000
1	3.5	63	1.71E+06	392	0.0002
1	4.5	53	2.91E+06	137	0.0000
1	5.5	47	4.10E+06	5	0.0000
1.5	4	85	6.82E+05	91	0.0001
1.5	4.5	79	8.60E+05	287	0.0003
1.5	5.5	71	1.21E+06	2	0.0000
2	4.5	106	3.62E+05	194	0.0005
2	5.5	94	5.09E+05	2	0.0000
2.5	5	124	2.23E+05	66	0.0003
2.5	5.5	118	2.60E+05	40	0.0002
Impact (MN) =	5.2	15.0	1.26E+08	1	7.926E-09
Inclinaion (MN)=	7.79	64.0	1.62E+06	2	1.231E-06
			Cumulative damage per installation	Dc =	0.0018
			Design fatigue factor	DFF =	1
			Total Damage per installation	Dd =	0.0017502
			No of installation	N_Insta	400
			Total Damage from the design life	D_td	0.7000813

Table 8.2: Fatigue check for the critical joint

From the table, it can be seen that the unity check is 0.7, where the remaining 0.3 is allocated to compensate for the other forms of fatigue loads which are not included in this analysis.

The final configuration of the jacket structure is shown in figures below. Note: For the top view diagram, as there are more members present in the structure, it was confusing a differentiate the truss members in the gripper frame and the X-bracing. Therefore, gripper frame with truss and plate is shown separately in figure-8.4, and the jacket structure without gripper frame is shown in figure 8.5.

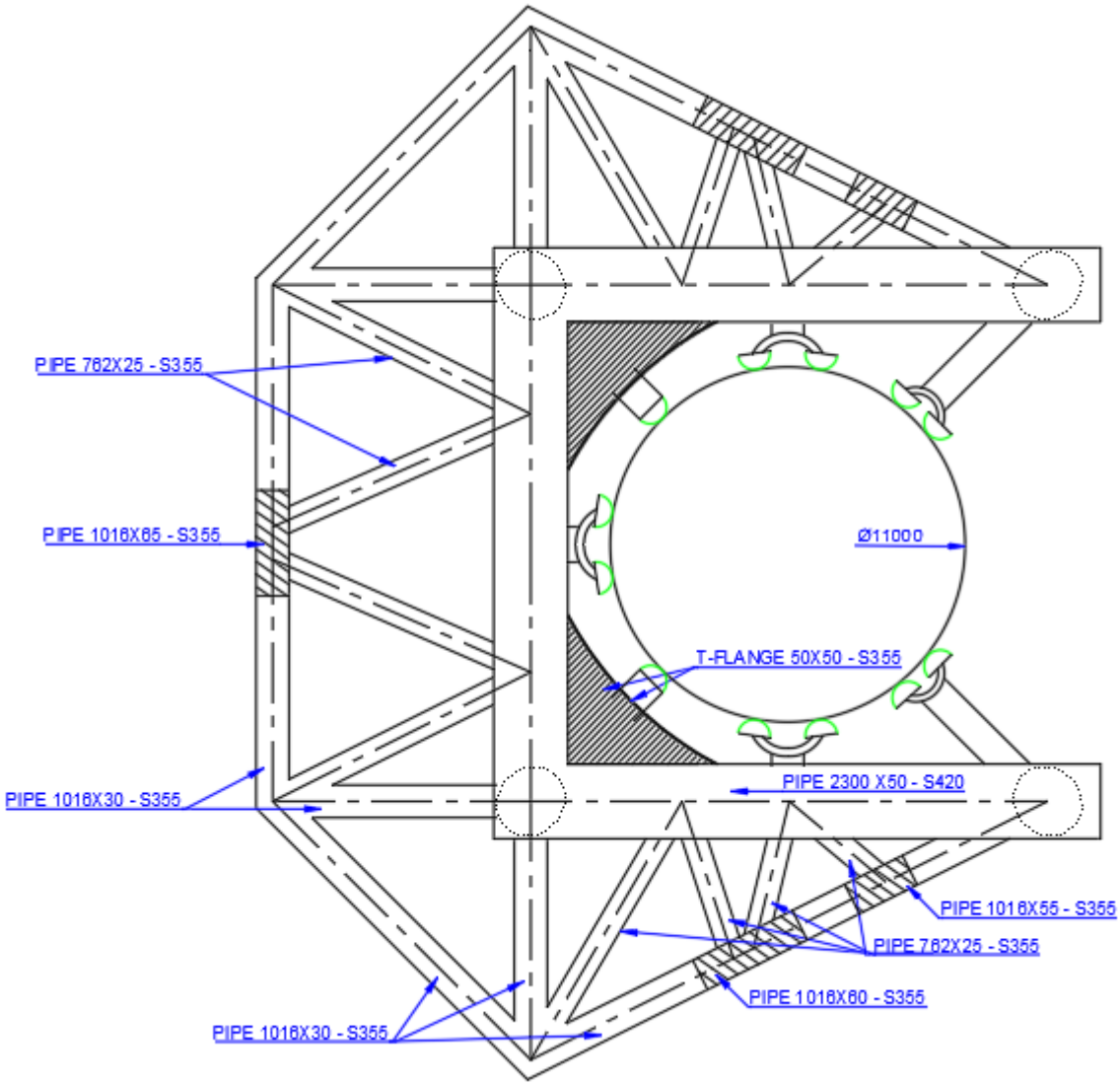

Figure 8.4: Top View - Gripper frame with truss and T flange

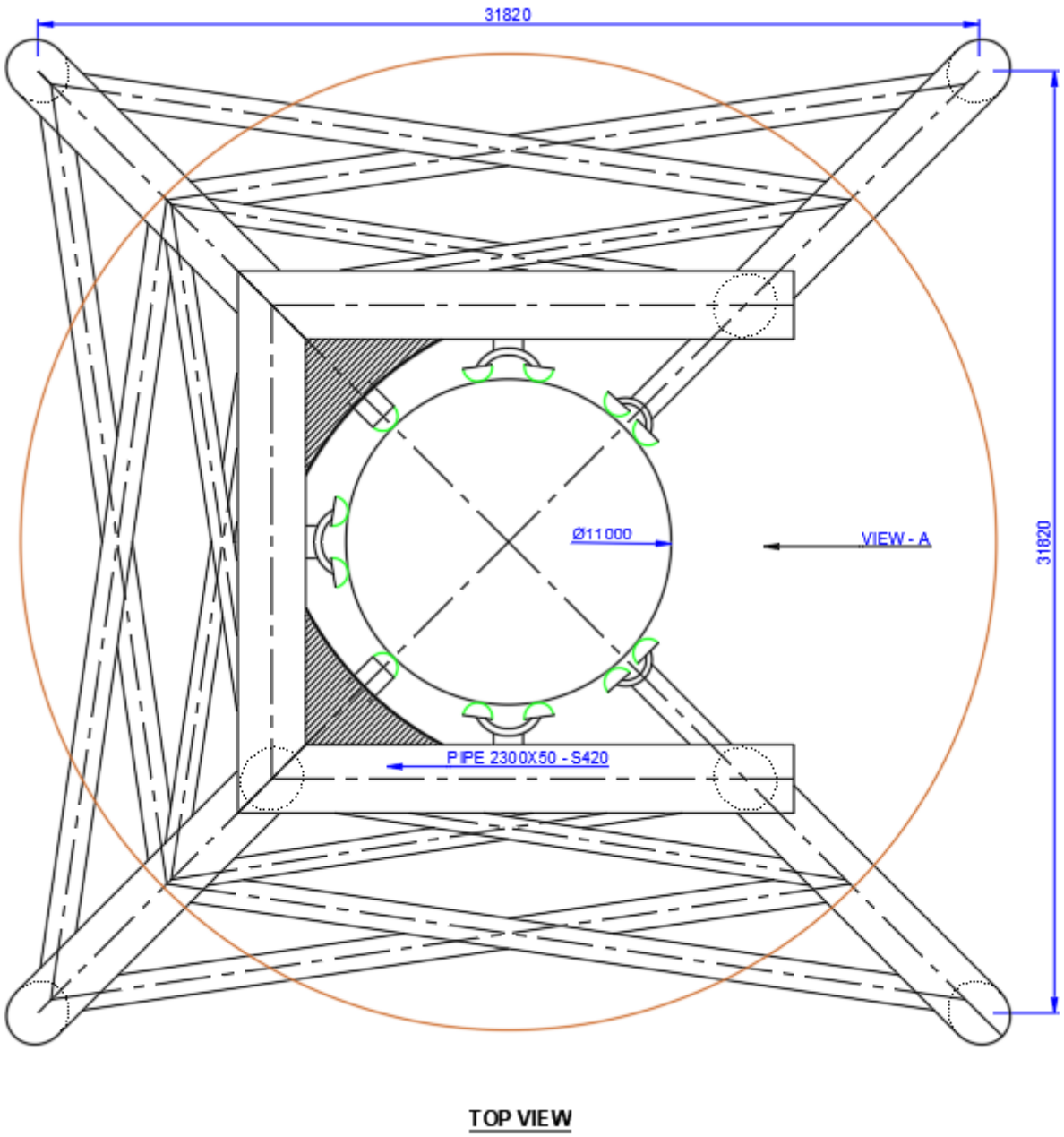

Figure 8.5: Top View - without gripper frame

Comparing the figures from ULS analysis (figure-6.8,6.9,6.10) and the figures from FLS analysis (8.4,8.5,8.6), it can be seen that the structure at the gripper frame is modified. Because of the inclusion of the truss structure, the load transfer is more efficient and there is no need of high grade steel anymore. The grade of steel for gripper frame is reduced from S500 to S420 and S355 is used for the remaining members. Three joints in the truss is strengthened

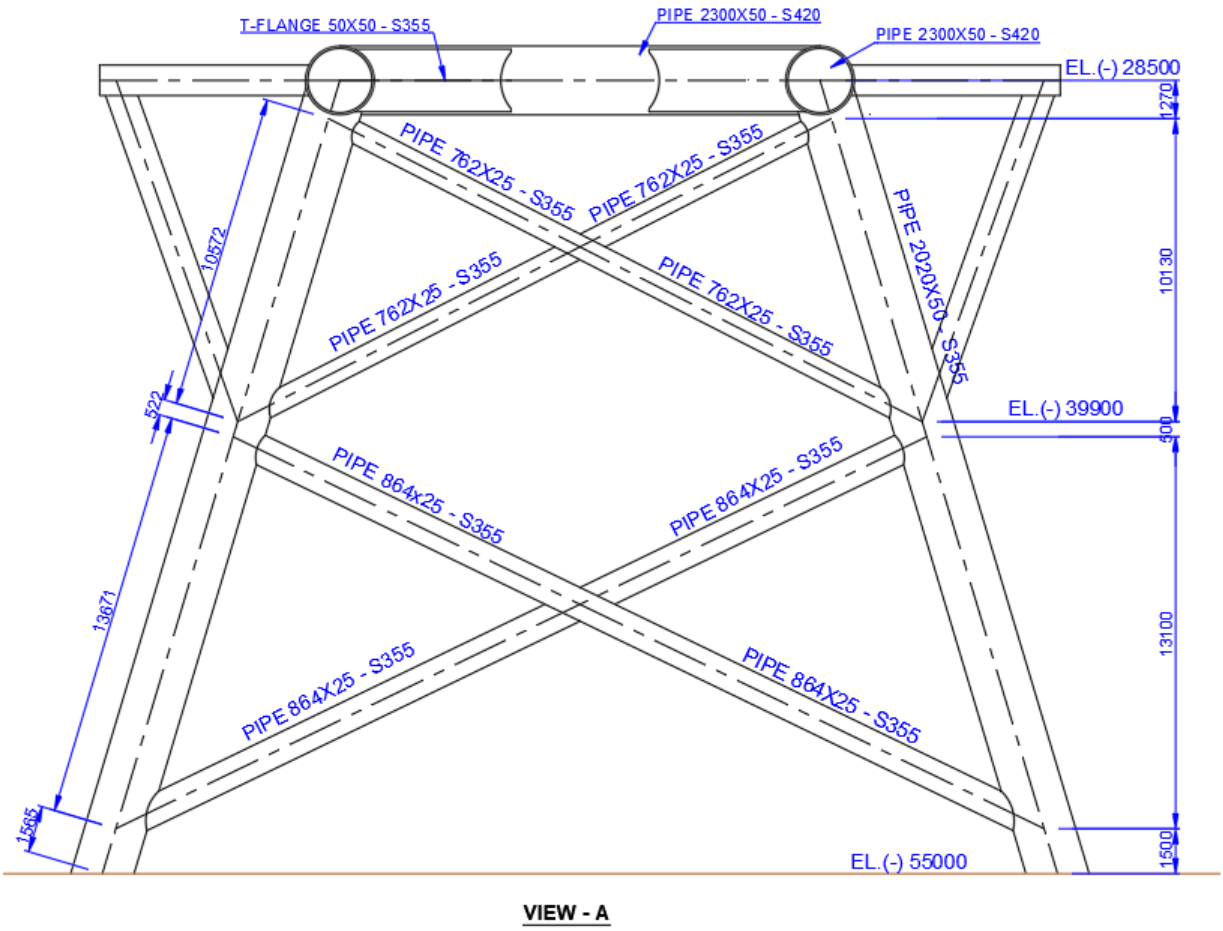

Figure 8.6: Front view

9

Case study of different installation scenarios

In this chapter, a case study has been performed for floating vessel with and without using the seabed gripper structure for the monopile installation. The main focus of the case study is to understand the economical feasibility of using a seabed gripper structure by evaluating the time taken and the cost associated to install a monopile. The different installation scenarios that are investigated in this thesis are:

1. Floating vessel with seabed gripper structure.
    - With helical pile foundation (Scenario-1)
    - With suction bucket foundation (Scenario-2)
2. Floating vessel with gripper on-board the vessel (i.e: without seabed gripper structure) (Scenario-3)

The input for the time taken for different operations involved in the installation of a monopile is given by Van Oord as a base condition and are shown in Appendix-**??**, table B.2. The total number of monopiles to be installed is taken as 400, which is the requirement as mentioned in section-8.1.

In all the scenarios, it is taken that the transition piece is installed after the monopile installation. Therefore, the time involved in the installation of TP is also taken into account. The maximum number of sets (i.e: Monopile and Transition piece) that the floating vessel can carry varies among the scenarios. For scenario-1,2, the vessel can carry 5 sets along with the seabed gripper structure on deck. For scenario-3, the vessel can carry 7 sets as it has more space due to the absence of seabed gripper structure.

As the total number of installations is 400, the number of trips needed to sail back to main port for reloading MP and TP depends on the number of sets the vessel can carry. For scenario-1,2, the vessel need to go back to shore for 79 trips to complete all the 400 installations and for scenario-3 it is 56 trips. This is one of the key factors for the time needed for the installation process.

The base condition for sailing to next location and to port for reloading is given in table 9.1. In the port, the sets need to be loaded and the time needed to load the sets is also given in table 9.1. As seen in the table, the first set needs more time than the remaining sets, since some adjustments and preparations need to be done on the vessel and also docking of the vessel.

Description	Value	unit
Sailing time to next location	45	minutes
Sailing distance	70	nautical miles
Sailing speed	11	knots
Sailing time to port (one way)	382	minutes
Loading first set	330	min/set
Loading remaining sets	120	min/set
Time at port	810	minutes

Table 9.1: Base condition for sailing of the vessel and loading in port [1]

The installation time of the seabed gripper depends on the type of foundation adopted. For the installation of helical piles, the time needed to upend the helical pile and place it inside the pile sleeve of the seabed gripper takes 30 minutes per pile [1] and to install the pile it takes a minimum of 30 minutes per pile[**?**]. The same 30 minutes will be taken for lifting the pile and placing on the deck [1]. For the removal of the helical pile it will be a minimum of 20 minutes to remove each pile. The total time taken to install four helical pile will be 240 minutes (4 hours) and to remove will be 200 minutes (3 hours 20 minutes). However, for the installation of suction bucket the maximum time taken to install the suction bucket will be 180 minutes (3 hours)[67] and to remove, it takes 120 minutes (2 hours). By comparing the time taken to install and remove the seabed gripper structure with both the foundations, suction bucket takes less time compared to helical piles (i.e: 140 minutes less per monopile installation or 39 days less for 400 monopile installation). The remaining installation processes to install the monopile are the same for the scenarios-1,2. Therefore, it will be optimal to use the jacket structure with suction bucket as the seabed gripper in terms of time taken for the installation of monopile.

Vessel name based on selected case	Floating vessel with DP system + MPT + Helical pile	Floating vessel with DP system + MPT + S.Bucket	Floating vessel with DP system - No MPT
No of sets (MP+TP) with MPT	5	5	7
Total No of Monopile installation	400	400	400
Positioning incl dp [min/unit]	60	60	60
MPT - hook on lifting gear [min/unit]	15	15	0
MPT - hook on template, place template on seabed [min/unit]	120	120	0
Installation of foundation	240	180	0
MPT -hook off template and back to deck [min/unit]	30	30	0
Set up for lifting/unlashing (relaesing seafasting?) [min/unit]	60	60	60
Upend MP & place in Gripper [min/unit]	60	60	60
Stab & remove upend tool [min/unit]	30	30	30
Hook up hammer & place [min/unit]	60	60	60
Hammer [min/unit]	180	180	180
Remove Hammer [min/unit]	30	30	30
Removal of foundation	200	120	0
MPT - hook on lifting gear for removal [min/unit]	15	15	0
MPT - connect to template [min/unit]	30	30	0
MPT - lift template and back to deck [min/unit]	60	60	0
Hook up TP [min/unit]	30	30	30
Install TP [min/unit]	90	90	90
First bolting campaign [min/unit]	64	64	64
Remainder of bolting [min/unit]	288	288	288
Clear TP replace cover [min/unit]	60	60	60
Seafasten & break-up [min/unit]	60	60	60
Installation time [min/unit]	*1842*	*1702*	*1132*
Total installation time [min]	736800	680800	452800
Total installation time [days]	***512***	***473***	***314***
Sail to next location [min/unit]	45	45	45
Sail back to M.Port for Reloading [min/trip]	382	382	382
Time taken at Port [min]	810	810	1050
No of times Sailing back to M.Port for Reloading	79	79	56
Total time for sailing back / next and loading [min]	124497	124497	102093
Total time for sailing back / next and loading [days]	***86***	***86***	***71***
Total no of days for the project [days]	***598***	***559***	***385***
Operating Hs [m]	2.5	2.5	1.0
No of days available in a year for installation [days]	342	342	179
Downtime during installation	23	23	186
Cost of the vessel for the project [M.EUR]	93	87	86
Weight of seabed gripper (tonnes)	1120	2297	0
Cost of Seabed gripper (M.EUR)	4	9	0
Total cost of the project	98	97	86
MPT - Monopile Template (i.e: Seabed gripper structure)			
DP - Dynamic Positioning			

Table 9.2: Different installation process involved in a monopile installation and their time[1]

From the table 9.2, it can be seen that the total installation time for suction bucket (473 days) is less than helical pile (512 days). The time taken to install the monopile by using floating vessel without seabed gripper is 314 days which is less compared to installing with seabed gripper. However, the operating weather window of the floating vessel without seabed

gripper is less (i.e: 1 m H_s) compared to floating vessel with seabed gripper structure (i.e: 2.5 m H_s). From the all year wave scatter table, the percentage of occurrence of wave is used to calculate the number of days the waves will occur and is shown in table-9.3.

Days	365	2	0	1	153	173	32	3	0	0	364.27
Hs [m]	7.5	0	0	0	0	0	0	0	0	0	0
	7	0	0	0	0	0	0	0	0	0	0
	6.5	0	0	0	0	0	0	0	0.0	0	0
	6	0	0	0	0	0	0	0.0	0.0	0	0
	5.5	0	0	0	0	0	0	0.1	0	0	0
	5	0	0	0	0	0	0	0.5	0	0	1
	4.5	0	0	0	0	0	0.1	0.9	0	0	1
	4	0	0	0	0	0	1.8	0.5	0	0	2
	3.5	0	0	0	0	0	5.8	0	0	0	6
	3	0	0	0	0	0.3	12.5	0	0	0	13
	2.5	0	0	0	0	15.8	9.5	0	0	0	25
	2	0	0	0	0.7	46.1	0.3	0	0	0	47
	1.5	0	0	0	21.6	68.3	0.3	0	0	0	90
	1	0	0	0	93.0	32.4	1.2	0	0	0	127
	0.5	1.8	0	0.9	37.7	10.5	0.8	0.5	0	0	52
		0.5	1.5	2.5	3.5	4.5	5.5	6.5	7.5	8.5	364.27
		Tz [s]									

Table 9.3: Occurrence of waves in days [1]

Based on the occurrence of waves and the operating weather condition, the number of days available in a year for installation is 342 days and 179 days for floating vessel with seabed gripper and without seabed gripper respectively. The downtime in installation while using a floating vessel without a seabed gripper is 135 days.

The cost per day of the floating vessel is taken as 150000 EUR. A cost per tonne of 4000 EUR is taken to fabricate the seabed gripper structure. This cost includes the high strength materials, complex fabrications and also the hydraulic components in the structure, etc. The total cost of the project including the cost for vessel and seabed gripper is also shown in table-9.2. The weight of the suction bucket is very high compared to helical pile, that reflects in the increase in cost of the seabed gripper using suction bucket as foundation.

From the table, the cost of using floating vessel without a seabed gripper is less compared to using a seabed gripper. However, maintaining the accuracy of the installation is difficult without using a seabed gripper.

Comparing the floating vessel with seabed gripper with both the foundations, the total cost of the project to install 400 monopiles is 1 million cheaper, using suction bucket as foundation for the seabed gripper.

The installation process of the helical pile can be changed to decrease the time taken for it to install and remove. If a second crane with a lifting capacity of 300 - 500 tonnes is available on the vessel, it can be used to install another helical pile simultaneously along with the big crane which is normally used. This way the installation and removal time of the helical pile can be cut into half. This reduces the total cost of the project from 98 M.EUR to 89 M.EUR.

After optimising the installation, the cost of the floating vessel with seabed gripper using helical piles as foundation (89 M.EUR) is close to the cost of the floating vessel without seabed gripper (86 M.EUR). With the seabed gripper, the monopiles can be installed accurately and vertical compared to floating vessel without seabed gripper.

10

Conclusions and Recommendations

The main goal of this thesis is an optimal design of a seabed gripper structure for the installation of a monopile foundation, to ensure the verticality of the monopile during installation and in addition is easy to install, remove and reuse. In addition, to see whether a realistic designed seabed gripper is a valuable add for Van Oord or not.

10.1. Conclusions

The outcomes of this thesis are based on literature study, reasonable assumptions and performed analysis as presented in the report. The requirements from Van Oord are taken as an input data to proceed with this thesis. The conclusions from this thesis are:

1. Jacket structure (four legged) with suction bucket is an optimal structure for a seabed gripper which is easy to install, remove and reuse while keeping the monopile vertical during installation. However, it is not an economical solution for Van Oord to use a seabed gripper for the installation of monopile.

2. Based on the soil-structure interaction, jacket structure was the optimal structure. The legs of the jacket structure are far away from the monopile and has less interaction with the monopile and vice versa compared to the tripod structure. The legs are also away from the armour layer of the scour protection.

3. To conclude with the design, the final optimised design of the jacket structure is as shown in figure-B.2, which is an optimised structure based on ULS and FLS analysis including member and joint checks.

4. Based on the case study, suction bucket takes less time to install compared to helical pile, which saves 34 days in the total installation time of the seabed gripper structure on a project of 400 monopile installations. Therefore, suction bucket can be adopted as the foundation for jacket structure.

5. Suction buckets have some challenges in the installation stage (i.e: the suction pressure differs with different layers of soil). Therefore, a detailed investigation and soil analysis is needed for each location where the monopile is being installed in the entire wind farm.

6. While comparing the installation of a monopile using floating vessel with and without seabed gripper structure, the floating vessel without a seabed gripper takes less time for the installation of a monopile. It takes 489 days and 337 days to complete the installation

of 350 monopiles for floating vessel with seabed gripper and without seabed gripper respectively.

7. The installation of monopile using floating vessel with and without seabed gripper has a certain operating weather conditions. For floating vessel with seabed gripper, the installation can be done for 342 days out 365 days per year. However, for floating vessel without seabed gripper, the installation can be done for 179 days out of 365 days per year. The downtime for using a floating vessel without seabed gripper is 163 days compared to installing with seabed gripper.

10.2. Recommendations

In this thesis, though an optimised design of a seabed gripper structure is proposed, it still needs further research and analysis which are listed below.

1. The design of hydraulics and rollers in the gripper frame should be done according to the gripper arrangement proposed in the section-5.2 to have a complete design of the gripper frame. This is a new type of arrangement that has been suggested particularly for this thesis. In addition, the gripper arrangements needs to be integrated with the jacket structure.

2. In ULS and FLS analysis, different soil models should be adopted, to have a better understanding of the response of the structure to different soil conditions.

3. The impact of the monopile on the gripper frame while slewing into the gripper frame will induce vibrations which may affect the re-usability of the structure and requires dynamic analysis to understand the effect of these vibrations.

4. During the hammering of the monopile, The vibrations that is caused while hammering the monopile will slightly transfer through the seabed gripper structure, due to the inclination of the monopile. It would be interesting to perform a dynamic analysis to understand the transfer of these vibrations through the seabed gripper and to the soil. There maybe fatigue damage induced by these vibrations if it passes through the seabed gripper.

5. Seabed gripper structure is a new type of structure to the industry in terms of using a separate structure on the seabed to install a monopile. The foundation of the seabed gripper and the monopile is close to each other. The monopile is hammered in between the legs of the seabed gripper structure. There is a research gap in the soil-structure interaction for this type of structure. A complete model of the monopile, soil and the seabed gripper should be modelled and analysed, to get an insight on the behaviour and influence of these three components on each other.

6. In fatigue analysis, a more detailed analysis needs to be done including all the fatigue loads that are not considered in this thesis. A more detailed fatigue analysis may influence the number of installations and removal of the seabed gripper. It would be interesting to perform a detailed Finite Element Analysis of the critical joints of the seabed gripper structure to derive the hot spot stresses in the joints, instead of using code to derive the stress concentration factor and finding the factored stresses.

7. During the case study, it has been seen that the suction bucket has less installation time compared to helical pile. Therefore, it is optimal to use suction bucket as the foundation

for jacket structure. However, it would be ideal to use water jets at the tip of the suction bucket for easy installation and removal and save more time if possible.

8. An alternative installation method can be used to pick helical pile and to have less installation time in comparison with suction bucket. Normally, piles are installed one by one for all the legs by using single crane. However, in this new method, if there is an extra availability of small crane on the vessel (i.e: maximum lifting capacity of 300 - 500 tonnes), it can be used to install and remove an additional helical pile. Therefore, the two cranes can be used to lift a helical pile each and both piles will be installed simultaneously. This results in less installation and removal time compared to the suction bucket. This is an option that can be adopted to optimise the installation process.

9. The connection between the jacket and suction bucket or helical pile needs to be designed based on which foundation is selected as the foundation for jacket. Normally, the connection between jacket and helical pile are done by grouting, but it cannot be adopted for this structure. Grouting needs some time to achieve its full load transfer capacity and needs to be removed after. Therefore, a new type of connection is needed between the jacket and the helical pile.

List of Figures

List of Tables

Bibliography

[1] Van Oord Offshore Wind bv.

[2] American Institute of Steel Construction (AISC), July 7,2016.

[3] DNVGL-OS-C101 - Design of offshore steel structures, general - LRFD method, July 2018.

[4] DNVGL-RP-C212 - Offshore soil mechanics and technical engineering, August 2017

[5] DNV-RP-C202 - Buckling strength of shells - tubular members, January 2013.

[6] DNVGL-ST-0126 - Support Structures for wind turbines, July 2018.

[7] DNVGL-RP-C203 - Fatigue design of offshore steel structures

[8] Hot rolled products of structural steels - Part 4: Technical delivery conditions for thermomechanical rolled weldable fine grain structural steels, August 2019.

[9] Kallehave Dan, Byrne Byron W., LeBlanc Thilsted Christian and Mikkelsen Kristian Kousgaard, 2015, Optimization of monopiles for offshore wind turbinesPhil. Trans. R. Soc. A.37320140100 http://doi.org/10.1098/rsta.2014.0100

[10] Giovanni Spagnoli, Cristina de Hollanda Cavalcanti Tsuha, Pierpaolo Oreste and Carlos Mauricio Mendez Solarte. Estimation of Uplift Capacity and Installation Power of Helical Piles in Sand for Offshore Structure. https://doi.org/10.1061/(ASCE)WW.1943-5460.0000471

[11] A.Sprince, L.Pakrastinsh. Helical pile behaviour analysis in different soils, January 2009. DOI: 10.2478/v10137-009-0012-2 https://www.researchgate.net/publication/245552664

[12] Byrne BW, Houlsby GT. 2015. Helical piles: an innovative foundation design option for offshore wind turbines. Phil. Trans. R. Soc. A 373: 20140081.http://dx.doi.org/10.1098/rsta.2014.0081

[13] Mohamed Elkasabgy and M. Hesham El Naggar. Lateral performance and p-y curves for Large-capacity helical piles installed in clayey glacial deposit, 2019. https://doi.org/10.1061/(ASCE)GT.1943-5606.0002063

[14] Howard A. Perko. Helical piles : A Practical Guide to Design and Installation, 2009.

[15] F. Bagheri & M. H. El Naggar (2015) Effects of installation disturbance on behavior of multi-helix piles in structured clays, DFI Journal - The Journal of the Deep Foundations Institute, 9:2, 80-91, http://dx.doi.org/10.1179/1937525515Y.0000000008

[16] Mr. Yaseen Umar Sharif, Dr. Michael Brown, Dr. Benjamin Cerfontaine, Mr. Craig Davidson, Dr. Matteo Oryem Ciantia, Dr. Jonathan Knappett, Mr. Jonathan David Ball, Dr. Andrew J. Brennan, Prof. Charles E. Augarde, Dr. William Coombs, Dr. Anthony Blake, Prof. David Richards, Dr. David White, Dr. Marco Huisman, and Mr. Marius Ottolini. Effects of screw pile installation on installation requirements and in-service performance using the Discrete Element Method. Canadian Geotechnical Journal. 0(ja): -.https://doi.org/10.1139/cgj-2020-0241

[17] Hoyt, R.M. and S.P. Clemence. 1989. "Uplift Capacity of Helical Anchors in Soil." Proceedings of the 12th International Conference on Soil Mechanics and Foundation Engineering, Rio de Janeiro, Brazil Vol. 2, pp. 1019–1022.

[18] Zeinoddini M, Nabipour M, Matin Nikoo H. An Investigation into the Pull-out Failure Mechanisms of Suction Caissons. ijmt. 2015; 4 :21-35. http://ijmt.ir/article-1-327-en.html

[19] Shucheng Jin, Yanhua Yang and Yongtao Zhang. Bucket Group Effect of the Composite Multi-bucket Structure. J. Marine Sci. Appl. (2014) 13: 62-66 DOI: 10.1007/s11804-014-1229-y

[20] Byrne BW, Houlsby GT. Design Procedure for installation of suction caissons in clay and other materials. Proceedings of the Institution of Civil Engineers Geotechnical Engineering 158, April 2005 Issue GE2 Pages 75–82

[21] Byrne BW, Houlsby GT. Design Procedure for installation of suction caissons in sand. Proceedings of the Institution of Civil Engineers Geotechnical Engineering 158, July 2005 Issue GE3 Pages 135–144

[22] Le ChiHung,Sung-RyulKim. Evaluation of combined horizontal-moment bearing capacities of tripod bucket foundations in undrained clay. https://doi.org/10.1016/j.oceaneng.2014.04.025

[23] Nghiem Xuan Tran, Le Chi Hung, Sung-Ryul Kim. Evaluation of horizontal and moment bearing capacities of tripod bucket foundations in sand. https://doi.org/10.1016/j.oceaneng.2017.05.012

[24] Sung-Ryul Kim, Le Chi Hung, Myounghak Oh. Group effect on bearing capacities of tripod bucket foundations in undrained clay. https://doi.org/10.1016/j.oceaneng.2013.12.017

[25] Koohyar Faizi, Asaad Faramarzi, Samir Dirar, David Chapman. Investigating the monotonic behaviour of hybrid tripod suction bucket foundations for offshore wind towers in sand. https://doi.org/10.1016/j.apor.2019.05.018

[26] Suction Installed Caisson Foundations for Offshore Wind: Design Guidelines, February 2019.

[27] Lian, J., Chen, F., and Wang, H. (2014a). Laboratory tests on soil-skirt interaction and penetration resistance of suction caissons during installation in sand. Journal of Ocean Engineering, 84:1–13.

[28] Chen, F., Lian, J., Wang, H., Liu, F. & Zhao, Y. (2016). Large-scale experimental investigation of the installation of suction caissons in silt sand. Journal of Applied Ocean Research 60, 109–120.

[29] Koteras, A. K. (2019). Jacking and suction installation of bucket foundation for offshore wind turbines. Aalborg Universitetsforlag. Ph.d.-serien for Det Ingeniør- og Naturvidenskabelige Fakultet, Aalborg Universitet

[30] Arunjyoti Sarkar, Ove T. Gudmestad. Study on a new method for installing a monopile and a fully integrated offshore wind turbine structure https://doi.org/10.1016/j.marstruc.2013.06.001

[31] Aliakbar Khosravi, Tuck Wai Yeong, Mohammed Parvez Anwar, Jayaprakash Jaganathana, Teck Leong Lau, Wael Elleithy. A Comparative Study between Three-Legged and Tripod Sub-structures in Design of Offshore Wind Turbines in the Transition Water Depth. International Journal of Engineering & Technology, 7 (3.36) (2018) 23-33

[32] Jan H.Vugts, Handbook of Bottom Founded Offshore Structures : Part 1. General Features of Offshore Structures and Theoretical Background, 2013.

[33] Jan H.Vugts, Handbook of Bottom Founded Offshore Structures : Part 2. Fixed Steel Structures, 2016.

[34] Jeroen Hoving, Frank Sliggers & Andre van der Stap, Course of Bottom founded structures from TU Delft, 2018.

[35] Deep Foundation Institute, Comparison of impact versus vibratory driven piles: with a focus on soil-structure interaction, 2014.

[36] R.A.W. Dubber, J.S. Hoving and S.W.G Huiskes, Hand-out - The equivalent stick-model, 2018.

[37] NORSOK Standard, N-004 - Design of Steel structures.

[38] Siciliano, R. J., Hamilton, J. M., Murff, J. D., & Phillips, R. J. (1990, January 1). Effect of Jackup Spud Cans on Piles. Offshore Technology Conference. https://doi.org/10.4043/6467-MS

[39] Wu, Yongren & Lu, Xiaobing & Zhang, Xuhui. (2010). Effects of the Spudcan Penetration on the Adjacent Foundations. The Open Ocean Engineering Journal. 3. 38-44. http://dx.doi.org/10.2174/1874835X01003010038

[40] Hawkins, A. D., Roberts, L., & Cheesman, S. (2014). Responses of free-living coastal pelagic fish to impulsive sounds. The Journal of the Acoustical Society of America, 135(5), 3101–3116. https://doi.org/10.1121/1.4870697

[41] Lesny, K. (2011). Foundations for Offshore Wind Turbines. Tools for Planning and Design. Essen, Germany: VGE Verlag GmbH.

[42] Koteras, A. K. (2019). Jacking and suction installation of bucket foundation for offshore wind turbines. Aalborg Universitetsforlag. Ph.d.-serien for Det Ingeniør- og Naturvidenskabelige Fakultet, Aalborg Universitet

[43] Oscar Yanguas Miñambres (2012), Assessment of Current Offshore Wind Support Structures Concepts – Challenges and Technological Requirements by 2020.

[44] A. Tsouvalas, Offshore noise generated by pile driving, no. november. 2015.

[45] B.J.M. Arntz, A feasibility study into an improved installation method for offshore foundation piles, 2018.

[46] Thieken, Klaus, Martin Achmus, and Christian Schröder. ”On the behavior of suction buckets in sand under tensile loads.” Computers and Geotechnics 60 (2014): 88-100.

[47] A. A. Rodger and G. S. Littlejohn, “A study of vibratory driving in granular soils,” Géotechnique, vol. 30, no. 3, pp. 269–293, 1980.

[48] Saleem Z., Alternatives and modifications of Monopile foundation or its installation technique for noise mitigation. Report for North Sea Foundation in TU Delft MSc. Thesis; 2011.

[49] Mitchell A. 1848 On submarine foundations; particularly screw pile and moorings. In Minutes of the Proc. of the Institution of Civil Engineers, vol. 7, pp. 108–132. London, UK: Institution of Civil Engineers.

[50] Hoyt AB, Clemence SP. 1989 Uplift capacity of helical anchors in soil. In Proc. 12th ICSMFE, Rio de Janeiro, 13–18 August 1989. Rotterdam, The Netherlands: A.A. Balkema.

[51] Sharif, Y., Brown, M., Cerfontaine, B., Davidson, C., Ciantia, M., Knappett, J., Brennan, A., Ball, J. D., Augarde, C., Coombs, W. M., Blake, A., Richards, D., White, D., Huisman, M., & Ottolini, M. (2020). Effects of screw pile installation on installation requirements and in-service performance using the Discrete Element Method. Canadian Geotechnical Journal. https://doi.org/10.1139/cgj-2020-0241

[52] Bradshaw, A., Zuelke, R., Hilderbranndt, L., Robertson, T. and Mandujano, R. 2019 ‘Physical Modelling of A Helical Pile Installed in Sand Under Constant Crowd’, in Davidson, C., Brown, M. J., Knappett, J. A., Brennan, A. J., Augarde, C. E., Coombs, W. M., Wang, L., Richards, D., White, D. J., and Blake, A. (eds) ISSPEA. Dundee, UK: University of Dundee, pp. 109–115. doi:10.20933/100001123.

[53] Cotter, O. (2010). The installation of suction caisson foundations for offshore renewable energy structures. PhD Thesis, Oxford University.

[54] Tjelta, T. I. (2015). The suction foundation technology. Frontiers in Offshore Geotechnics, III:85–93.

[55] Christos Alexandridis, A.M., Ship’s anchors(June,2017).

[56] Sebastian Schreier, Course of Floating structures and offshore moorings from TU Delft, 2019.

[57] R.R. Damiani, Design of offshore wind turbine towers (2016).

[58] Tripile Support Structures by 4C Offshore [Internet]. Available from: https://www.4coffshore.com/news/tripile-support-structures-aid6.html

[59] Segeren, Maxim Lourens, Eliz-Mari Tsouvalas, A. Zee, T.J.J.. (2014). Investigation of a slip joint connection between the monopile and the tower of an offshore wind turbine. Renewable Power Generation, IET. 8. 422-432. 10.1049/iet-rpg.2013.0163.

[60] Frank van Gerven, Optimising the design of a steel substructure of offshore wind turbines in deep waters, 2011. Master Thesis,TU Delft.

[61] Jutta Stutzmann, Lisa Ziegler, Michael Muskulus,2017, Fatigue crack detection for lifetime extension of monopile-based offshore wind turbines.

[62] IHC IQIP takes next step in development of BLUE Piling Technology, Press release, April,2019.

[63] Statoil (Equinor). https://www.equinor.com/en/what-we-do/fields-and-platforms.html#

[64] Hao Wang, Xiaohui Cheng, Undrained Bearing Capacity of Suction Caissons for Offshore Wind Turbine Foundations by Numerical Limit Analysis, April 2015. 10.1080/1064119X.2015.1004766

[65] Saleh Jalbi *, Joseph Hilton and Luke Jacques, Assessment of Practical Methods to Predict Accumulated Rotations of Monopile-Supported Oshore Wind Turbines in Cohesionless, July 2020. Ground Profiles

[66] https://contecompany.com/helical-pile-foundation-fast-construction

[67] https://www.imeche.org/news/news-article/%27game-changing%27-suction-bucket-foundation-helps-install-turbines-in-record-time

A

Preliminary design

For the calculations that are done in this chapter, certain values are given as mentioned in Chapter 2 - Requirements.

The self-weight of the monopile is found by,

$$\begin{aligned} S.W &= 3000\ tonnes * 9.81 \\ &= 29430\ kN \end{aligned} \tag{A.1}$$

To calculate the buoyancy weight of the monopile, the volume of water displaced by the monopile (is equal to the volume of monopile underwater) needs to be found. To find the volume, a reasonable thickness should be used. D/t ratio of 110 is used to find the thickness of the monopile for the buoyancy weight calculation. With this D/t ratio, the thickness of the monopile wall is found as 100 mm.

The buoyancy weight of the monopile is,

$$\begin{aligned} Buoyancy\ weight &= \frac{\pi}{4} * (D_{out} - D_{in}) * L_{MP} * \rho_w \\ &= \frac{\pi}{4} * (11^2 - 10.8^2) * 55 * \frac{1025}{1000} * 9.81 \\ &= 1893.8\ kN \end{aligned} \tag{A.2}$$

The requirements from Van Oord which is taken for the load calculation is shown in table A.1.

For the wind load calculation, the velocity of air at the top of the MP above water and the top of the hammer is found using the formula 5.5. With these velocity and substituting in equation 5.6, the calculated wind loads are shown in table A.2.

The wave loads are calculated using the calculation sheet available within Van Oord, which calculates the wave load with respect to time and shows final load at a time where the loads are maximum. In this case, the maximum load acting on the MP is at 4.36th sec of a 5.6 sec wave period. The excel sheet is shown in table A.3.

Load Calculation					
Monopile properties					
Min MP dia	7	m			
Max Mp dia	11	m			
Min MP wall thickness	D/t =	1/125	0.09	m	
Length Max	110	m			
Weight Max	3000	ton			
Hammer properties					
Total weight	1750	ton			
COG 15m above pile top		H_hammer	30	D_hammer	8.5
Wind Load area	8,5*30		255	m2	
Environmental conditions					
During Installation					
Assumed all load in same direction, hammer on pile					
Hs	2.5	m			
6<= T <= 8	sec		T	5.6	sec
V_current	1			7.22	sec
V_wind_10	20	m/s			
Gripper Capabilities					
Correct for verticality, maximum MP inclination 1 deg, correct to 0,25 deg					
Resist Environmental loading					
water depth upto	55	m			

Figure A.1: Requirement from Van Oord used for load calculation

Wind Load			
Self penetration		9.6	m
MP above water =		45.4	m
	MP @ 45m	Hammer @ 75.4m	
V_wind	23.27	24.48	m/s
V_wind	24	25	m/s
Cd_tubular	0.7	0.7	
rho_air	1.29	1.29	kg/m3
Q_wind	0.260064	0.2821875	kN/m2
Shear force at seabed			
F_wind_sb_MP		129.875962	kN
F_wind_sb_hammer		71.9578125	kN
F_wind_sb		**201.833774**	kN
Moment at seabed			
M_wind_sb_MP		10091.3622	kNm
M_wind_sb_hammer		8303.93156	kNm
M_wind_sb		**18395.2938**	kNm

Figure A.2: Wind load calculation

Linear small amplitude wave theory (Airy) with Wheeler stretching

Door R.J.N.J. Luiken v1.1 27-02-2013

INPUT

H	5.00	[m]	wave height
T	5.60	[s]	wave period
d	55.00	[m]	water depth
C_d	1.00	[-]	Drag coefficient
C_m	2.00	[-]	Inertia coefficient
g	9.81	[m/s^2]	Gravity
ρ	1025.00	[kg/m^3]	Water density
D	11.00	[m]	Diameter pile
V0	1.00	[m/s]	Current top
V1/4	1.00	[m/s]	
V1/2	1.00	[m/s]	
V3/4	1.00	[m/s]	
V1	1.00	[m/s]	Current bottom
H_{crest}/H	0.50	[-]	Ratio of wave above mean water level {Default 0.5. See also validity Airy sheet}

CALCULATION

λ	48.96	[m]	Wave length
ω	1.12	[rad/s]	
k	0.13	[1/m]	
ξ_a	2.50	[m]	Max wave height above still water level
λ_0	48.96	[m]	Deep water wave length
H_b	6.95	[m]	Miche criterium breaking wave height
H_b/d	0.13	[-]	

Calculate wave

OUTPUT

t = 4.36 (t = 0 to 5.60 [s])

q = 0.99

True depth z	Wheeler depth z1	Hor. Velocity u [m/s]	Hor. Acceleration a [m/s^2]	Current v [m/s]	Drag force F_d [N/m]	Inertia force F_m [N/m]	Total force F_{tot} [N/m]	Total force F [kN]	M at seabed M [kNm]
0.43	0.00	0.49	3.10	1.00	12466.85	603816.40	616283.25	1708.16	92322.87
-2.34	-2.75	0.34	2.18	1.00	10156.70	424271.64	434428.34	1204.11	61742.50
-5.11	-5.50	0.24	1.53	1.00	8674.95	298114.73	306789.68	850.33	41245.17
-7.88	-8.25	0.17	1.08	1.00	7703.65	209470.83	217174.48	601.94	27528.79
-10.65	-11.00	0.12	0.76	1.00	7055.66	147185.51	154241.17	427.51	18366.50
-13.42	-13.75	0.08	0.53	1.00	6617.38	103421.15	110038.53	304.99	12257.65
-16.20	-16.50	0.06	0.37	1.00	6317.83	72670.71	78988.54	218.93	8192.04
-18.97	-19.25	0.04	0.26	1.00	6111.51	51064.71	57176.23	158.48	5490.60
-21.74	-22.00	0.03	0.18	1.00	5968.60	35884.41	41853.01	116.00	3697.59
-24.51	-24.75	0.02	0.13	1.00	5869.21	25219.59	31088.80	86.17	2507.77
-27.28	-27.50	0.01	0.09	1.00	5799.90	17728.25	23528.14	65.21	1717.14
-30.05	-30.25	0.01	0.06	1.00	5751.47	12467.73	18219.19	50.50	1189.71
-32.83	-33.00	0.01	0.05	1.00	5717.60	8776.07	14493.68	40.17	835.09
-35.60	-35.75	0.00	0.03	1.00	5693.93	6188.75	11882.68	32.94	593.37
-38.37	-38.50	0.00	0.02	1.00	5677.41	4380.18	10057.59	27.88	424.96
-41.14	-41.25	0.00	0.02	1.00	5665.94	3122.79	8788.73	24.36	303.83
-43.91	-44.00	0.00	0.01	1.00	5658.06	2258.35	7916.41	21.94	212.86
-46.68	-46.75	0.00	0.01	1.00	5652.77	1678.09	7330.87	20.32	140.80
-49.46	-49.50	0.00	0.01	1.00	5649.41	1308.99	6958.41	19.29	80.19
-52.23	-52.25	0.00	0.01	1.00	5647.55	1104.61	6752.16	18.72	25.94
-55.00	-55.00	0.00	0.01	1.00	5646.96	1039.23	6686.18		
							Σ	5997.94	278875.36

Figure A.3: Hydrodynamic load calculation

B

Finite Element Analysis

B.1. Member check

The complete excel that was made to check the members is shown in the figure below and the final values of each check is shown in table B.1. As this was a compression member, in some parts it will say NOT APPLICABLE, because that is a check for tension members. The cells with blue color are the inputs given and the other values are calculated based on the formulas showed from equation 6.5 till 6.1.2.

Tension	Nt	NA	<=1	NA
Compression	Nc	0.176	<=1	SAFE
Moment	Mb	0.791	<=1	SAFE
Shear	Vs	0.166	<=1	SAFE
Torsion	Ts	0.258	<=1	SAFE
Hydrostatic pressure	Fh	0.113	<=1	SAFE
Tension & Moment	Nt , Mb	NA	<=1	NA
Compression & Moment	Nc , Mb	0.877	<=1	SAFE
Shear & Moment	Vs , Mb	0.791	<=1	SAFE
Shear, Moment & Torsion	Vs,Mb,Ts	0.815	<=1	SAFE
Tension,Bending & Hydrostatic	Nt,Mb,Fh	NA	<=1	NA
		NA	<=1	NA
Compression, Bending & Hydrostatic	Nc,Mb,Fh	0.904	<=1	SAFE
		0.996	<=1	SAFE

Do =	2.02	m
Di =	1.92	m
t =	0.05	m

	Fx	Fy	Fz	Mx	My	Mz
Element 6	-16.90	-2.73	4.23	-15.05	48.03	-8.42

6.3.2 - Axial Tension

$$N_{Sd} \le N_{t,Rd} = \frac{A f_y}{\gamma_M}$$

Nsd = Design axial force (tension positive)	-16.9	MN	
fy = characteristic yield strength	390	MN/m2	
A = Cross sectional area	0.309	m2	
ym = 1.15	1.15		

Nsd =	-17	MN
Nt,Rd =	104.943	MN

NOT APPLICABLE

Grade steel - S	420
<=16	420
<=40	400
<=63	390
<=80	380
<=100	370
<=150	365

Figure B.1: Final check values of all checks.

B.2. Joint Check

The steps followed to check for the joints are shown below.

The table below shows the joint check done for the critical joint on the Jacket structure using the above mentioned steps.

G.F. Main			G.F. Sub		
D_Out	2.3	m	D_Out	1.62	m
D_In	2.11	m	D_In	1.52	m
t	0.095	m	t	0.05	m
g	0.611	m	βA	0.704	
g/D	0.2657		τA	0.526	
Qg	1.0		Q_βA	1.031	1.031
Y	12.10526				

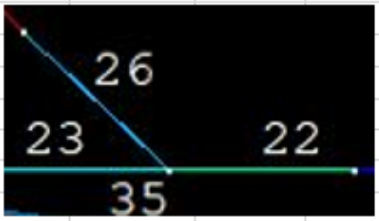

Values for Strength factor - Qu				
Joint	Axial T	Axial C	In-plane	out-plane
Y	21.13	19.74	8.85	5.28

G.F. Main		
D_Out	2.3	m
D_In	2.11	m
t	0.095	m

G.F. Sub		
D_Out	1.62	m
D_In	1.52	m
t	0.050	m

Values for chord action factor Qf								
σasd =	-4.9052	MN/m2	From table for T/Y joint				F & M	Stress
σ_my,sd =	-263.846	MN/m2	C1	C2	C3	Fx_t	9.12	13.86
σ_mz,sd =	-75.4812	MN/m2	0.3	0	0.8	My_t	-100.06	-287.19
fy =	450	MN/m2	0.2	0	0.4	Mz_t	-24.10	-69.17
A^2	0.230			Iyy	0.401	Fx_b	-18.93	-28.77
Qf_Axial	0.81		Element 22,23 - 464,465	Izz	0.401	My_b	-83.80	-240.51
Qf_Bending	0.91					Mz_b	-28.50	-81.80

NRd =	85.8	MN	Top X	NSd =	40.72	MN	Element 26 - 504
My,Rd =	64.9	MN.m	In-plane	My,Sd =	-16.83	MN.m	
Mz,Rd =	38.7	MN.m	Out-plane	Mz,Sd =	-14.81	MN.m	
0.92	<=	1					
SAFE							

Table B.1: Joint check

6.3.3 - Axial Compression

$$N_{Sd} \le N_{c,Rd} = \frac{Af_c}{\gamma_M}$$

Nsd = Design axial force (comp positive)	16.9	MN
fc = Charac axial compression strength	357.626	MN/m2
ym = See 6.3.7	1.150	

In the absence of hydrostatic pressure the charac axial comp strength for tubular members shall be the smaller of the inplane or out of plane buckling strength from eqns below

$$f_c = [1.0 - 0.28\bar{\lambda}^2]f_{cl} \quad \text{for } \bar{\lambda} \le 1.34$$

$$f_c = \frac{0.9}{\bar{\lambda}^2} f_{cl} \quad \text{for } \bar{\lambda} > 1.34$$

$$\bar{\lambda} = \sqrt{\frac{f_{cl}}{f_E}} = \frac{kl}{\pi i}\sqrt{\frac{f_{cl}}{E}}$$

$$f_{cl} = f_y \quad \text{for } \frac{f_y}{f_{cle}} \le 0.170$$

$$f_{cl} = \left(1.047 - 0.274\frac{f_y}{f_{cle}}\right) f_y \quad \text{for } 0.170 < \frac{f_y}{f_{cle}} \le 1.911$$

$$f_{cl} = f_{cle} \quad \text{for } \frac{f_y}{f_{cle}} > 1.911$$

and

$$f_{cle} = 2C_e E\frac{t}{D}$$

fcl = Char local buckling strength	390	MN/m2
λ` = column slenderness parameter	0.544	
fE = smaller Euler buckling strength in y or z direction		
E - Younds modulus of elasticity 2.1*e5 Mpa	210000	MN/m2
k = Effective length factor, see 6.3.8.2	1	
l = longer unbraced length in y or z direction	27.655	m
i = radius of gyration	0.697	m
A - Cross sectional area	0.309	m
fy /fcle	0.125	
fcle = characteristic elastic local buckling strength	3118.812	MN/m2
Ce = critical elastic buckling coef	0.3	
D = outside diameter	2.02	m
t = wall thickness	0.05	m

For fy/fcle > 0.17, the tubular is a class 4 cross section and may behave as a shell. Shell structure may have brittle failure 6.2. So ym should be increased.

Nsd =	16.9	MN	
Nc,Rd =	96.232	MN	SAFE

6.3.4 - Bending

$$M_{Sd} \le M_{Rd} = \frac{f_m W}{\gamma_M}$$

Msd = Design bending moment	48.762	MN.m
fm = characteristice bending strength	476.59	MN/m2
W = elastic section modulus	0.1487	m3
ym = see 6.3.7	1.15	

$$f_m = \frac{Z}{W} f_y \quad \text{for } \frac{f_y D}{Et} \le 0.0517$$

$$f_m = \left(1.13 - 2.58\left(\frac{f_y D}{Et}\right)\right)\left(\frac{Z}{W}\right) f_y \quad 0.0517 < \frac{f_y D}{Et} \le 0.1034$$

$$f_m = \left(0.94 - 0.76\left(\frac{f_y D}{Et}\right)\right)\left(\frac{Z}{W}\right) f_y \quad 0.1034 < \frac{f_y D}{Et} \le 120\frac{f_y}{E}$$

fy*D/E*t	0.0750		
Msd=	48.762	MN.m	
Mrd=	61.636	MN.m	SAFE
Z/W * fy=	508.948	MN/m2	
W=	0.1487	m3	
Z=	0.1941	m3	

W = elastic section modulus $= \frac{\pi}{32}\frac{\left[D^4 - (D-2t)^4\right]}{D}$

Z = plastic section modulus $= \frac{1}{6}\left[D^3 - (D-2t)^3\right]$

For fy/fcle > 0.17, the tubular is a class 4 cross section and may behave as a shell. Shell structure may have brittle failure 6.2. So ym should be increased.

6.3.5 - Shear

$$V_{Sd} \le V_{Rd} = \frac{Af_y}{2\sqrt{3}\gamma_M}$$

Vsd = Design shear force	5.03	MN
fy = Yield strength	390	MN/m2
A = cross sectional area	0.309	m2
ym = 1.15	1.15	

Vsd=	5.03026	MN	
Vrd=	30.2944	MN	SAFE

Tubular members subjected to shear from torsional moment should be designed to statisfy the following conditio

$$M_{T,Sd} \le M_{T,Rd} = \frac{2I_p f_y}{D\sqrt{3}\gamma_M}$$

$M_{T,Sd}$ = design torsional moment

I_p = polar moment of inertia $= \frac{\pi}{32}\left[D^4 - (D-2t)^4\right]$

	-15.05	MN.m
	0.3004	m4

Mtsd=	-15.052	MN.m	
Mtrd=	58.2402	MN.m	SAFE

6.3.6 - Hydrostatic pressure

6.3.6.1 - Hoop buckling | **In our case we don't use stiffener, so this hoop criteria should be SAFE**

$$\sigma_{p,Sd} \le f_{h,Rd} = \frac{f_h}{\gamma_M}$$

$$\sigma_{p,Sd} = \frac{p_{Sd} D}{2t}$$

fh = characteristic hoop buckling strength	113.22419	MN/m2
σpsd = design hoop stress due to hydrostatic pressure (compression positive)	11.171383	MN/m2
psd = Design hydrostatic pressure	0.553	MN/m2
γm = see 6.3.7	1.15	

If out-of-roundness tolerance do not meet the requirements in NORSOK M-101, guidance on calculating the reduced strength is given in Clause 12

$f_h = f_y$, for $f_{he} > 2.44 f_y$

$f_h = 0.7 f_y \left[\frac{f_{he}}{f_y}\right]^{0.4}$ for $2.44 f_y \ge f_{he} > 0.55 f_y$

$f_h = f_{he}$, for $f_{he} \le 0.55 f_y$

$f_{he} = 2 C_h E \frac{t}{D}$

σpsd=	11.17138	MN	
fh,Rd=	98.45582	MN	SAFE
D/t =	40.4		
fhe=	113.2242	MN/m2	
Ch =	0.011		

C_h = 0.44 t/D for $\mu \ge 1.6D/t$
= 0.44 t/D + 0.21 $(D/t)^3/\mu^4$ for $0.825D/t \le \mu < 1.6D/t$
= 0.737/(μ - 0.579) for $1.5 \le \mu < 0.825D/t$
= 0.80 for $\mu < 1.5$

$\mu = \frac{L}{D}\sqrt{\frac{2D}{t}}$ μ = 123.0631

L = length of tubular between stiffening rings, diaphragms or end connecti 27.655 m

μ = Geometric parameter

6.3.7 - Material Factor

$\gamma_M = 1.15$ for $\bar{\lambda}_s < 0.5$
$\gamma_M = 0.85 + 0.60\bar{\lambda}_s$ for $0.5 \le \bar{\lambda}_s \le 1.0$
$\gamma_M = 1.45$ for $\bar{\lambda}_s > 1.0$

γm =	1.15
γm =	1.07
γm =	1.45

$$\bar{\lambda}_s = \frac{|\sigma_{c,Sd}|}{f_{cl}} \cdot \lambda_c + \left(\frac{\sigma_{p,Sd}}{f_h}\right)^2 \cdot \lambda_h$$

λs = 0.365

$\lambda_c = \sqrt{\frac{f_y}{f_{cle}}}$, and $\lambda_h = \sqrt{\frac{f_y}{f_{he}}}$

λc =	0.4
λh =	1.9

$$\sigma_{c,Sd} = \frac{N_{Sd}}{A} + \frac{\sqrt{M_{y,Sd}^2 + M_{z,Sd}^2}}{W}$$

σcsd= 382.481 MN/m2

Nsd=	16.9	MN	(Tension or Compression) Nsd is -ve in tension
My,sd=	48.03	MN.m	Design bending moment about member y-axis (in-plane)
Mz,sd=	-8.42	MN.m	Design bending moment about member z-axis (out-of-plane)

6.3.8 - Tubular members subjected to combined loads without hydrostatic pressure

6.3.8.1 - Axial tension and bending

$$\left(\frac{N_{Sd}}{N_{t,Rd}}\right)^{1.75}+\frac{\sqrt{M_{y,Sd}^2+M_{z,Sd}^2}}{M_{Rd}}\le 1.0$$

#NUM!	<=	1

NOT APPLICABLE

If shear and torsion is of importance the bending capacity Mrd needs to be substituted with Mred,rd calculated according to subclause 6.3.8.3 or 6.3.8.4

6.3.8.2 - Axial compression and bending

$$\frac{N_{Sd}}{N_{c,Rd}}+\frac{1}{M_{Rd}}\left\{\left[\frac{C_{my}M_{y,Sd}}{1-\frac{N_{Sd}}{N_{Ey}}}\right]^2+\left[\frac{C_{mz}M_{z,Sd}}{1-\frac{N_{Sd}}{N_{Ez}}}\right]^2\right\}^{0.5}\le 1.0$$

0.877	<=	1

SAFE

and at all cross sections along their length

$$\frac{N_{Sd}}{N_{cl,Rd}}+\frac{\sqrt{M_{y,Sd}^2+M_{z,Sd}^2}}{M_{Rd}}\le 1.0$$

$$N_{cl,Rd}=\frac{f_{cl}\cdot A}{\gamma_M}$$

$$N_{Ey}=\frac{\pi^2 EA}{\left[\frac{kl}{i}\right]_y^2}\qquad N_{Ez}=\frac{\pi^2 EA}{\left[\frac{kl}{i}\right]_z^2}$$

Nsd = Design axial compression force

Cmy = moment reduction factor corresponds y axes	0.85	0.98	
Cmz = moment reduction factor corresponds z axes	0.85	0.98	
ky = Effective length corresponds to y axes	1		
kz = Effective length corresponds to z axes	1		
Ney = Euler buckling strength corresponds to y axes	407.08	MN	
Nez = Euler buckling strength corresponds to z axes	407.08	MN	
Ncl,rd = design axial local buckling resistance	104.94	MN	

To select k and Cm for the loads see table 6-2 in next sheet

6.3.8.2 -Interaction shear and bending moment

Tubular members subjected to beam shear force and bending moment should be designed to statisfy the following condition provided that the direction of the shear force and moment vectors are othogonal within +- 20 deg

$$\frac{M_{Sd}}{M_{Rd}}\le\sqrt{1.4-\frac{V_{Sd}}{V_{Rd}}}\quad\text{for}\ \frac{V_{Sd}}{V_{Rd}}\ge 0.4$$

$$\frac{M_{Sd}}{M_{Rd}}\le 1.0\quad\text{for}\ \frac{V_{Sd}}{V_{Rd}}<0.4$$

Vsd / Vrd =	0.2
Msd / Mrd =	0.79

SAFE

6.3.8.2 -Interaction shear and bending moment and torsional moment

Tubular members subjected to beam shear force,bending moment and torsional moment should be designed to statisfy the following condition provided that the direction of the shear force and moment vectors are othogonal

$$\frac{M_{Sd}}{M_{Red,Rd}}\le\sqrt{1.4-\frac{V_{Sd}}{V_{Rd}}}\quad\text{for}\ \frac{V_{Sd}}{V_{Rd}}\ge 0.4$$

$$\frac{M_{Sd}}{M_{Red,Rd}}\le 1.0\quad\text{for}\ \frac{V_{Sd}}{V_{Rd}}<0.4$$

Vsd / Vrd =	0.2
Msd / Mred,rd =	0.81

SAFE

$$M_{Red,Rd}=\frac{Wf_{m,Red}}{\gamma_M}$$

$$f_{m,Red}=f_m\sqrt{1-3\left(\frac{\tau_{T,Sd}}{f_d}\right)^2}$$

$$\tau_{T,Sd}=\frac{M_{T,Sd}}{2\pi R^2 t}$$

$$f_d=\frac{f_y}{\gamma_M}$$

R = radius of tubular member

γ_M = see 6.3.7

Mred,rd=	59.84	
fm,red=	462.68	MN/m2
τ_t,sd=	-46.97	MN/m2
fd =	339.13	MN/m2

6.3.9 - Tubular members subjected to combined loads with hydrostatic pressure

The equations in this section are not applicable if the section 6.3.6 is not statisfied

Method - A - assumed that the capped end compressive force due to external hydrostatic pressure are not included in the structural analysis. Method - B - assume that such forces are included in the analysis as external nodal forces.

6.3.9.1 - Axial tension, bending and hydrostatic pressure

It should statisfy equations either in Method A or B at all cross sections alon their length

Method A (σ_{asd} is in tension) | **(b) condition**

(a) For $\sigma_{a,sd} >= \sigma_{q,sd}$ (net axial tension condition)

$$\frac{\sigma_{a,Sd} - \sigma_{q,Sd}}{f_{th,Rd}} + \frac{\sqrt{\sigma_{my,Sd}^2 + \sigma_{mz,Sd}^2}}{f_{mh,Rd}} \le 1.0$$

0.635	<=	1

NOT APPLICABLE

σ_{asd} = design axial stress that excludes the effect of capped end axial compression arising from the external hyrostatic pressure (tension positive) — -54.6136 MN/m2

σ_{qsd} = capped end design axial compression stress due to external hydrostatic pressure (=0.5*σpsd) (compression positive) — 5.58569 MN/m2

$\sigma_{my,sd}$ = design in plane bending stress — -56.6142 MN/m2

$\sigma_{mz,sd}$ = design out-of plane bending stress — 322.943 MN/m2

$f_{th,Rd}$ = design axial tensile resistance in the presence of external hydrostatic pressure — 327.78 MN/m2

$f_{mh,Rd}$ = design bending resistance in the presence of external hydrostatic pressure — 400.56 MN/m2

$$f_{th,Rd} = \frac{f_y}{\gamma_M}[\sqrt{1+0.09B^2} - B^{2\eta} - 0.3B] \qquad B = \frac{\sigma_{p,Sd}}{f_{h,Rd}}, \quad B \le 1.0 \qquad \eta = 5 - 4\frac{f_h}{f_y}$$

$$f_{mh,Rd} = \frac{f_m}{\gamma_M}[\sqrt{1+0.09B^2} - B^{2\eta} - 0.3B]$$

B = 0.113 η = 3.84

γ_M = see 6.3.7

(b) For $\sigma_{a,sd} < \sigma_{q,sd}$ (net axial compression condition)

$$\frac{|\sigma_{a,Sd} - \sigma_{q,Sd}|}{f_{cl,Rd}} + \frac{\sqrt{\sigma_{my,Sd}^2 + \sigma_{mz,Sd}^2}}{f_{mh,Rd}} \le 1.0$$

0.996	<=	1

NOT APPLICABLE

$$f_{cl,Rd} = \frac{f_{cl}}{\gamma_M}$$

$f_{cl,Rd}$ = 339.13 MN/m2

When $\sigma_{c,Sd} > 0.5\frac{f_{bo}}{\gamma_M}$ and $f_{clo} > 0.5 f_{bo}$, Equation (6.41) should also be satisfied:

382.481	49.2279	Needed
3118.81	56.6121	Needed

$$\frac{\sigma_{c,Sd} - 0.5\frac{f_{bo}}{\gamma_M}}{\frac{f_{clo}}{\gamma_M} - 0.5\frac{f_{bo}}{\gamma_M}} + \left[\frac{\sigma_{p,Sd}}{\frac{f_{bo}}{\gamma_M}}\right]^2 \le 1.0$$

0.128	<=	1

NOT APPLICABLE

in which $\sigma_{c,Sd} = \sigma_{m,Sd} + \sigma_{q,Sd} - \sigma_{a,Sd}$; $\sigma_{c,Sd}$ should reflect the maximum combined compressive stress.

$$\sigma_{m,Sd} = \frac{\sqrt{M_{z,Sd}^2 + M_{y,Sd}^2}}{W}$$

γ_M = see 6.3.7

σ_{msd} = 327.868 MN/m2

σ_{csd} = 388.067 MN/m2

6.3.9 - Tubular members subjected to combined loads with hydrostatic pressure

6.3.9.2 - Axial compression, bending and hydrostatic pressure

Method A ($\sigma_{a,sd}$ is in compression)

$$\frac{\sigma_{a,Sd}}{f_{ch,Rd}} + \frac{1}{f_{mh,Rd}}\left[\left(\frac{C_{my}\sigma_{my,Sd}}{1-\frac{\sigma_{a,Sd}}{f_{Ey}}}\right)^2 + \left(\frac{C_{mz}\sigma_{mz,Sd}}{1-\frac{\sigma_{a,Sd}}{f_{Ez}}}\right)^2\right]^{0.5} \le 1.0$$

0.904	<=	1
	SAFE	

$$\frac{\sigma_{a,Sd}+\sigma_{q,Sd}}{f_{cl,Rd}} + \frac{\sqrt{\sigma_{my,Sd}^2+\sigma_{mz,Sd}^2}}{f_{mh,Rd}} \le 1.0$$

0.996	<=	1
	SAFE	

σ_{asd} = design axial stress that excludes the effect of capped end axial compression arising from the external hyrostatic pressure (compression positive) 54.614 MN/m2

$$f_{Ey} = \frac{\pi^2 E}{\left[\frac{kl}{i}\right]_y^2}$$

f_{Ey} = 1315.51 MN/m2

$$f_{Ez} = \frac{\pi^2 E}{\left[\frac{kl}{i}\right]_z^2}$$

f_{Ez} = 1315.51 MN/m2

$f_{ch,Rd}$ = Design axial compression strength in the presence of external hydrostatic pressure

$$f_{ch,Rd} = \frac{1}{2}\frac{f_{cl}}{\gamma_M}\left[\xi - \frac{2\sigma_{q,Sd}}{f_{cl}} + \sqrt{\xi^2 + 1.12\bar{\lambda}^2\frac{\sigma_{q,Sd}}{f_{cl}}}\right] \quad \text{for } \bar{\lambda} < 1.34\sqrt{\left[(1-\frac{2\sigma_{q,Sd}}{f_{cl}})\right]^{-1}}$$

$$f_{ch,Rd} = \frac{0.9}{\bar{\lambda}^2}\frac{f_{cl}}{\gamma_M}, \quad \text{for } \bar{\lambda} \ge 1.34\sqrt{\left[(1-\frac{2\sigma_{q,Sd}}{f_{cl}})\right]^{-1}}$$

$f_{ch,Rd}$ = 306.56 MN/m2

0.17815

$$\xi = 1 - 0.28\bar{\lambda}^2$$

ξ = 0.91699

When $\sigma_{c,Sd} > 0.5\frac{f_{bo}}{\gamma_M}$ and $f_{clo} > 0.5 f_{bo}$, Equation (6.41) should also be satisfied:

$$\frac{\sigma_{c,Sd} - 0.5\frac{f_{bo}}{\gamma_M}}{\frac{f_{clo}}{\gamma_M} - 0.5\frac{f_{bo}}{\gamma_M}} + \left[\frac{\sigma_{p,Sd}}{\frac{f_{bo}}{\gamma_M}}\right]^2 \le 1.0$$

0.130	<=	1
	SAFE	

in which $\sigma_{c,Sd} = \sigma_{m,Sd} + \sigma_{q,Sd} + \sigma_{a,Sd}$

σ_{msd} =

σ_{Csd} = 388.067

Figure B.2: Strength check of members

The characteristic resistances for simple tubular joints are defined as follows:

$$N_{Rd} = \frac{f_y T^2}{\gamma_M \sin\theta} Q_u Q_f$$

$$M_{Rd} = \frac{f_y T^2 d}{\gamma_M \sin\theta} Q_u Q_f$$

where

N_{Rd} = the joint design axial resistance
M_{Rd} = the joint design bending moment resistance
f_y = the yield strength of the chord member at the joint
γ_M = 1.15

For joints with joint cans, N_{Rd} shall not exceed the resistance limits defined in 6.4.3.5

6.4.3.3 Strength factor Q_u

Q_u varies with the joint and action type, as given in Table 6-3.

Table 6-3 Values for Q_u

	Brace action			
Joint Classification	**Axial Tension**	**Axial Compression**	**In-plane Bending**	**Out-of-plane bending**
K	$\min\begin{cases}(16+1.2\gamma)\beta^{1.2}Q_g \\ 40\beta^{1.2}Q_g\end{cases}$		$(5+0.7\gamma)\beta^{1.2}$	$2.5+(4.5+0.2\gamma)\beta^{2.5}$
Y	30β	$\min\begin{cases}2.8+(20+0.8\gamma)\beta^{1.6} \\ 2.8+36\beta^{1.6}\end{cases}$		
X	$6.4\gamma^{(0.6\beta^2)}$	$(2.8+(12+0.1\gamma)\beta)Q_\beta$		

The following notes apply to Table 6-3:

(a) Q_β is a geometric factor defined by:

$$Q_\beta = \frac{0.3}{\beta(1-0.833\beta)} \qquad \text{for } \beta > 0.6$$

$$Q_\beta = 1.0 \qquad \text{for } \beta \le 0.6$$

(b) Q_g is a gap factor defined by:

$$Q_g = 1+0.2\left(1-\frac{2.8\,g}{D}\right)^3 \qquad \text{for } \frac{g}{D} \ge 0.05, \text{ but } Q_g \ge 1.0$$

$$Q_g = 0.13+0.65\phi\gamma^{0.5} \qquad \text{for } \frac{g}{D} \le -0.05$$

6.4.3.4 Chord action factor Q_f

Q_f is a design factor to account for the presence of factored actions in the chord.

$$Q_f = 1.0 + C_1\frac{\sigma_{a,Sd}}{f_y} - C_2\frac{\sigma_{my,Sd}}{1.62\,f_y} - C_3 A^2$$

$$A^2 = \left(\frac{\sigma_{a,Sd}}{f_y}\right)^2 + \left(\frac{\sigma^2_{my,Sd}+\sigma^2_{mz,Sd}}{1.62\,f_y^2}\right) \qquad (6.55)$$

where

$\sigma_{a,Sd}$ = design axial stress in chord, positive in tension
$\sigma_{my,Sd}$ = design in-plane bending stress in chord, positive for compression in the joint footprint
$\sigma_{mz,Sd}$ = design out-of-plane bending stress in chord
f_y = yield strength
C_1, C_2, C_3 = coefficients depending on joint and load type as given in Table 6-4

Table 6-4 Values for C_1, C_2 and C_3

Joint type	C_1	C_2	C_3
K joints under balanced axial loading	0.2	0.2	0.3
T/Y joints under brace axial loading	0.3	0	0.8
X joints under brace axial tension loading 1)			
$\beta \le 0.9$	0	0	0.4
$\beta = 1.0$	0.2	0	0.2
X joints under brace axial compression loading 1)			
$\beta \le 0.9$	0.2	0	0.5
$\beta = 1.0$	-0.2	0	0.2
All joints under brace moment loading	0.2	0	0.4

1) Linear interpolated values between $\beta = 0.9$ and $\beta = 1.0$

The average of the chord loads and bending moments on either side of the brace intersection should be used in Equations (6.54) and (6.55). The chord thickness at the joint should be used in the above calculations.

$$\frac{N_{Sd}}{N_{Rd}} + \left(\frac{M_{y,Sd}}{M_{y,Rd}}\right)^2 + \frac{M_{z,Sd}}{M_{z,Rd}} \le 1$$

where

N_{Sd} = design axial force in the brace member
N_{Rd} = the joint design axial resistance
$M_{y,Sd}$ = design in-plane bending moment in the brace member
$M_{z,Sd}$ = design out-of-plane bending moment in the brace member
$M_{y,Rd}$ = design in-plane bending resistance
$M_{z,Rd}$ = design out-of-plane bending resistance

C

Fatigue Analysis

All year

Hs [m] \ Tz [s]	0	1	2	3	4	5	6	7	8	9		
							1:7	1:10				
7.5									0.0		1:18	0.0
7									0.0			0.0
6.5								0.0	0.1		1:20	0.1
6								0.1	0.1			0.2
5.5								0.3	0.0			0.3
5								1.4				1.4
4.5							0.4	2.6			1:30	2.9
4							4.8	1.5				6.3
3.5						0.0	16.0	0.0				16.0
3						0.8	34.2				1:40	35.0
2.5					0.0	43.2	26.1					69.3
2					1.8	126.4	0.9					129.0
1.5					59.2	187.1	0.8					247.0
1					254.9	88.9	3.2					347.1
0.5												
0	4.9		2.6	103.3	28.7	2.3	1.4	0.0	0.0			143.3
Total	4.9		2.6	419.1	475.2	88.6	7.3	0.3	0.0			998.0
											Calms	*2.0*
												Total

Number of Observations, Total: 245053

Table C.1: All year wave scatter for North Sea

S-N curve	$N \le 10^7$ cycles		$N > 10^7$ cycles	Fatigue limit at 10^7 cycles [MPa] *)	Thickness exponent k	Structural stress concentration embedded in the detail (S-N class), see also equation (2.3.2)
	m_1	$\log \bar{a}_1$	$\log \bar{a}_2$ $m_2 = 5.0$			
B1	4.0	15.117	17.146	106.97	0	
B2	4.0	14.885	16.856	93.59	0	
C	3.0	12.592	16.320	73.10	0.05	
C1	3.0	12.449	16.081	65.50	0.10	
C2	3.0	12.301	15.835	58.48	0.15	
D	3.0	12.164	15.606	52.63	0.20	1.00
E	3.0	12.010	15.350	46.78	0.20	1.13
F	3.0	11.855	15.091	41.52	0.25	1.27
F1	3.0	11.699	14.832	36.84	0.25	1.43
F3	3.0	11.546	14.576	32.75	0.25	1.61
G	3.0	11.398	14.330	29.24	0.25	1.80
W1	3.0	11.261	14.101	26.32	0.25	2.00
W2	3.0	11.107	13.845	23.39	0.25	2.25
W3	3.0	10.970	13.617	21.05	0.25	2.50
*) See also [2.12].						

Figure C.1: S-N curve for air environment

Environment	m_1	$\log \bar{a}_1$	m_2	$\log \bar{a}_2$	Fatigue limit at 10^7 cycles [MPa]*)	Thickness exponent k
Air	$N \le 10^7$ cycles		$N > 10^7$ cycles			
	3.0	12.48	5.0	16.13	67.09	0.25
Seawater with cathodic protection	$N \le 1.8 \cdot 10^6$ cycles		$N > 1.8 \cdot 10^6$ cycles			
	3.0	12.18	5.0	16.13	67.09	0.25
Seawater free corrosion	3.0	12.03	3.0	12.03	0	0.25
*) See also [2.12].						

Figure C.2: S-N curve for air environment specially for tubular members